Estimating Global Impacts to Agriculture from Climate Change Accounting for Adaptation

Andrew Hultgren*[1], Tamma Carleton[3,4], Michael Delgado[6], Diana R. Gergel[6], Michael Greenstone[2,4,5], Trevor Houser[6], Solomon Hsiang*[4,7], Amir Jina[4,5], Robert E. Kopp[8], Steven B. Malevich[6], Kelly E. McCusker[6], Terin Mayer[9], Ishan Nath[2], James Rising[10], Ashwin Rode[2], and Jiacan Yuan[11]

[1]Department of Agricultural and Consumer Economics, University of Illinois Urbana-Champaign; Urbana, IL, USA

[2]Department of Economics, University of Chicago; Chicago, IL, USA

[3]Bren School of Environmental Science and Management, University of California; Santa Barbara, CA, USA

[4]National Bureau of Economic Research; Cambridge, MA, USA

[5]Harris School of Public Policy University of Chicago; Chicago, IL, USA

[6]Rhodium Group; Oakland, CA, USA

[7]Global Policy Laboratory, Goldman School of Public Policy, University of California; Berkeley, CA, USA

[8]Department of Earth and Planetary Sciences and Institute of Earth, Ocean, and Atmospheric Sciences, Rutgers University; New Brunswick, NJ, USA

[9]Humbert H. Humphrey School of Public Affairs, University of Minnesota; Minneapolis, MN, USA

[10]School of Marine Science and Ocean Policy, University of Delaware; Newark, DE, USA

[11]Fudan University; Shanghai, China

September 17, 2022

*Correspondence: ahultgr@illinois.edu, shsiang@berkeley.edu

Abstract

Climate change threatens global food systems, but the extent to which adaptation will reduce losses remains unknown. Here, we empirically estimate the net impact of producer adaptations around the world using longitudinal data on six staple crops spanning 12658 sub-national units, capturing two-thirds of global crop calories. We project that adaptation and income growth nearly halve global losses at end-of-century, but substantial residual losses remain for all staples except rice. Global damages are dominated by losses to modern-day breadbaskets that currently exhibit limited adaptation due to favorable climates. We estimate global production declines 5.8×10^{14}kCal annually per 1°C rise in global mean surface temperature (4.6% of current production or 130kCal/person/day, per 1°C; $p < 0.001$). These results suggest a scale of innovation, cropland expansion and/or additional adaptation that might be necessary to ensure global food security in a changing climate.

Climate change and the global food supply

Disruptions of the global food system due to climate change threaten human well-being (*1*, *2*, *3*) and social stability (*4*, *5*), but researchers lack a complete understanding of the magnitude and structure of potential impacts of warming on food systems globally (*6*, *7*). It is known that changes to the climate will alter the distribution of weather events experienced across the planet (*8*) and that biophysical processes in agricultural systems will respond to these changes (*9*, *10*, *11*). However, the degree to which humans around the world are likely to effectively adapt their agricultural practices in reaction to these changes remains unknown (*6*, *9*, *12*, *13*). For this reason, existing global projections have been unable to account for the adoption rates and efficacy of producer adaptations (*9*, *10*, *14*) and it remains unresolved whether producers' compensatory responses are likely to overcome the challenges posed by climate change (e.g. *15*, *16*).

Here, we develop a unified empirical approach to measure the effect of climate change on staple crop production, accounting for the costs, benefits, and adoption rates of producer adaptations as they are observed in practice around the world. We focus on staple crops and study one of the most comprehensive samples of subnational crop yields ever assembled, representing two-thirds of global cropped calorie production, which allows our results to be globally representative. Using high-resolution data from populations across diverse contexts allows us to understand the real-world response of producers to weather events, changes in climate, and economic development. We then apply our empirical results to project probabilistic global climate change impacts on yields that account for environmental changes, biophysical processes, and producers' compensatory responses.

Prior analyses employing process-based models have provided crucial insights about the potential impacts of climate change on food systems (*9*, *10*, *13*, *14*). These models explicitly characterize the biophysical processes that generate yields (e.g. root depth, evapotranspiration, light utilization) and are calibrated to precisely managed experimental fields (*10*, *14*), thereby providing detailed insight into the agronomic mechanisms by which climatic changes influence future yields. However, to date, these models have not attempted to incorporate data on the decisions real producers make; instead they generally assume producers optimize yields subject to exogenously imposed constraints that reflect scenarios selected by the modeler (e.g. "no adaptation" or "optimal varietal switching") (*9*, *10*, *13*, *14*). As with most scenario-based analyses, these scenarios describe what is theoretically possible but are not intended to reflect real world conditions across diverse socioeconomic contexts (*9*, *10*), which are influenced by credit constraints (e.g. *17*), imperfect information (e.g. *18*), market failures (e.g. *19*), and other social and environmental conditions (e.g. *19*, *20*). Furthermore, because global process-based models are parameterized based on a relatively small sample of scientific farms, it is well known that they are not representative of actual producer decisions in diverse and resource-constrained contexts around the world (*7*, *9*, *10*, *11*, *13*, *21*).

To address this challenge, we develop an econometric approach that simultaneously captures the combined impact of biophysical crop responses and producer decision-making. Rather than a modeler prescribing scenarios for exactly how producers might adapt, our approach empirically estimates the effect of actual adaptations observed in historical data around the world in response to underlying climatic and economic conditions faced by producers. This reduced-form approach does not attempt the complex and difficult task of identifying and modeling each of the individual mechanisms through which these adaptations occur (e.g. optimizing over all combinations of producer decisions and inputs). Instead, we measure the total impact of all adaptive adjustments that producers make in response to the climate (e.g. changing varietals, altering planting dates, adjusting fertilizer) without modeling these intermediary processes explicitly (see Supplementary Appendix A.2). We then apply these measurements — which capture the extent, intensity, and efficacy of real-world producer adaptations as a function of local climates and economic conditions — in simulations of future crop production under climate change and economic development over the coming decades.

Prior empirical work has demonstrated how reduced form econometric approaches can be calibrated to the behavior of large populations of producers in specific regions (*6*, *11*, *22*, *23*, *24*), such as maize producers in the United States (*11*). Follow-up work demonstrated that application of this econometric approach is complementary to, rather than a replacement for, detailed process-based models (*9*, *13*, *21*, *23*, *25*, *26*). Our work here represents, to the best of our knowledge, the first global analysis of staple crops that (i) accounts for observed adaptation behavior and how it varies globally, (ii) uses these results to generate global projections of climate impacts on yields over the 21st century, and (iii) transforms these projections into an empirically-derived "damage function" that links changes in global calorie production to changes in global mean surface temperature ($\Delta GMST$). The scale and scope of our projections are comparable to global gridded process-based models, such as those underlying the Agricultural Model Intercomparison and Improvement Project (AgMIP) (*10*); but unlike those models, our analysis is based on globally representative data and accounts for the adoption rates and efficacy of adaptive behaviors that producers choose to undertake in practice across diverse environmental and economic contexts.

Challenges to projecting global climate impacts on staple crops

Here we address four key challenges to projecting global impacts of climate change on agriculture, all of which are essential to the objective of accurately capturing adaptive behavior in projections but none of which have been previously addressed at global scale.

First, it has been difficult to empirically quantify climate impacts on agriculture globally and at high resolution. Prior global econometric analyses have relied on country-level data and estimate global aver-

age responses (e.g. *27*). This leaves varied climates, food systems, and socioeconomic contexts within and between countries unresolved. We address this challenge by assembling one of the largest datasets of sub-national crop production available to researchers,[1] covering over 12,658 sub-national administrative units from 55 countries for six globally and regionally important crops that represent two thirds of global crop caloric production (Figure 1A-C and G, Supplementary Figure S1, Supplementary Table S1). This allows us to understand how local climate changes in diverse socioeconomic conditions induce local adaptations and influence local yields, all at a global scale (e.g. see Figures 1D-F and H-J, Figure S2, Appendices A.2 and D).

Second, there has been extensive unresolved debate over what aspects of weather are statistically important for the production of each crop (*6*, *11*, *29*, *30*, *31*, *32*, *33*, *34*, *35*). For example, it has been debated if the evenness of rainfall within a season is influential for crop yields(*34*) once seasonal precipitation is accounted for, whether nighttime temperature (*32*) or vapor-pressure-deficit (*35*) are important variables once daytime temperature is accounted for, and whether temperature effects are nonlinear and/or contain critical thresholds (*11*). These various measures all describe aspects of the distribution of weather at a location and they tend to be highly correlated, making it difficult to isolate and distinguish their impacts. Furthermore, those variables that are important for one crop might be less important for a different crop. We endeavor to "let the data speak" and select the independent weather variables in our models via cross-validation, an approach commonly used in machine learning (Appendix C, Appendix Figure S2A, Appendix Figures S3–S4). We assemble many candidate model structures based on weather variables studied in previous research(*11*, *32*, *34*, *35*, *36*), then select a parsimonious global model for each crop based on its ability to predict yields in portions of the sample that are withheld during model-fitting (Appendix A.2, Tables S7 & S8).

Third, it is widely believed that agricultural producers will adapt to climate change, but it has been debated how to measure the impact of this adaptation and account for it in future projections (*6*, *11*, *12*, *15*, *16*, *22*, *37*, *38*). Unlike process-based yield models, where all components of adaptation decisions are fully specified by the modeler, in statistical approaches the net effects of all real-world adaptive decisions are observed. For example, if a producer is or is not adapted to drought conditions, then we may observe that actual drought events have limited or large effects on their crop yields (*24*, *38*), respectively. To build a model that expresses these changes in vulnerability, we follow prior research by using summary statistics that describe the climate (e.g. average temperature, average rainfall, or their product; e.g. see bars in Figure 1D-F and H-J) to identify sub-populations that are likely to be similarly adapted (Appendix Figures S2B & S6–S7, Appendices A.2 and D)(*11*, *15*, *38*, *39*, *40*, *41*). Distinct from prior research, we determine measures

[1] Ray et al. (*28*) analyze the only comparable data set we are aware of, containing "∼13,500 spatial units" and four crops, but have not made their data public and declined to provide access to it.

of the climate that proxy for adaptation via cross-validation separately for each crop (Appendix Figure S2C), similar to our approach for identifying key weather variables. We then estimate the characteristic production patterns within each group, reflecting the range of real-world adaptations they undertake. In projections, as the climate evolves, the impact of weather on a producer is adjusted to reflect the level of adaptation observed for producers inhabiting a similar climate (see Appendices A.2 and F). This approach accounts for any adaptation measure that varies with climatological conditions (e.g. varietal selection, shifting of planting dates and cultivation windows, and optimization of inputs such as fertilizer or irrigation intensity in response to climate). Importantly, we account for both the costs and benefits of these adaptations at each location around the world, using the method developed in ref. (*40*) (see Appendix Figure S10, Appendix G); failing to account for costs would overstate the value of adaptation (*16*).

Last, we account for the possibility that agricultural producers with access to different resources (e.g. fertilizer, farming capital, or crop technologies) may produce food differently. This is particularly important in projections of climate change, since future economic development is likely to alter agricultural practices and their socioeconomic contexts in ways that could make agriculture more resilient or vulnerable to weather (*42*). We account for the overall net effect of different populations' access to resources, both public and private, by allowing income and access to irrigation to continuously alter all components of each crop model (Figures S2B, & S6–S7, Appendix A.2, Appendix D). In projections, we then alter how climate and weather influence crop production in response to projected economic development(*43*). Theoretically, other types of non-income resources could be accounted for explicitly (e.g. market access), but we restrict our analysis to focus on income because (i) socioeconomic variables correlated with global incomes (e.g. roads, institutions) will be captured by income, and (ii) income is the only variable for which standard projections are available, via the Shared Socioeconomic Pathways (*43*, *44*).

Estimating the effect of climate and weather on global staple crops

Econometric implementation We estimate a separate model for each of six crops — maize, soybeans, rice, wheat, cassava and sorghum — allowing yields in each subnational unit to be a function of weather, climate, income, and irrigation access simultaneously (see Supplementary Appendix A.2, e.g. Equation A.13). For each year, we compute a set of weather measures previously identified in prior literature as important for some staple crops in our sample: vapor pressure deficit (*35*), degree days (*11*), minimum temperature (*32*), drought (*45*), first- through fifth-order polynomials in growing season precipitation (*36*), precipitation by phase of growing season (*45*), the count of rainy days (*34*), the count of extreme rain days (*34*), and the total amount of extreme rain (*45*). To estimate a plausibly causal impact of each weather measure on crop yields, we account for time-invariant and trending confounds by residualizing yields and weather measures on a set

of location-specific (e.g. county or municipality) constants, country-by-year constants, and quadratic trends for each first-level adminstrative unit (e.g. state or province). This procedure nonparametrically absorbs the influence of time-invariant local confounds such as soil quality, country-by-year confounds such as prices and trade policy, and time-varying state or province confounds such as the diffusion of new technologies or local variation in prices (see Supplementary Appendix A.2).

We select a parsimonious set of independent weather variables for each crop using cross-validation over random folds of this residualized data set. In a few cases, we also used published expert judgement(*46*, *47*, *48*) to limit the set of candidate variables, restricting our search to variables that are reliably projected by global climate models. Our procedure evaluates the out-of-sample performance of candidate models that include all combinations of weather variables that we draw from the literature and allows for varying degrees of nonlinearity (Figure 1, Appendix Figures S2A and S4; see Supplementary Appendices A.2, D, and C).

We then estimate how adaptive responses to long-term climate variables (average temperature, average precipitation, and their interaction), income, and access to irrigation mediate the influence of all weather variables by constructing continuous interactions between weather and these variables (e.g. Figure 1D-F and H-J; see Appendix Figure S2B and Supplementary Appendices A.2, D, and C). These mediating factors allow the yield response-function to evolve non-linearly as a simultaneous function of the climate, income, and irrigation in each location. Inclusion of climate and irrigation mediating variables is determined via cross-validation, with folds in the data blocked by first-level administrative unit (e.g. state or province, see Supplementary Appendices A.2, D, and C).

The final global model for each crop that results from this procedure is high-dimensional, nonlinear, and dependant on the underlying economic and climatic characteristics of each location – but nonetheless fully interpretable. Each crop model includes multiple measures of weather that are all interacted with multiple measures of climate, as well as income and possibly irrigation (Appendix Figure S2C). This approach allows yields in a given year and location to be computed based on (i) weather in that location-year, which is an argument to (ii) a location-and-time-specific function determined by crop-specific measures of climate, income and irrigation. The resulting crop models are relatively parsimonious compared to global process-based models (*9*, *10*) because the influence of many additional factors and confounders not explicitly included in the model (e.g. soil type and quality) is captured indirectly and/or nonparametrically (see Supplementary Appendix A.2).

Weather variables that influence crop yields

We use cross-validation to evaluate over 8,000 candidate empirical models across all six crops, where each model predicts residual changes in historical crop yields using a different combination of weather variables

proposed by prior studies (*11*, *32*, *34*, *35*, *36*) (see Supplementary Appendices A.2 and D). Based on out-of-sample performance, we find that nonlinear degree days are the most important determinant of yields, on average across crops, by a considerable margin (Appendix Figures S2A and S4). Degree days increases model out-of-sample (OOS) fit (Table S7) across crops by 49.2% on average (relative to the second best model), with the largest gain for sorghum (101.6%, a doubling of model OOS fit) and the smallest gains for rice and cassava (9.1% and 9.4%). In general, exposure to cool daily temperatures ($< 11°C$ for wheat, and $< 29 - 31°C$ for all other crops) modestly increase yields, while daily temperatures above these thresholds cause sharp declines in yields; for example lowering end-of-season maize yields by -5% for each day that shifts from a 25°C to a 40°C day (Figure 1K, Appendix Figure S6). This finding generalizes prior results from the US (e.g. *11*) globally and across crops.

Seasonal precipitation is the second most important determinant of yields across all crops, to the exclusion of a wide range of other candidate weather variables put forward in the literature (Figures S2A and S4). Nonlinear measures of seasonal precipitation increase model OOS fit across crops by 14.6%, with the largest gains for rice and maize (22.8% and 22.2%) and the smallest gains for wheat, soy, and sorghum (8.2%, 9.2%, and 9.4%, Table S8). Across crops, increasing seasonal monthly precipitation raises yields on average 0.2% per mm at low rainfall levels (<100 mm/month), has little effect at intermediate levels (250-300mm/month), and reduces yields -0.6% per mm at higher levels (>400mm/month, Figures S6 & S7).

In contrast to reports from individual empirical studies (e.g., *32*, *34*, *35*, *49*), we find monthly average minimum temperatures (t_{min}), vapor-pressure deficit (VPD), drought, the count of rain days, the count of extreme rain days, and the amount of extreme rain generally only contribute modest gains to yield model fits (average % gains in OOS fit range from 1.2% to 3.6% excluding drought for cassava, discussed below). Minimum temperatures are important predictors for rice and wheat yields but not other crops (Figure S4 and Tables S7 & S8).

There are exceptions for individual crops. Cassava yields are generally insensitive to weather overall (maximum OOS variance predicted is 2.3%), motivating its cultivation in contexts where the climate is not conducive to other staple crops that are more sensitive (*50*). We found that growing season drought is the most important factor for predicting cassava yields (24.0% gain in variance predicted, Table S7). Drought is also important for rice yields, as is the count of rain days (6.4% and 8.0% gain in variance predicted, Table S7). The count of rain days is also moderately important for maize yields (6.6% gain in variance predicted, Table S7). Taken together, these results indicate the importance of nuanced projections of future precipitation distributions for a restricted set of global staple crops.

Accounting for human adaptation to climate and economic development

Because our data span climatic zones around the world, we are able to empirically measure how adaptive practices in different climates mediate the influence of environmental conditions (Figure 1, Figure S2C). In contrast to detailed process-based models (*9*, *10*, *13*, *14*) that explicitly model each adaptive action and prescribe whether it is taken, we adopt a top-down "reduced form" approach that captures the overall net consequences of all adaptive actions that are associated with changes in climatic conditions (see Supplementary Appendix A.2). This approach does not provide the granular detail contained in process-based models, but it ensures that the net consequence of all climate-associated adaptive actions are accounted for without requiring that each is explicitly modeled or observed (*22*). Because access to resources also alters producer actions through multiple channels— such as access to technology (*19*, *51*, *52*), inputs like fertilizer (*19*, *53*), or labor markets (*19*, *54*)—we also account for the mediating effects of income and irrigation access. This allows us to minimize confounding, since resources and climate tend to be correlated, and it allows us to project future changes associated with economic development.

Adaptation to climate We find that producers adapt to higher temperatures such that, across crops and around the world, yields are systematically less sensitive to daily temperature and generally more sensitive to seasonal precipitation in locations that are hotter on average (Figures 1; S2B; S6A,E; S7A,E). Similarly, yields are less responsive to temperature and more responsive to precipitation in locations that are drier on average (Figures S2B; S6B,F; S7B,F). Because climate-associated adaptations influence numerous—possibly correlated—aspects of weather-crop responses, we estimate the mediating influence of all dimensions of climate simultaneously on all dimensions of weather for each crop, generating a multi-dimensional function describing these interacting relationships (Figures S6 and S7). This function serves as the basis for projecting adaptation to climate change (Appendices A.2 and F) and has not been previously represented in global process-based models (*9*, *10*).

Economic development We also find that rising incomes enable producers to respond to environmental conditions in important but varied ways, thereby mediating the effects of different climates. For example, maize and sorghum yields become more sensitive to temperature as incomes rise while rice and cassava become less sensitive (Figures S2B, and S6C). These differences could be due to differences in how access to improved technologies, infrastructure, banking and credit, or insurance (*17*, *19*, *51*, *55*) influence producer strategies (*20*, *19*). Notably, however, we find that higher incomes and access to irrigation are associated with greater resilience to precipitation extremes across all crops (Figures S2B; S6G; S7G), consistent with access to improved irrigation technologies increasing with income.(*19*, *55*)

Accounting for adaptation costs

We are able to empirically observe the benefits of adaptive management among producing regions because adaptation decisions have costs (*16*, *39*). If adaptations were free, then we would expect all regions to adopt uniform management practices and varieties using only the most climate-resilient technology available, since this strategy would convey benefits at no cost (*16*, *40*). To capture the full impact of climate change on agricultural systems it is therefore essential that these costs of adaptation are accounted for, in addition to adaptation benefits, since these costs would not be incurred in the absence of climate change.

We cannot observe these costs directly, but they can be inferred under the assumption that producers undertake adaptations where the benefits exceed costs, but not those where costs exceed benefits (*40*). This is referred to as a revealed preference approach and is widely used in the economics research (*56*). Specifically, we follow the approach developed in ref. (*40*) to track these costs for each crop and in each region until 2100 (see Appendix G, Figure S10). We follow ref. (*16*) and deduct these costs from yield changes to develop a complete measure of climate change impacts (*40*). Thus, our projections of climate change impacts on yields should be interpreted as capturing both the costs and benefits of voluntary producer adaptations in each location.

Projecting the effects of climate change

We use our empirical estimates of yield-weather responses, which account for adaptation to climate and economic development, to project potential yields across 24,378 administrative regions that span the entire globe until the end of the century. We report results based on where crops are cultivated today, noting that our approach also allows us to estimate changes to theoretical yields for a crop in locations where it is not presently cultivated (Figures S11 and S12). We focus on a high emissions scenario (RCP8.5, Figure 2) and a moderate emissions scenario (RCP4.5, Figure S12) matched to two socioeconomic scenarios (*43*) (Appendix A.1). We project the annual evolution of yields in each of 33 climate models and model surrogates that represent the full range of climate-sensitivities (*57*) while also accounting for statistical uncertainty in our empirically estimated relationships via 1,920 Monte Carlo simulations per crop, following the approach developed in refs (*40*, *41*, *58*)].

The Global Distribution of Impacts

The projected effects of climate change on crop yields vary around the world (Figure 2, Figure S14). Regions exhibit different initial climates and socioeconomic conditions, and they experience different changes in temperature distributions, precipitation, and incomes. These in turn alter the environmental factors crops

are exposed to as well as the adaptive decisions by humans that influence how a crop in a given context responds to those factors.

For all crops, temperature changes (via degree days, and minimum temperature for rice and wheat) generally dominate the sign of local projected climate impacts. Precipitation strongly influences inter-annual variability in yields— which is important to producers, consumers, and government planners (*59*)— but does not generally drive overall trends. Global patterns in yield losses reflect the nonlinear response of crops to temperatures, with increasing extreme heat depressing yields and reductions in cold days increasing yields. Adaptive responses to rising average temperature moderate losses to extreme heat (e.g. Figure S6A), consistent with producers taking protective measures to prepare for expected temperature extremes (*16*). However, benefits from these protective measures are partially offset by decreased yield gains during moderate temperatures. The trade-off between temperature-resilience and average yield has been documented and is understood to reflect physiological compromises across varietals (*16*, *33*), although its potential global impact on future food production has not been previously demonstrated nor quantified.

A second general pattern across multiple crops spans equatorial regions of the world with high rainfall, such as central Africa, Southeast Asia, and South America. In these regions, the benefits of moderate temperatures are amplified by increasing levels of precipitation, driven by an intensifying water cycle (*60*). While rising temperatures may ultimately reduce yields in these regions, benefits of high rainfall in these regions partially offset those effects.

Maize In 2100 under a high emissions scenario, our projected losses of maize yields are severe ($\sim -40\%$) in the grain belt of the U.S., Eastern China, Central Asia, Southern Africa, and the Middle East (Figures 2a and S14). Losses in South America and Central Africa are more moderate ($\sim -15\%$), mitigated in part by high levels of precipitation and increasing long-run precipitation (see Figure S6B). Impacts in Europe vary strongly with latitude, ranging from $+10\%$ gains in the north to severe losses up to -40% along the Mediterranean. Gains in theoretical yield potentials occur in many northern regions where maize is not widely grown (Figure S11).

Soybeans The spatial distribution of impacts on soybean yields is similar in structure to maize, although the magnitude of impacts tends to be accentuated (Figures 2b and S14), e.g. $\sim -50\%$ in the US and $\sim +20\%$ in wet regions of Brazil.

Rice Projected impacts on rice yields are mixed in India and Southeast Asia, where it is primarily grown, with small gains of around $+3\%$ in India and losses of -1% in Southeast Asia. This regional result is broadly consistent with earlier work (*27*). In remaining areas of the world where rice is grown, central estimates

for projected impacts are generally negative, with the magnitude of yield impacts in Sub-Saharan Africa, Europe, and Central Asia exceeding −50% across each region (Figures 2C and S14).

Wheat Wheat losses are notably consistent across major wheat growing regions of the world, with yield losses of −15 to −25% in India, Eastern Europe, Western Europe, and South America, and −30 to −40% in China, Russia, the U.S., and Canada (Figures 2D and S14). Areas of Africa exhibit modest gains, but these tend to be places where wheat is not widely cultivated and overall Sub-Saharan Africa exhibits significant losses of −20% by end of century (Figure S14).

Cassava Cassava is projected to have uniformly negative projected impacts in nearly all regions where it is currently grown, with the largest losses in Sub-Saharan Africa (−40% on average). While cassava is not a large portion of global agricultural revenues, it is an important subsistence crop in low and middle income countries. Thus these potential yield losses may be a substantial future threat to the nutritional intake of the global poor (Figures 2E and S14).

Sorghum Sorghum losses are widespread in almost all major regions where it is currently grown: North America (−40%), South Asia (including India) (−10%), and Sub-Saharan Africa (−25%). Projected gains emerge in Western Europe (+28%) and Northern China (+3%) (Figures 2F and S14).

Impacts on Global Yields

We aggregate losses of yields globally, based on the current distribution of global croplands, accounting for the benefits and costs of measured adaptations (Figure 3A). For all crops except rice, we estimate that warming will likely reduce global yields in these regions by 2050 (probability of loss $>$ 0.704 [sorghum] to 0.729 [maize]) after accounting for both statistical and climate model uncertainty. Central estimates for global end-of-century (EOC) losses under the high/moderate emissions scenarios (RCP8.5/RCP4.5) are $-26.1\%/-9.8\%$ ($p < 0.269/0.332$) for maize, $-1.3\%/-0.9\%$ ($p < 0.522/0.509$) for rice, $-36.8\%/-17.8\%$ ($p < 0.169/0.253$) for soy, $-33.5/-12.1\%$ ($p < 0.231/0.297$) for cassava, $-20.4\%/-7.1\%$ ($p < 0.340/0.422$) for sorghum, and $-28.5\%/-12.7\%$ ($p < 0.001/0.085$) for wheat. EOC uncertainty ranges may be substantial, with the largest 90% credible range for rice [q5=-66.3%; q95=177.7%; RCP 8.5) and the narrowest range for wheat [q5=-25.5%; q95=2.0%; RCP 4.5). These ranges allow for moderate likelihood that high emissions impacts on global yields are positive for rice (prob>0.522), maize (prob>0.269), and sorghum (prob>0.340) or more negative than −30% for rice (prob>0.243), maize (prob>0.392), sorghum (prob>0.340), wheat (prob>0.414), soy (prob>0.554), and cassava (prob>0.435).

Impacts by Climate Although the impact of heat on yields is nonlinear and dramatic for many crops (Figures S6 & S7), global aggregate yields are not driven downward most strongly by the hottest regions of the world. Accounting for all patterns of adaptation simultaneously, we find that the 70% of regions with the lowest average temperatures tend to suffer the largest yield losses (Fig 3B). This is due primarily to the fact that hotter locations tend to already be relatively highly adapted to heat, so additional warming has a reduced impact on yields. In addition, high average rainfall rates, prevalent in many hot locations, are linked to increased gains from moderate warming (Figures S6B & S7B). This finding underscores the importance of accounting for real-world patterns of differentiated adaptation in global-scale analyses.

Impacts by Income Our projections suggest that changes in global yields affect populations around the world unequally. We estimate that total calorie production is generally impacted more heavily by climate change in regions that are richer today (Figure 3C), as well as for the lowest income decile, which is heavily affected due to a reliance on cassava. Between the third and top income deciles, we estimate that yield impacts change by -3.2% (95% CI = -3.36% – -2.95%, $p < 0.001$) per decile on average. This result is partially driven by lower income populations tending to live in hotter climates, where current baseline rates of adaptation are higher and, in the tropics, where high average precipitation reduce impacts of warming on yields (Figure 3B). This result has important implications for global damages, since high income regions tend also to be more productive today, and include many of the world's breadbaskets. Because yield losses are greatest (in relative terms) in regions where modern production is concentrated, they have an amplified influence on global production of calories under climate change.

Global Calorie Production We combine our projections across all six crops to estimate the total potential impact of warming on global production of calories (*61*) (see Appendices A.2 and J). Following the approach in refs (*40*, *41*, *58*), we index lost calorie production against $\Delta GMST$ expressed in each climate model simulation. We thereby recover a *damage function* describing the joint distribution of $\Delta GMST$ and lost calorie production for these six staple crops in each five-year moving window of the 21st century (Figure 3C). We estimate that the magnitude of impacts to current croplands increase nearly linearly at a rate of -5.78×10^{14} kcal (p< 0.001, 95% credible interval -5.88–-5.69×10^{14} kcal) of calorie production per +1∘C in GMST in 2100 (see Appendix J for other decades), amounting to ~ -126 kCal/day/1°C per person based on the 2100 global population projections in SSP3, or 4.6% of current per capita consumption per 1°C. (For example, warming of 4°C in GMST in 2100 would correspond to an estimated calorie loss of $\sim$ 18.4% of current per capita consumption.)

The Role of Adaptation and Development In contrast to prior global analyses (*9*, *10*), the projections in this analysis account for rates of adaptation by producers that reflect observed behavior. We find that accounting for adaptation to climate change and changes in producer behavior associated with rising incomes have substantial impact on projections for all crops and regions, accounting for adaptation costs and benefits (Table 1). We estimate that the net influence of adaptive adjustments is to reduce the magnitude of global calorie impacts (relative to a "no adaptation" scenario) by roughly 33% in 2050 (column 1a vs 1b in Table 1) and 47% in 2100 (column 2a vs. 2b), due to the growing extent of adjustment that accompanies greater climatic change. The relative impact of adaptation is largest for rice (96% reduction of impacts in 2100) and smallest for wheat (23% reduction) (Table S10). Regionally, the largest benefits of adaptation accrue to Southeast Asia (94% reduction of impacts in 2100) mostly due to a heavy reliance on rice, while the smallest benefits emerge in North Africa (20% reduction). Our results suggest (i) producer adaptations are likely to have strong influence over the net impact of climate change in agriculture, highlighting the critical importance of accounting for these adaptations; however (ii) our central estimates for the potential overall impact of climate change on production of staples remain negative and meaningful, even once the net effects of adaptation are accounted for. In addition, we note that substantial uncertainty persists in these estimates, originating both from econometric uncertainty and climate model uncertainty, such that overall risks should be assessed across the full range of projected impacts.

Adjustments for CO_2 fertilization Results above do not account for the effects of CO_2 fertilization, which have been challenging to measure empirically (*62*, *63*, *64*, *65*). However, we are able to adjust our results post-estimation to incorporate CO_2 fertilization using estimates from prior studies (*13*) (Appendices I and J). Adjusting for CO_2 fertilization does not qualitatively alter the structure of our findings (Supplementary Figures S17 – S22) but it does reduce the central estimate for overall yield losses by 5.0−9.5% at end of century (Figure 3A) and increases the likelihood of positive aggregate effects. We do not account for the decreased crop nutrient content that might result from CO_2 fertilization (*66*).

Valuing the Impact of Current CO_2 Emissions on Future Crops

Losses to future global yields can be incorporated into present day climate policy. One approach to doing so is to compute the net present value of future economic harms that result from the emission of an additional ton of CO_2, a value known as the Social Cost of Carbon (SCC). We compute a component of the SCC—a "partial SCC"—that results from changes in global yields by integrating these projections into the Data-driven Spatial Climate Impact Model (DSCIM) developed in refs (*40*, *41*) (see Appendices A.2 and J). To do this, we assign country-specific average prices to total calorie production following the approach in ref. (*61*),

allowing producers to intensify/reduce production in order to meet demand in their market at increasing marginal cost (see Appendix J). (In general, aggregate yield losses under climate change harm consumers as caloric consumption is lower and prices are higher; producers are also harmed by production losses, but this harm may be offset by profit gains from higher prices.) In all scenarios, our approach to modeling human adaptation implicitly allows the spatial distribution of varieties within each crop to adjust optimally within currently cropped locations (see Figure S2 and Appendix A.2). In some additional scenarios, we deflate these estimates based on prior estimates for the potential role of crop-switching and international trade (*67*, *68*, *69*, *70*), which might cause the spatial distribution of crop types to shift (see Appendix J).

Across different modeling assumptions, the partial SCC for the six staple crops we study ranges from $0.41 (5% discounting; adjusted for flexible crop switching, movement of cropped land, and international trade; moderately elastic demand and supply, frictionless trade within continents, RCP 4.5) to $11.53 (Ramsey discounting (*71*), crop type and land distributions mirror present day, moderately elastic demand and supply (*61*), frictionless trade within continents, RCP 8.5). See Extended Data Tables S12 & S13 for a complete set of partial SCC estimates.

Discussion

Our analysis of staple crops is the first to measure how much producers adapt to climate around the world and to apply these measurements to projections of global agricultural damages. Our econometric results complement findings from process-based models that resolve the underlying mechanics of crop production but which take producer behavior as exogenous (*9*, *10*, *14*, *21*). Our results indicate a substantial and statistically significant rate at which $\Delta GMST$ reduces the ability of current global food systems to produce calories, net of adaptation. However, in the absence of adaptation, we project that agricultural outcomes would be materially worse.

A key finding is that populations around the world exhibit extensive adaptation to climate already, with some of the most intensive adaptation already occurring in relatively low-income and hot regions of the world – with the exception of the world's poorest who depend heavily on cassava and face higher potential losses. However, we also observe that the breadbaskets of the world, where the climate is moderate and most global production occurs, exhibit more limited baseline adaptation at present. This finding is consistent with earlier detailed analysis of the US indicating that crop systems are optimized for high average yields, not robustness to climatic changes (*33*). Because such a large fraction of global agricultural production is concentrated in these wealthy-but-low-adaption regions, they dominate projections of global calorie production, generating much of the risk to global food security that we document.

Our projection of net declines in overall productivity due to climate change contrasts with process-based

model results that are calibrated to experimental farms, that do not account for observed adaptations, and which generally tend to indicate productivity gains globally. For example, ensemble mean projections of process-based models participating in the AgMIP (*10*) indicate end-of-century productivity gains for maize (+1.3%, RCP8.5), wheat (+9.9%), soy (+15.3%) and rice (+23.3%). These differ substantially from the generally negative impacts we predict, with central estimates that range from -36.8% (soy) to -1.3% (rice) at end of century (Table S10, RCP8.5), although both sets of projections exhibit large uncertainties. We believe that these differences highlight the importance of using globally representative data and accounting for real-world adaptive behaviors in projections of climate change damages.

It is possible that future adaptation of food producers to climate change will differ from the historically observed patterns of adaptation that we recover here. For example, technological breakthroughs in agriculture, such as the industrial fixation of nitrogen (*72*), transformed what is understood about the limit of global productivity. However, the repeatability and penetration of these innovations has been uneven and perhaps should be interpreted cautiously—e.g. synthetic fertilizers remain incompletely deployed despite their invention over a century ago (*73*) and progress towards heat tolerance for some staple crops has stalled (*74*). Nonetheless, to the extent that these advances have been and will be correlated with income, they are implicitly accounted for in our projections. Importantly, though, novel adaptations or policy interventions could maintain staple crop production even in the presence of warming, causing reality to diverge from our projections. Our findings provide a sense of the scale and scope that would be required of such innovations or interventions in order to maintain global food security.

A challenge to this analysis is the limited way in which future resource access has been projected (*75*), i.e. relying on standardized scenarios contained in the SSPs (*44*). Numerous types of resources likely influence how staple crops are managed, however we restricted our analysis to consider only the mediating effects of income and irrigation. We treat income as a proxy measure for access to resources associated with economic development, such as fertilizer or extension services. These variables are intentionally omitted from regression models so that their influence will be captured by the income variable, allowing them to be represented in standard socioeconomic projections where income is projected and available to us, but these other variables are not (*44*). Mediating effects of irrigation are accounted for explicitly because they are influential and irrigation presence is dependant on groundwater geology, local topography, or surface water flows, which are not well-captured by income nor climate measures. An important area for future work is to develop projections of irrigation for use in crop yield projections.

Our monetization of agricultural damages from climate change is limited as it is unlikely to fully capture the human impact of all future changes, such as the potential linkages between climate change, food availability, and social instability (*4*, *5*). Nonetheless, synthesizing the complex global response of agriculture into a

partial SCC is an important step toward representing these damages in climate policies (*76*). Comparison of the partial SCC we compute using DSCIM with existing estimates provides context for these findings. The FUND model (*77*), the only integrated assessment model used in US federal rule-making for which direct comparison is possible, reports a partial SCC for agriculture of $-2.70 per ton CO_2 globally (*78*) using a 3% discount rate (i.e. warming improves global welfare via agriculture, a negative cost). Because this value relies on mainly older (pre-2000) studies for calibration (*79*), Moore et al. (*13*) construct an updated estimate based on a meta-analysis of previous research (*9*), most of which are from process-based models. Inserting these meta-analysis-based projections into a computable general equilibrium model for 16 regions, Moore et al. apply the resulting damage estimates to a modified version of FUND and estimate a partial SCC of $8.50 per ton in net costs, opposite in sign from the original FUND partial SCC. Because this estimate is derived from process-based models it cannot account for observed rates of producer-level adaptation, and it is 3-8× larger than the range of our comparable estimates $1.09-$2.79 (3% discount rate, see Table S12) that do account for autonomous adaptation. In addition, neither set of estimates account for non-staple crops or livestock, an important area for future work, and neither estimate accounts for the unequal impact that crop losses are expected to impose on the global poor (Figure 3C), for whom lost agricultural revenues and/or consumption may be particularly damaging with acute consequences (*3*, *4*, *5*, *80*). In ongoing work (*81*), we are developing techniques to more fairly represent these unequal costs in global estimates of monetized damages.

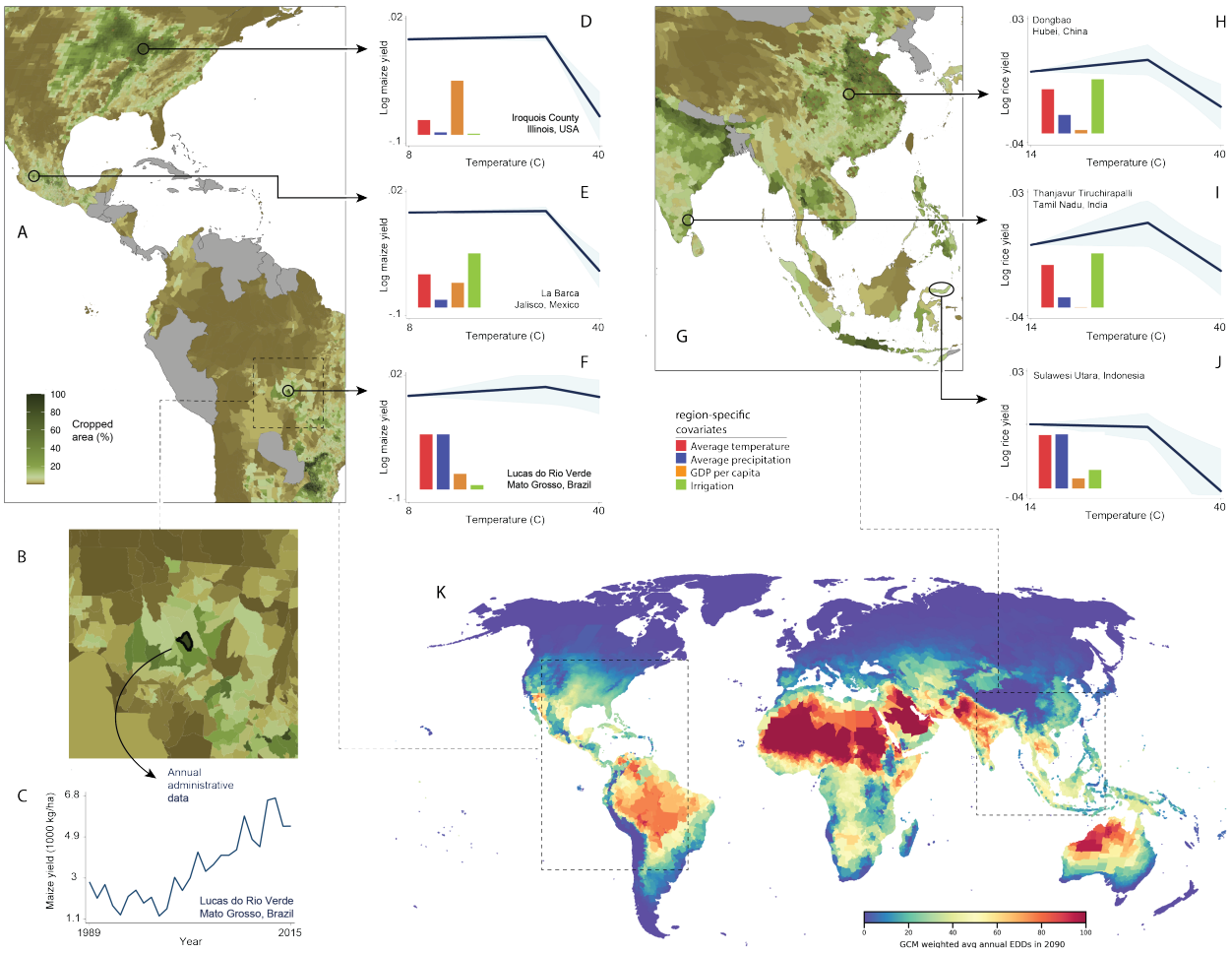


Fig. 1: Global econometric analysis of longitudinal sub-national administrative data enables empirical estimation of crop-specific climate impacts that vary with local economic and environmental conditions. Region- and crop-specific impacts are projected to evolve in the future based on changes to economic conditions (e.g. GDP per capita) and climate (e.g. average temperature), reflecting economic development and adaptation. **(A)** Fraction of cropped area observed in our administrative data in sub-national units, for example regions spanning North, Central, and South America. **(B)** Inset example of regions surrounding Luca do Rio Verde municipality in Mato Grosso state, Brazil. **(C)** Time-series of administrative data describing maize yields from Luca do Rio Verde used in this analysis. **(D)** Empirically estimated relationship between daily temperature and log maize yields (shaded region: 95% CI) in Iroquois County, Illinois, USA, conditional on other factors that include rainfall (see Methods), climate, and access to inputs and technology. Bars indicate county-specific values for variables used to predict the local, county-level effects of temperature and rainfall. **(E)** Same as (D), but for La Barca municipality in Jalisco, Mexico. **(F)** Same as (D), but for Luca do Rio Verde. **(G)** Same as (A), but for an example region of Asia. **(H)** Same as (D), but for the response of rice to daily temperature in Dongbao district in Hubei, China. **(I)** same as (H), but for the cities of Thanjavur and Tiruchirapalli in Tamil Nadu, India. **(J)** Same as (H), but for Sulawesi Utara, Indonesia. **(K)** Expected exceedance degree days (EDDs) over 30C projected for each of 24,378 regions in 2090 in a high emissions scenario (RCP8.5). EDD projections (and other variables) from each model are combined with econometric results, such as (D)-(F) and (H)-(J), to project crop-specific climate impacts that account for adaptation.

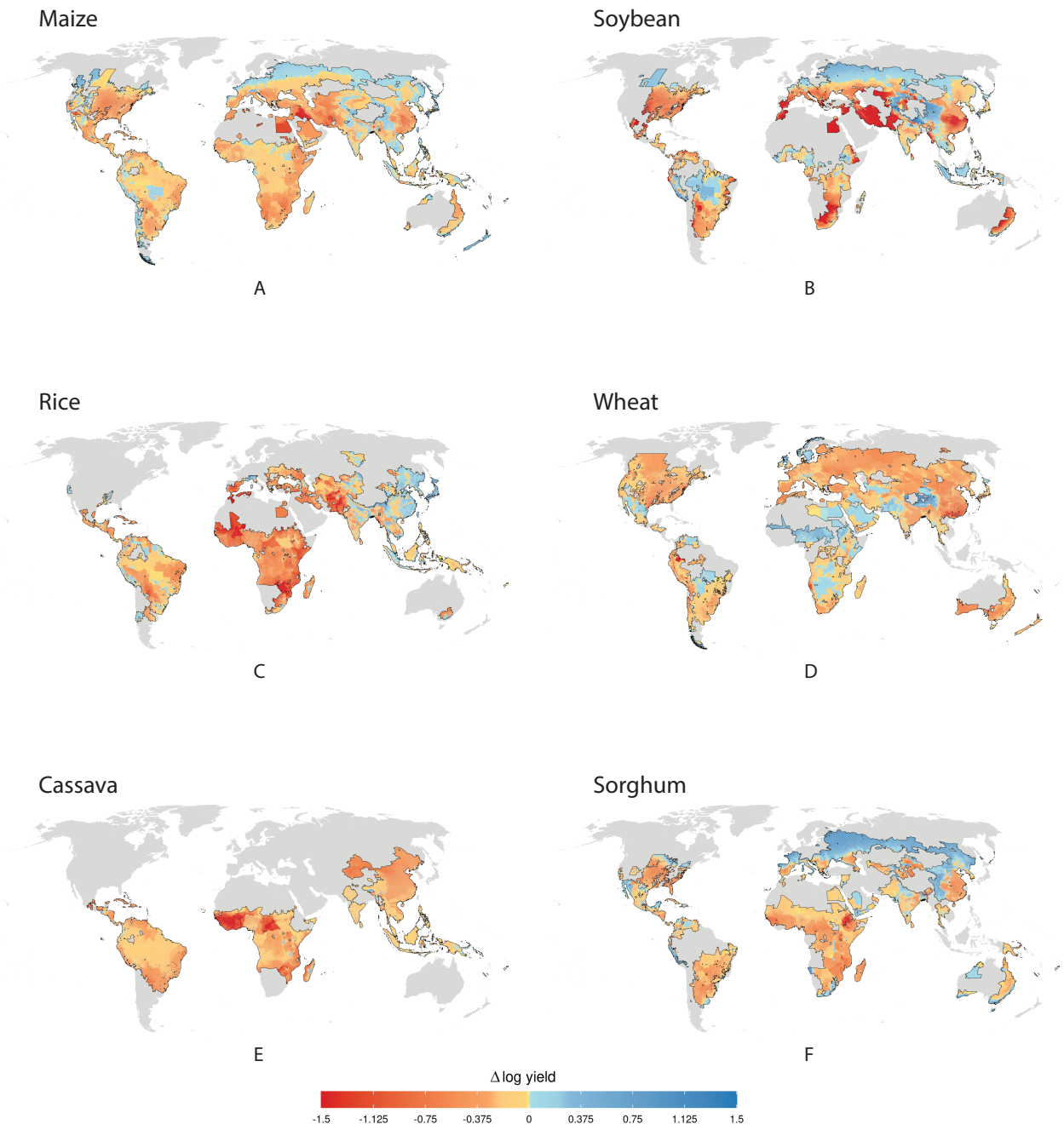


Fig. 2: Projected end-of-century change in log crop yields due to climate change, accounting for adaptation to climate and rising incomes. Colors indicate central estimate in a high emissions (RCP 8.5) scenario, net of adaptation costs and benefits, for **(A)** maize, **(B)** soybean, **(C)** rice, **(D)** wheat, **(E)** cassava, and **(F)** sorghum for 2089 - 2098. Projections computed for 24,378 subnational units, uncropped regions are shaded in grey. Wheat shows winter wheat and spring wheat projections combined, weighted by their area share in each region. Estimates in each location are ensemble means across climate and statistical uncertainty. Incomes from SSP3 (*44*). Results for a moderate emissions scenario (RCP 4.5) shown in Figure S12 and adjusting for CO_2 fertilization in Appendix I.

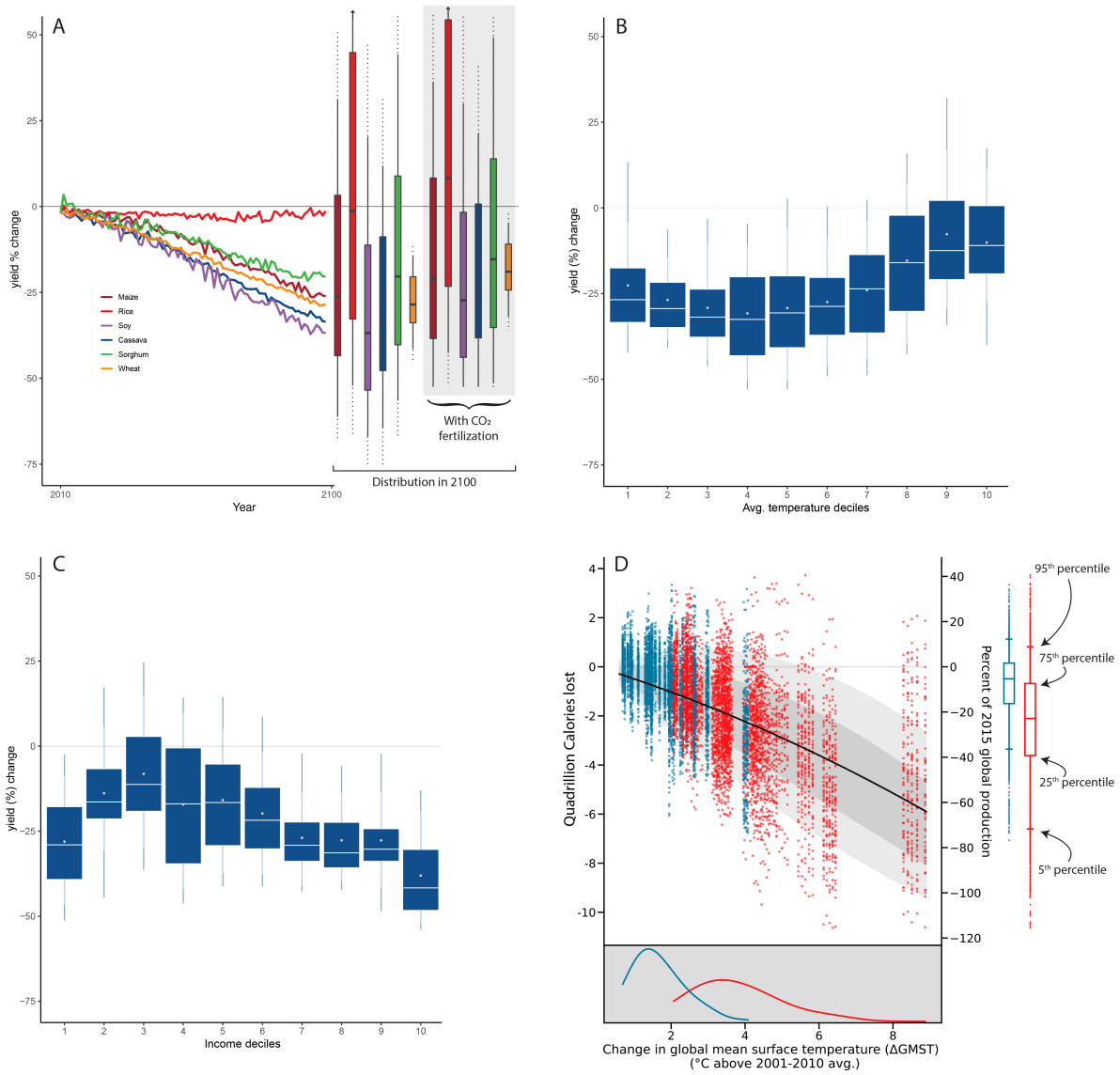


Fig. 3: Global impact of climate change on staple crops. (A) Time series of projected climate change impacts on global average crop yields (area-weighted) in a high emissions (RCP 8.5) scenario, accounting for producer adaptations and adaptation costs. Box and whisker plots show total distribution of end-of-century projections accounting for both statistical uncertainty and climate model uncertainty (boxes=25^{th}-75^{th} percentiles; whiskers=5^{th}-95^{th} percentiles). Projections adjusted for the estimated effect of CO_2 fertilization from ref. (*13*) on right. Results for moderate emissions RCP 4.5 are shown in Figure S13, time series for CO_2 fertilization is in Appendix I. Time series showing uncertainty and decomposing contributions in Figures S8 (RCP 8.5) and S9 (RCP 4.5). **(B)** Projected impacts on yields, by deciles of present-day average temperature in each of 24,378 regions for year 2098 (the last year for which all climate models have downscaled precipitation projections, see Appendix F). Impacts across crops are weighted within region according to their cropped-area and caloric content; distributions across regions are weighted by total cropped area. **(C)** Same as **(B)**, but by decile of present-day income for each of 24,378 regions. **(D)** Empirical end-of-century damage function describing Calories (kCal) lost as a quadratic function of the global mean surface temperature anomaly (ΔGMST). Each point represents a single climate-model-by-Monte-Carlo run for RCP 4.5 (blue) or RCP 8.5 (red) in 2093-2097. Grey bands indicate 10-90 and 25-75 quantile bands, conditional on ΔGMST. Bottom panel shows the distribution of warming under each RCP across 33 climate models and model surrogates (see Appendix F), boxplots to the right show the distribution of damages collapsed by RCP. The right axis describes Calorie losses normalized by 2015 global Calorie production for the six crops studied here.

	2050		2098	
	(1a) Producer behavior unchanged	(1b) Accounting for adaptation & development	(2a) Producer behavior unchanged	(2b) Accounting for adaptation & development
World	**-13.4**	**-9.0**	**-45.0**	**-23.7**
United States	-16.8	-14.3	-64.0	-42.6
Russia	-16.9	-14.4	-43.3	-31.8
North Africa	-19.6	-16.8	-46.8	-37.5
Sub-Saharan Africa	-16.5	-12.2	-44.7	-28.0
Western Europe	-10.1	-9.0	-38.6	-25.2
China	-11.0	-6.1	-41.0	-19.0
South America	-13.9	-7.7	-53.7	-19.0
India	-11.6	-4.4	-31.7	-9.3
Southeast Asia	-9.2	-3.6	-28.4	-1.8

Table 1: Projected percent change in staple crop yields (calories per hectare) due to climate change in a high emission scenario, comparing estimates with and without accounting for adaptation and economic development. Yield changes are expected change in calories produced per unit of cropped area, aggregated across six staple crops based on planted areas. Values indicate estimates in a high emissions (RCP 8.5) scenario for mid-century (columns 1a – 1b), and end-of-century (columns 2a – 2b). For all regions, see Fig. S14. For uncertainty and projections that include estimated CO_2 fertilization effects, see Table S10.

References

[1] C. B. Field and V. R. Barros, *Climate change 2014–Impacts, adaptation and vulnerability: Regional aspects*. Cambridge University Press, 2014.

[2] S. S. Myers, M. R. Smith, S. Guth, C. D. Golden, B. Vaitla, N. D. Mueller, A. D. Dangour, and P. Huybers, "Climate change and global food systems: potential impacts on food security and undernutrition," *Annual review of public health*, vol. 38, no. 1, pp. 259–277, 2017.

[3] R. E. Baker and J. Anttila-Hughes, "Characterizing the contribution of high temperatures to child undernourishment in sub-saharan africa," *Scientific reports*, vol. 10, no. 1, pp. 1–10, 2020.

[4] A. Missirian and W. Schlenker, "Asylum applications respond to temperature fluctuations," *Science*, vol. 358, no. 6370, pp. 1610–1614, 2017.

[5] M. Burke, S. M. Hsiang, and E. Miguel, "Climate and conflict," *Annu. Rev. Econ.*, vol. 7, no. 1, pp. 577–617, 2015.

[6] M. Auffhammer and W. Schlenker, "Empirical studies on agricultural impacts and adaptation," *Energy Economics*, vol. 46, pp. 555–561, 2014.

[7] T. W. Hertel and D. B. Lobell, "Agricultural adaptation to climate change in rich and poor countries: Current modeling practice and potential for empirical contributions," *Energy Economics*, vol. 46, pp. 562–575, 2014.

[8] "Climate change 2013: The physical science basis. contribution of working group i to the fifth assessment report of the intergovernmental panel on climate change," *IPCC*, p. 1535, 2013.

[9] A. J. Challinor, J. Watson, D. B. Lobell, S. Howden, D. Smith, and N. Chhetri, "A meta-analysis of crop yield under climate change and adaptation," *Nature Climate Change*, vol. 4, no. 4, pp. 287–291, 2014.

[10] C. Rosenzweig, J. Elliott, D. Deryng, A. C. Ruane, C. Müller, A. Arneth, K. J. Boote, C. Folberth, M. Glotter, N. Khabarov, *et al.*, "Assessing agricultural risks of climate change in the 21st century in a global gridded crop model intercomparison," *Proceedings of the national academy of sciences*, vol. 111, no. 9, pp. 3268–3273, 2014.

[11] W. Schlenker and M. J. Roberts, "Nonlinear temperature effects indicate severe damages to us crop yields under climate change," *Proceedings of the National Academy of Sciences*, vol. 106, no. 37, pp. 15594–15598, 2009.

[12] R. Mendelsohn, W. D. Nordhaus, and D. Shaw, "The impact of global warming on agriculture: A ricardian analysis," *The American Economic Review*, pp. 753–771, 1994.

[13] F. C. Moore, U. Baldos, T. Hertel, and D. Diaz, "New science of climate change impacts on agriculture implies higher social cost of carbon," *Nature communications*, vol. 8, no. 1, pp. 1–9, 2017.

[14] C. Müller, J. Elliott, D. Kelly, A. Arneth, J. Balkovic, P. Ciais, D. Deryng, C. Folberth, S. Hoek, R. C. Izaurralde, *et al.*, "The global gridded crop model intercomparison phase 1 simulation dataset," *Scientific data*, vol. 6, no. 1, pp. 1–22, 2019.

[15] E. Butler and P. Huybers, "Adaptation of us maize to temperature variations," *Nature Climate Change*, vol. 3, no. 1, pp. 68–72, 2013.

[16] W. Schlenker, M. J. Roberts, and D. B. Lobell, "Us maize adaptability," *Nature Climate Change*, vol. 3, no. 8, pp. 690–691, 2013.

[17] K. S. Mohamed and A. E. Temu, "Access to credit and its effect on the adoption of agricultural technologies: the case of zanzibar," *African Review of Money Finance and Banking*, pp. 45–89, 2008.

[18] D. L. Kelly, C. D. Kolstad, and G. T. Mitchell, "Adjustment costs from environmental change," *Journal of Environmental Economics and management*, vol. 50, no. 3, pp. 468–495, 2005.

[19] M. Mwangi and S. Kariuki, "Factors determining adoption of new agricultural technology by smallholder farmers in developing countries," *Journal of Economics and sustainable development*, vol. 6, no. 5, 2015.

[20] F. Annan and W. Schlenker, "Federal crop insurance and the disincentive to adapt to extreme heat," *American Economic Review*, vol. 105, no. 5, pp. 262–66, 2015.

[21] M. J. Roberts, N. O. Braun, T. R. Sinclair, D. B. Lobell, and W. Schlenker, "Comparing and combining process-based crop models and statistical models with some implications for climate change," *Environmental Research Letters*, vol. 12, no. 9, p. 095010, 2017.

[22] O. Deschênes and M. Greenstone, "The economic impacts of climate change: evidence from agricultural output and random fluctuations in weather," *The American Economic Review*, vol. 97, no. 1, pp. 354–385, 2007.

[23] D. B. Lobell and M. B. Burke, "On the use of statistical models to predict crop yield responses to climate change," *Agricultural and forest meteorology*, vol. 150, no. 11, pp. 1443–1452, 2010.

[24] T. A. Carleton and S. M. Hsiang, "Social and economic impacts of climate," *Science*, vol. 353, no. 6304, p. aad9837, 2016.

[25] D. B. Lobell, G. L. Hammer, G. McLean, C. Messina, M. J. Roberts, and W. Schlenker, "The critical role of extreme heat for maize production in the united states," *Nature climate change*, vol. 3, no. 5, pp. 497–501, 2013.

[26] B. Schauberger, S. Archontoulis, A. Arneth, J. Balkovic, P. Ciais, D. Deryng, J. Elliott, C. Folberth, N. Khabarov, C. Müller, *et al.*, "Consistent negative response of us crops to high temperatures in observations and crop models," *Nature communications*, vol. 8, no. 1, pp. 1–9, 2017.

[27] D. B. Lobell, M. B. Burke, C. Tebaldi, M. D. Mastrandrea, W. P. Falcon, and R. L. Naylor, "Prioritizing climate change adaptation needs for food security in 2030," *Science*, vol. 319, no. 5863, pp. 607–610, 2008.

[28] D. K. Ray, N. Ramankutty, N. D. Mueller, P. C. West, and J. A. Foley, "Recent patterns of crop yield growth and stagnation," *Nature communications*, vol. 3, no. 1, pp. 1–7, 2012.

[29] D. B. Lobell and M. B. Burke, "Why are agricultural impacts of climate change so uncertain? the importance of temperature relative to precipitation," *Environmental Research Letters*, vol. 3, no. 3, p. 034007, 2008.

[30] "Nonlinear heat effects on african maize as evidenced by historical yield trials," *Nature Climate Change*, vol. 1.

[31] W. Dong, J. Chen, L. Wang, Y. Tian, B. Zhang, Y. Lai, Y. Meng, C. Qian, and J. Guo, "Impacts of nighttime post-anthesis warming on rice productivity and grain quality in east china," *The Crop Journal*, vol. 2, no. 1, pp. 63 – 69, 2014.

[32] J. R. Welch, J. R. Vincent, M. Auffhammer, P. F. Moya, A. Dobermann, and D. Dawe, "Rice yields in tropical/subtropical asia exhibit large but opposing sensitivities to minimum and maximum temperatures," *Proceedings of the National Academy of Sciences*, vol. 107, no. 33, pp. 14562–14567, 2010.

[33] D. B. Lobell, M. J. Roberts, W. Schlenker, N. Braun, B. B. Little, R. M. Rejesus, and G. L. Hammer, "Greater sensitivity to drought accompanies maize yield increase in the us midwest," *Science*, vol. 344, no. 6183, pp. 516–519, 2014.

[34] R. Fishman, "More uneven distributions overturn benefits of higher precipitation for crop yields," *Environmental Research Letters*, vol. 11, p. 024004, feb 2016.

[35] M. J. Roberts, W. Schlenker, and J. Eyer, "Agronomic weather measures in econometric models of crop yield with implications for climate change," *American Journal of Agricultural Economics*, vol. 95, no. 2, pp. 236–243, 2013.

[36] D. B. Lobell, W. Schlenker, and J. Costa-Roberts, "Climate trends and global crop production since 1980," *Science*, vol. 333, no. 6042, pp. 616–620, 2011.

[37] M. Burke and K. Emerick, "Adaptation to climate change: Evidence from us agriculture," *American Economic Journal: Economic Policy*, vol. 8, pp. 106–40, August 2016.

[38] S. Hsiang, "Climate econometrics," *Annual Review of Resource Economics*, vol. 8, pp. 43–75, 2016.

[39] S. M. Hsiang and D. Narita, "Adaptation to cyclone risk: Evidence from the global cross-section," *Climate Change Economics*, vol. 3, no. 02, p. 1250011, 2012.

[40] T. Carleton, M. Delgado, M. Greenstone, T. Houser, S. Hsiang, A. Hultgren, A. Jina, R. E. Kopp, K. McCusker, I. Nath, *et al.*, "Valuing the global mortality consequences of climate change accounting for adaptation costs and benefits," *University of Chicago, Becker Friedman Institute for Economics Working Paper No. 2018-51*, 2020.

[41] A. Rode, T. Carleton, M. Delgado, M. Greenstone, T. Houser, S. Hsiang, A. Hultgren, A. Jina, R. E. Kopp, K. McCusker, I. Nath, J. Rising, and J. Yuan, "Estimating a social cost of carbon for global energy consumption," *Nature*, in press.

[42] J. Porter, L. Xie, A. Challinor, K. Cochrane, S. Howden, M. Iqbal, D. Lobell, and M. Travasso, "Food security and food production systems. in: Climate change 2014: Impacts, adaptation, and vulnerability. part a: Global and sectoral aspects. contribution of working group ii to the fifth assessment report of the intergovernmental panel on climate change," *IPCC*, pp. 485–533, 2014.

[43] R. Dellink, J. Chateau, E. Lanzi, and B. Magné, "Long-term economic growth projections in the shared socioeconomic pathways," *Global Environmental Change*, 2015.

[44] K. Riahi, D. P. Van Vuuren, E. Kriegler, J. Edmonds, B. C. O'neill, S. Fujimori, N. Bauer, K. Calvin, R. Dellink, O. Fricko, *et al.*, "The shared socioeconomic pathways and their energy, land use, and greenhouse gas emissions implications: An overview," *Global environmental change*, vol. 42, pp. 153–168, 2017.

[45] M. Auffhammer, V. Ramanathan, and J. R. Vincent, "Climate change, the monsoon, and rice yield in india," *Climatic Change*, vol. 111, no. 33, pp. 411–424, 2012.

[46] V. V. Kharin, F. W. Zwiers, X. Zhang, and M. Wehner, "Changes in temperature and precipitation extremes in the cmip5 ensemble," *Climatic Change*, vol. 119, pp. 345–357, 2013.

[47] Z. Liu, A. Mehran, T. J. Phillips, and A. AghaKouchak, "Seasonal and regional biases in cmip5 precipitation simulations," *Climate Research*, vol. 60, pp. 35–50, 2014.

[48] A. Mehran, A. AghaKouchak, and T. J. Phillips, "Evaluation of cmip5 continental precipitation simulations relative to satellite-based gauge-adjusted observations," *Journal of Geophysical Research: Atmospheres*, vol. 119, no. 4, pp. 1695–1707, 2014.

[49] M. Auffhammer and A. Aroonruengsawat, "Simulating the impacts of climate change, prices and population on california's residential electricity consumption," *Climatic Change*, vol. 109, no. 1, pp. 191–210, 2011.

[50] A. Burns, R. Gleadow, J. Cliff, A. Zacarias, and T. Cavagnaro, "Cassava: the drought, war and famine crop in a changing world," *Sustainability*, vol. 2, no. 11, pp. 3572–3607, 2010.

[51] F. Ellis and H. A. Freeman, "Rural livelihoods and poverty reduction strategies in four african countries," *Journal of development studies*, vol. 40, no. 4, pp. 1–30, 2004.

[52] T. Reardon, K. Stamoulis, and P. Pingali, "Rural nonfarm employment in developing countries in an era of globalization," *Agricultural Economics*, vol. 37, pp. 173–183, 2007.

[53] S. Makokha, S. Kimani, W. Mwangi, H. Verkuijl, and F. Musembi, *Determinants of fertilizer and manure use for maize production in Kiambu District, Kenya*. Cimmyt, 2001.

[54] C. R. Doss and M. L. Morris, "How does gender affect the adoption of agricultural innovations? the case of improved maize technology in ghana," *Agricultural economics*, vol. 25, no. 1, pp. 27–39, 2001.

[55] W. Muzari, W. Gatsi, and S. Muvhunzi, "The impacts of technology adoption on smallholder agricultural productivity in sub-saharan africa: A review," *Journal of Sustainable Development*, vol. 5, no. 8, p. 69, 2012.

[56] I. Crawford and B. De Rock, "Empirical revealed preference," *Annu. Rev. Econ.*, vol. 6, no. 1, pp. 503–524, 2014.

[57] D. J. Rasmussen, M. Meinshausen, and R. E. Kopp, "Probability-weighted ensembles of u.s. county-level climate projections for climate risk analysis," *Journal of Applied Meteorology and Climatology*, vol. 55, no. 10, pp. 2301–2322, 2016.

[58] S. Hsiang, R. Kopp, A. Jina, J. Rising, M. Delgado, S. Mohan, D. Rasmussen, R. Muir-Wood, P. Wilson, M. Oppenheimer, *et al.*, "Estimating economic damage from climate change in the united states," *Science*, vol. 356, no. 6345, pp. 1362–1369, 2017.

[59] J. Schmidhuber and F. N. Tubiello, "Global food security under climate change," *Proceedings of the National Academy of Sciences*, vol. 104, no. 50, pp. 19703–19708, 2007.

[60] I. M. Held and B. J. Soden, "Robust responses of the hydrological cycle to global warming," *Journal of climate*, vol. 19, no. 21, pp. 5686–5699, 2006.

[61] M. J. Roberts and W. Schlenker, "Identifying supply and demand elasticities of agricultural commodities: Implications for the us ethanol mandate," *American Economic Review*, vol. 103, no. 6, pp. 2265–95, 2013.

[62] S. P. Long, E. A. Ainsworth, A. D. Leakey, and P. B. Morgan, "Global food insecurity. treatment of major food crops with elevated carbon dioxide or ozone under large-scale fully open-air conditions suggests recent models may have overestimated future yields," *Philosophical Transactions of the Royal Society B: Biological Sciences*, vol. 360, no. 1463, pp. 2011–2020, 2005.

[63] S. P. Long, E. A. Ainsworth, A. D. Leakey, J. Nösberger, and D. R. Ort, "Food for thought: lower-than-expected crop yield stimulation with rising co2 concentrations," *science*, vol. 312, no. 5782, pp. 1918–1921, 2006.

[64] E. A. Ainsworth, "Rice production in a changing climate: a meta-analysis of responses to elevated carbon dioxide and elevated ozone concentration," *Global change biology*, vol. 14, no. 7, pp. 1642–1650, 2008.

[65] C. A. Taylor and W. Schlenker, "Environmental drivers of agricultural productivity growth: Co2 fertilization of us field crops," tech. rep., National Bureau of Economic Research, 2021.

[66] S. S. Myers, A. Zanobetti, I. Kloog, P. Huybers, A. D. Leakey, A. J. Bloom, E. Carlisle, L. H. Dietterich, G. Fitzgerald, T. Hasegawa, *et al.*, "Increasing co 2 threatens human nutrition," *Nature*, vol. 510, no. 7503, pp. 139–142, 2014.

[67] J. Rising and N. Devineni, "Crop switching reduces agricultural losses from climate change in the united states by half under rcp 8.5," *Nature communications*, vol. 11, no. 1, pp. 1–7, 2020.

[68] A. Costinot, D. Donaldson, and C. Smith, "Evolving comparative advantage and the impact of climate change in agricultural markets: Evidence from 1.7 million fields around the world," *Journal of Political Economy*, vol. 124, no. 1, pp. 205–248, 2016.

[69] U. L. Baldos, T. W. Hertel, and F. C. Moore, "Understanding the spatial distribution of welfare impacts of global warming on agriculture and its drivers," *American Journal of Agricultural Economics*, vol. 101, no. 5, pp. 1455–1472, 2019.

[70] C. Gouel and D. Laborde, "The crucial role of domestic and international market-mediated adaptation to climate change," *Journal of Environmental Economics and Management*, vol. 106, p. 102408, 2021.

[71] National Academies of Sciences, Engineering, and Medicine, *Valuing Climate Damages: Updating Estimation of the Social Cost of Carbon Dioxide*. Washington, DC: The National Academies Press, 2017.

[72] J. N. Galloway, A. M. Leach, A. Bleeker, and J. W. Erisman, "A chronology of human understanding of the nitrogen cycle," *Philosophical Transactions of the Royal Society B: Biological Sciences*, vol. 368, no. 1621, p. 20130120, 2013.

[73] N. D. Mueller, J. S. Gerber, M. Johnston, D. K. Ray, N. Ramankutty, and J. A. Foley, "Closing yield gaps through nutrient and water management," *Nature*, vol. 490, no. 7419, pp. 254–257, 2012.

[74] M. J. Roberts and W. Schlenker, "The evolution of heat tolerance of corn: Implications for climate change," in *The economics of climate change: adaptations past and present*, pp. 225–251, University of Chicago Press, 2011.

[75] S. Hsiang and R. E. Kopp, "An economist's guide to climate change science," *Journal of Economic Perspectives*, vol. 32, no. 4, pp. 3–32, 2018.

[76] T. Carleton and M. Greenstone, "Updating the united states government's social cost of carbon," *University of Chicago, Becker Friedman Institute for Economics Working Paper*, no. 2021-04, 2021.

[77] D. Anthoff and R. Tol, "Fund-climate framework for uncertainty, negotiation and distribution," *Available at www. fund-model. org. Accessed October*, vol. 26, p. 2015, 2014.

[78] D. Diaz, "Evaluating the key drivers of the us government's social cost of carbon: A model diagnostic and inter-comparison study of climate impacts in dice, fund, and page," *FUND, and PAGE (October 3, 2014)*, 2014.

[79] D. Diaz and F. Moore, "Quantifying the economic risks of climate change," *Nature Climate Change*, vol. 7, no. 11, pp. 774–782, 2017.

[80] S. Maccini and D. Yang, "Under the weather: Health, schooling, and economic consequences of early-life rainfall," *American Economic Review*, vol. 99, no. 3, pp. 1006–26, 2009.

[81] I. Nath and et al., "The welfare economics of a data driven social cost of carbon," *Mimeo*, 2021.

[82] S. Heft-Neal, "The non-linear relationship between agricultural productivity and the environment and its effects on human health and the economy," *Dissertation, U.C. Berkeley*, 2015.

[83] N. Gatti, K. Baylis, and B. Crost, "The effects of market access on the market structure in zambia," *Working Paper*, 2020.

[84] J. Sheffield, G. Goteti, and E. F. Wood, "Development of a 50-year high-resolution global dataset of meteorological forcings for land surface modeling," *Journal of Climate*, vol. 19, no. 13, pp. 3088–3111, 2006.

[85] B. Thrasher, E. P. Maurer, C. McKellar, and P. Duffy, "Technical note: Bias correcting climate model simulated daily temperature extremes with quantile mapping," *Hydrology and Earth System Sciences*, vol. 16, no. 9, pp. 3309–3314, 2012.

[86] K. E. Taylor, R. J. Stouffer, and G. A. Meehl, "An overview of cmip5 and the experiment design," *Bulletin of the American Meteorological Society*, vol. 93, no. 4, p. 485, 2012.

[87] K. Riahi, S. Rao, V. Krey, C. Cho, V. Chirkov, G. Fischer, G. Kindermann, N. Nakicenovic, and P. Rafaj, "Rcp 8.5—a scenario of comparatively high greenhouse gas emissions," *Climatic Change*, vol. 109, no. 1-2, pp. 33–57, 2011.

[88] D. P. Van Vuuren, J. Edmonds, M. Kainuma, K. Riahi, A. Thomson, K. Hibbard, G. C. Hurtt, T. Kram, V. Krey, J.-F. Lamarque, *et al.*, "The representative concentration pathways: An overview," *Climatic Change*, vol. 109, no. 1-2, p. 5, 2011.

[89] N. Gennaioli, R. L. Porta, F. L. D. Silanes, and A. Shleifer, "Growth in regions," *Journal of Economic Growth*, vol. 19, pp. 259–309, September 2014.

[90] K. Samir and W. Lutz, "The human core of the shared socioeconomic pathways: Population scenarios by age, sex and level of education for all countries to 2100," *Global Environmental Change*, 2014.

[91] Food and Agriculture Organization, "Aquastat fao's information system on water and agriculture," 1999. data retrieved from FAO AQUASTAT, http://www.fao.org/aquastat/en/.

[92] T. Deryugina and S. Hsiang, "The marginal product of climate," tech. rep., National Bureau of Economic Research, 2017.

[93] D. B. Lobell, W. Schlenker, and J. Costa-Roberts, "Climate trends and global crop production since 1980," *Science*, vol. 333, no. 6042, pp. 616–620, 2011.

[94] N. Ramankutty, A. T. Evan, C. Monfreda, and J. A. Foley, "Farming the planet: 1. geographic distribution of global agricultural lands in the year 2000," *Global Biogeochemical Cycles*, vol. 22, no. 1, 2008.

[95] R. Frisch and F. V. Waugh, "Partial time regressions as compared with individual trends," *Econometrica: Journal of the Econometric Society*, pp. 387–401, 1933.

[96] S. Peng, J. Huang, J. E. Sheehy, R. C. Laza, R. M. Visperas, X. Zhong, G. S. Centeno, G. S. Khush, and K. G. Cassman, "Rice yields decline with higher night temperature from global warming," *Proceedings of the National Academy of Sciences*, vol. 101, no. 27, pp. 9971–9975, 2004.

[97] E. S. Cassidy, P. C. West, J. S. Gerber, and J. A. Foley, "Redefining agricultural yields: from tonnes to people nourished per hectare," *Environmental Research Letters*, vol. 8, no. 3, p. 034015, 2013.

[98] S. Berry and W. Schlenker, "Technical report for the icct: Empirical evidence on crop yield elasticities," *Weather*, pp. 1–18, 2011.

[99] P. T. Scott, "Indirect estimation of yield-price elasticities," *Unpublished manuscript. New York University, New York, USA*, 2013.

[100] T. Hastie, R. Tibshirani, J. H. Friedman, and J. H. Friedman, *The elements of statistical learning: data mining, inference, and prediction*, vol. 2. Springer, 2009.

[101] H. R. Varian, "Big data: New tricks for econometrics," *Journal of Economic Perspectives*, vol. 28, no. 2, pp. 3–28, 2014.

[102] S. Athey, "Beyond prediction: Using big data for policy problems," *Science*, vol. 355, no. 6324, pp. 483–485, 2017.

[103] S. Athey and G. Imbens, "Recursive partitioning for heterogeneous causal effects," *Proceedings of the National Academy of Sciences*, vol. 113, no. 27, pp. 7353–7360, 2016.

[104] S. Athey, "The impact of machine learning on economics," in *The economics of artificial intelligence: An agenda*, pp. 507–547, University of Chicago Press, 2018.

[105] V. Chernozhukov, D. Chetverikov, M. Demirer, E. Duflo, C. Hansen, and W. Newey, "Double/debiased/neyman machine learning of treatment effects," *American Economic Review*, vol. 107, no. 5, pp. 261–65, 2017.

[106] V. Chernozhukov, D. Chetverikov, M. Demirer, E. Duflo, C. Hansen, W. Newey, and J. Robins, "Double/debiased machine learning for treatment and structural parameters," 2018.

[107] V. Chernozhukov, M. Demirer, E. Duflo, and I. Fernandez-Val, "Generic machine learning inference on heterogeneous treatment effects in randomized experiments, with an application to immunization in india," tech. rep., National Bureau of Economic Research, 2018.

[108] R. L. Snyder, "Hand calculating degree days," *Agricultural and forest meteorology*, vol. 35, no. 1-4, pp. 353–358, 1985.

[109] NOAA Defense Meteorological Satellite Program (DMSP), "Nighttime lights," 1995.

[110] R. S. Tol, "On the optimal control of carbon dioxide emissions: an application of fund," *Environmental Modeling & Assessment*, vol. 2, no. 3, pp. 151–163, 1997.

[111] M. Meinshausen, S. J. Smith, K. Calvin, J. S. Daniel, M. L. Kainuma, J.-F. Lamarque, K. Matsumoto, S. A. Montzka, S. C. Raper, K. Riahi, *et al.*, "The rcp greenhouse gas concentrations and their extensions from 1765 to 2300," *Climatic change*, vol. 109, no. 1, pp. 213–241, 2011.

[112] B. D. Wright and J. C. Williams, "The economic role of commodity storage," *The Economic Journal*, vol. 92, no. 367, pp. 596–614, 1982.

[113] Food and Agriculture Organization, "Global agro-ecological zones (gaez) v3: Land & water division, food and agricultural organization of the united nations," 2012. data retrieved from GAEZ data portal, https://gaez.fao.org/.

[114] J. I. Dingel, K. C. Meng, and S. M. Hsiang, "Spatial correlation, trade, and inequality: Evidence from the global climate," tech. rep., National Bureau of Economic Research, 2019.

[115] M. Stevanović, A. Popp, H. Lotze-Campen, J. P. Dietrich, C. Müller, M. Bonsch, C. Schmitz, B. L. Bodirsky, F. Humpenöder, and I. Weindl, "The impact of high-end climate change on agricultural welfare," *Science advances*, vol. 2, no. 8, p. e1501452, 2016.

[116] R. J. Millar, Z. R. Nicholls, P. Friedlingstein, and M. R. Allen, "A modified impulse-response representation of the global near-surface air temperature and atmospheric concentration response to carbon dioxide emissions," *Atmospheric Chemistry and Physics*, vol. 17, no. 11, pp. 7213–7228, 2017.

[117] C. Gollier and J. K. Hammitt, "The long-run discount rate controversy," *Annu. Rev. Resour. Econ.*, vol. 6, no. 1, pp. 273–295, 2014.

[118] S. Berry, "Biofuels policy and the empirical inputs to gtap models," *California Air Resources Board Expert Workgroup Working Paper*, 2011.

[119] P. Scott, "Dynamic discrete choice estimation of agricultural land use," 2014.

Acknowledgements

This project is an output of the Climate Impact Lab consortium that gratefully acknowledges funding from the Carnegie Corporation, Energy Policy Institute of Chicago (EPIC), International Growth Centre, National Science Foundation (#SES1463644), Sloan Foundation, and Tata Center for Development. We thank Laura Alcocer, Thomas Bearpark, Trinetta Chong, Zaya Delgerjargal, Greg Dobbels, Radhika Goyal, Simon Greenhill, Iván Higuera Dylan Hogan, Azhar Hussain, Theodor Kulczycki, Ruixie Li, Maya Norman, Odiche Nwabuikwu, Sebastien Phan, Yuqi Song, Kit Schwarz, Nishka Sharma, Emile Tenezakis, Jingyuan Wang, and Jong-kai Yang for invaluable research assistance during all stages of this project, and we thank Samantha Anderson, Jack Chang, and Megan Landín for excellent project management. We acknowledge the World Climate Research Programme's Working Group on Coupled Modeling, which is responsible for CMIP, and we thank the climate modeling groups (listed in *Appendix* Table S9) for producing and making available their model output. For CMIP, the U.S. Department of Energy's Program for Climate Model Diagnosis and Intercomparison provides coordinating support and led development of software infrastructure in partnership with the Global Organization for Earth System Science Portals. We would like to thank Kathy Baylis and Sam Heft-Neal for generously sharing subnational yield data for this project.

Author contributions AH, TC, MD, MG, SH, TH, AJ, RK, JR, AR conceived of and planned the study. AH, JY, TC, MD, DG, AJ, RK, KMC, AR prepared historical climate data. JY, DG, RK, KMC, AH created and prepared climate projection data. AH, TC, AJ, IN, TM, AR prepared agricultural data. AH, TC, MG, SH, AJ, IN, AR, JR performed cross-validation and estimated yield-climate response functions. AH, SM, JR, TC computed projected impacts of future climate change. IN, AH developed methods for valuation of impacts. AH, IN, TC, MD, DG, MG, SH, AJ, KMC, AR, JR constructed damage functions and computed partial social cost of carbon. AH, SH wrote the main text, AH, SH, AJ, IN, wrote the supplementary materials appendix.

Supplementary Information for:

Estimating Global Impacts to Agriculture from Climate Change Accounting for Adaptation

Andrew Hultgren,[1] Tamma Carleton,[2,3] Michael Delgado,[5] Diana R. Gergel,[5] Michael Greenstone,[1,3] Trevor Houser,[5] Solomon Hsiang,[3,6] Amir Jina,[3,4] Robert E. Kopp,[7] Steven B. Malevich,[5] Kelly E. McCusker,[5] Terin Mayer,[8] Ishan Nath,[1] James Rising,[9] Ashwin Rode,[1] Jiacan Yuan,[10]

[1]Department of Economics, University of Chicago; Chicago, IL, USA
[2]Bren School of Environmental Science and Management, University of California; Santa Barbara, CA, USA
[3]National Bureau of Economic Research; Cambridge, MA, USA
[4]Harris School of Public Policy University of Chicago; Chicago, IL, USA
[5]Rhodium Group; Oakland, CA, USA
[6]Goldman School of Public Policy, University of California; Berkeley, CA, USA
[7]Department of Earth and Planetary Sciences and Institute of Earth, Ocean, and Atmospheric Sciences, Rutgers University; New Brunswick, NJ, USA
[8]Humbert H. Humphrey School of Public Affairs, University of Minnesota; Minneapolis, MN, USA
[9]School of Marine Science and Ocean Policy, University of Delaware; Newark, DE, USA
[10]Fudan University; Shanghai, China

Supplementary Materials Contents

A Materials and Methods Overview SI-1

B Agricultural Data SI-13

C Two-Stage Cross Validation in a Causal Inference Context SI-16

D Econometric Estimation: Crop Specifications SI-22

E Econometric Estimation: Additional Results and Robustness SI-33

F Projections: Approach SI-39

G Accounting for the costs of adaptation SI-45

H Projections: Additional Results and Robustness SI-51

I Projections: Accounting for CO_2 Fertilization SI-61

J Valuation and the Partial Social Cost of Carbon SI-68

A Materials and Methods Overview

This section provides a detailed overview of the data and methods used in the paper to estimate the relation between agricultural yields and variation in weather, accounting for adaptation to climate and economic development.

A.1 Data

Agricultural data. Sub-national yields, production and harvested area, primarily at 2$^{\text{nd}}$-administrative level (ADM2) were collected from the statistical offices of 55 countries (Figure S1 and Table S1). Additional data were generously shared for Burma, Cambodia, Laos, Malaysia, and Thailand (*82*) and Zambia (*83*). This yields a dataset for six crops in 12,658 locations (41,186 location-crop pairs) spanning up to 137 years. Detailed information is provided in Appendix B.

Historical weather data. The main weather dataset used in this analysis is the Global Meteorological Forcing Dataset (GMFD v1) (*84*). Data are available on a 0.25°×0.25° resolution grid from 1948-2010. We obtain daily maximum and minimum temperatures and daily average precipitation for all grid cells globally. These data provide surface temperature and precipitation information using a combination of both observations and reanalysis, based on the NCEP/NCAR reanalysis, which is downscaled and bias-corrected using a number of station-based observational datasets to remove biases in monthly temperature and precipitation.

Projected weather data. We use the NASA Earth Exchange (NEX) Global Daily Downscaled Projections (GDDP) dataset for future projections of climate change. This comprises 21 climate projections, which are downscaled to 0.25°×0.25° resolution (*85*) from global climate model (GCM) runs in the Coupled Model Intercomparison Project Phase 5 (CMIP5) archive (*86*). NEX-GDDP uses GMFD (*84*) to adjust the GCM outputs in historical and in future time periods so that the systemic bias of the GCMs is removed. Climate is projected under emissions from Representative Concentration Pathways 4.5 and 8.5 (RCP4.5 and RCP8.5) up to 2100(*87*, *88*), though some models' NEX-GDDP outputs lack precipitation data past 2098 so that "end-of-century" in this paper is the year 2098. The CMIP5 ensemble of GCMs described above is not a systematic sample of possible futures. Therefore, to provide an ensemble of climate projections with a probability distribution of global mean surface temperature (GMST) responses consistent with that estimated by a probabilistic simple climate model, we use the method outlined in (*57*) to assign probabilistic weights to climate projections. A full list of models and their weights is given in Table S9. For a more complete description, see ref. (*40*).

Historical income data. We obtain national and sub-national income data for 1,503 administrative regions from 83 countries from ref. (*89*). Data are provided by (*89*) at the first administrative subdivision for each country (i.e., ADM1). We use these subnational data to allocate national GDP data from the Penn

World Tables (PWT),[2] under the assumption that the within-country distributions of GDP recorded in (*89*) are accurate, but the exact levels may not be. Using these data we contruct a consistent panel dataset of subnational incomes for all areas in our crop dataset that sum to national GDP from PWT for all countries in the sample.

Projected income data. Future projections of national incomes are derived from the Organization for Economic Co-operation and Development (OECD) Env-Growth model (*43*) and the International Institute for Applied Systems Analysis (IIASA) GDP model (*90*), as part of the "socioeconomic conditions" of the Shared Socioeconomic Pathways (SSPs). These are the only models which provide GDP per capita projections for a wide range of countries in the SSP database. The SSPs propose a set of plausible scenarios of socioeconomic development over the 21st century in the absence of climate impacts and policy. Data are interpolated to annual frequency and downscaled following (*40*).

Irrigation data. We obtain data on the area equipped for irrigation from FAO Aquastat(*91*). These data are a single cross-section centered around the year 2000 at $0.08^\circ \times 0.08^\circ$ resolution, and we hold the values fixed in climate projections. (Increases in incomes and extreme heat exposure may drive increases in future irrigation while aquifer and reservoir draw-down may drive decreases in future irrigation.)

A.2 Methods

We develop a reduced-form approach to modeling crop yields and producer adaptation, allowing us to recover plausibly causal effects of weather on yields based on data from real-world farms, without having to observe all of the biophysical processes in a given crop that mediate these effects. The approach allows us to account for the total costs and benefits of numerous real-world adaptive adjustments producers undertake, without requiring that we observe or model each adjustment explicitly. This approach builds on ideas and techniques developed in refs. (*15*, *16*, *39*, *92*), adopting the method for capturing the benefits of adaptation in ref. (*41*) and accounting for its costs based on the revealed preference approach in ref. (*40*).

In the empirical portion of this analysis, we apply cross-validation techniques common in machine learning, but adapted to our particular case, i.e., model selection in a causal inference context. Our cross-validation approach has three stages: (i) we remove variation in outcomes that is associated with non-parametric controls that condition out the influence of unobservables, (ii) we apply cross-validation to this residualized data to select weather measures, and (iii) we apply cross-validation a second time, modifying the model chosen in the previous step to select dimensions of climate that matter for adaptation. We perform the sequence (i)-(iii) for each of the six crops separately in order to identify the most suitable model for each crop. (In this section below, we use maize as an example and provide detailed model specifications for each of the other crops in Appendix D.) Having selected and fit an empirical model that accounts for adaptation and weather, we then apply the model in projections of climate change impacts. Each of these steps is detailed below.

[2]Penn World Tables (PWT) database: https://www.rug.nl/ggdc/productivity/pwt/.

Accounting for adaptation: Strategy Conceptually, our approach accounts for two pathways through which climate change will affect agricultural outcomes. First, climate change will alter what weather occurs at each location, and this change in weather will have a direct effect on crops through biophysical processes. Second, producers will adjust to changes in the climate, which will alter their yields and how crops respond to weather. The relative reduction in losses to due to these changes are adaptations. For example, an unexpected heat wave may harm crop yields for all producers (a direct effect). But in a typically cool location, the impact may be more damaging to maize yields than a physically similar heat wave experienced in a hotter location would be—since in hotter locations heat waves happen more routinely and producers are likely to select more heat- and drought-tolerant varietals of maize when planting. Global process-based crop models capture many of the former direct effects of climate change, but they lack data to realistically model how a resource-constrained producer would make the latter adaptive adjustments (*9*, *10*, *13*).

Heuristically, if the function $weather(climate)$ describes how weather changes with the climate and the function $adaptation(climate)$ describes how producers adjust their behavior in response to the climate, then a highly simplified model of yields would be an indirect function of *climate* via these two pathways:

$$yield = yield(weather(climate), adaptation(climate)). \tag{A.1}$$

A general formulation is discussed in detail in refs (*24*, *38*). If the climate were to change, we would be interested in the total change in yields that results from the change in climate, i.e. the derivative of yields with respect to climate, accounting for both pathways. The total derivative of this simple yield model would be

$$\frac{\mathrm{d}\, yield}{\mathrm{d}\, climate} = \underbrace{\frac{\partial\, yield}{\partial\, weather}}_{\text{direct effects } (\beta)} \times \frac{\partial\, weather}{\partial\, climate} + \frac{\partial\, yield}{\partial\, adaptation} \times \underbrace{\frac{\partial\, adaptation}{\partial\, climate}}_{\text{farmer adjustments}} . \tag{A.2}$$

Prior process-based modeling captured the direct effects in the first term, and sometimes also contains a mechanistic model for how ideal adaptations (based on test fields) would affect yields (*9*)–described by the factor $\frac{\partial\, yield}{\partial\, adaptation}$. However, these models are unable to measure the extent to which large numbers of producers around the world actually adapt, since such idealized adaptations on the scientifically-managed farms used for calibration are unlikely to be representative of behavior around the world, particularly in resource-constrained settings. Thus the second term, specifically the factor $\frac{\partial\, adaptation}{\partial\, climate}$ describing the extent of producer adjustment, is unknown and unaccounted for in prior global models (*9*, *10*). Conceptually, our approach aims to recover analogs for both the first and second terms empirically from global data, although the equation we actually estimate is substantially more complex.

Eq. A.2 illustrates how accounting for adaptation may be important for estimating the effect of small changes in climate on crop yields, yet accounting for adaptation may be even more important when estimating the effect of large changes in climate. The first term in Eq. A.2, denoted slope β, describes a relationship between yields and weather that is locally linear (i.e. it is a slope evaluated at a point on the surface of the function $yield(\cdot)$). However, yields may be nonlinear functions of weather (*11*) and producer adaptations may interact with climate, causing the slope in Eq. A.2 to itself change as a function of both climate and

adaptations. For example, the effect of one degree warming of daily temperature on yields may be positive in a cold climate but negative in a hot one. Likewise, negative effects of one degree of warming on yields may be larger if a producer does not adapt compared to if they do adapt. Allowing for these possibilities requires that the slope β is not constant, but rather varies as a function of of climate and adaptation.

$$\frac{\partial\, yield}{\partial\, weather} = \beta(climate, adaptation) \tag{A.3}$$

Accounting for the structure of $\beta(\cdot)$ becomes increasingly important as one considers larger changes in climate, since a change in $\beta(\cdot)$ will cause projections of yields to diverge from a linear extrapolation of a local derivative measured in the current climate with current levels of adaptation.

We would, in principle, like to estimate the slope of the yield-weather relation β as a function of adaptation, but this cannot be done explicitly since we do not observe adaptation directly. As noted in the main text, attempting to account for all possible dimensions of adaptation explicitly is likely infeasible, since there exist a vast number of potential adjustments that producers might make as the climate changes. To circumvent this issue, we do not attempt to measure and account for adaptation explicitly but instead do so implicitly. Specifically, we do not estimate how $\beta(\cdot)$ changes as a function of *adaptation* directly, but instead we estimate how it changes as a function of those factors that determine *adaptation*. In this heuristic example, we assumed *adaptation* was a function of *climate*. Thus we can circumvent the challenge of observing *adaptation* by estimating $\beta(\cdot)$ as a function of *climate* only

$$\frac{\partial\, yield}{\partial\, weather} = \beta(climate, adaptation(climate)) = \tilde{\beta}(climate) \tag{A.4}$$

which is far simpler to implement because *climate* can be observed. Here, $\tilde{\beta}$ denotes the same slope, but written as a function that does not contain *adaptation* as an argument. Thus, in this example, allowing the slope of the yield-weather relation to be a flexible function of climate at every point would implicitly account for the effects of *adaptation* on yields. This can be seen by differentiating Eq. A.4 with respect to climate.

Note that in the heuristic example above, we assume *adaptation* is only a function of *climate*, but in our actual implementation we allow for *adaptation* to be determined by other factors as well, including income and access to irrigation, and *climate* is allowed to be multi-dimensional. Furthermore, there are many dimensions of *weather* to account for in each crop model. Thus, fully accounting for adaptation requires that, for each crop, we estimate the structure of a highly nonlinear yield-weather surface in which the response to each dimension of weather (e.g. growing degree days, nighttime temperature, seasonal precipitation) is allowed to interact with each potential mediator of adaptation (e.g. average temperature, average precipitation, average temperature times average precipitation, income, irrigation access). Heuristically, we are

estimating

$$\frac{\partial\, yield}{\partial\, weather_1} = \tilde{\beta}_1(climate_1, climate_2, ..., income, irrigation)$$
$$\frac{\partial\, yield}{\partial\, weather_2} = \tilde{\beta}_2(climate_1, climate_2, ..., income, irrigation)$$
$$\frac{\partial\, yield}{\partial\, weather_3} = ...$$

where $weather_i$ describes the ith dimension of weather and $climate_j$ describes the jth dimension of climate. Figure S2 depicts the interacting relations between each measure of $weather_i$ (down the rows) and each measure of $climate_j$ and other factors that mediate adaptation (across the columns). All of these interacted elements are accounted for simultaneously in a single model.

This reduced-form approach captures the benefits of adaptation by conditioning the yield-weather relationship on multiple dimensions of climate (in addition to other factors that influence adaptation). We account for the unobserved costs of these implicit adaptations using the revealed-preference approach developed in ref. (*40*) and detailed in Appendix G. The intuition of this cost calculation is that observing patterns of adaptations that are or are not undertaken is informative of their costs: if a producer chooses to adapt voluntarily, they will do so because they expect it to be beneficial on net, such that the benefits outweigh the costs (this included non-monetary costs). If we observe that producers do not adopt an adaptation strategy initially, but after a change in the climate they do, then we can infer that the costs out-weighted the benefits in the initial climate but not so after the change. Because we can compute benefits of this adjustment (since we know the climate in both states), it allows us to place a bound on the what the costs of the adaptation strategy must be. We estimate the structure of these costs, as a function of the climate, and track them over the course of our projections following the approach in (*40*).

Accounting for multi-dimensional adaptation in a reduced form yield model As discussed heuristically above, we employ a reduced-form approach to modeling crop yields and producer adaptation, allowing us to recover the effect of climate change on yields – accounting for producer adaptation in observable data – without having to observe the full range of biophysical processes or the set of constrained producer decisions that mediate this effect. Here we formalize the setup. Additionally, we note that while a large number of non-climate factors also influence crop yields around the world, our reduced form approach non-parametrically accounts for factors unique to each location (e.g. soil quality), as well as those that trend over time within each location (e.g. technology diffusion), without modeling either explicitly.

Formally, yields y may be affected by a vector of exogenous weather variables $\mathbf{w} = [w_1, ..., w_K]$, whose effect on yields is mediated through a vector $\mathbf{x} = [x_1, ..., x_N]$ of biophysical variables (e.g. stomatal control of transpiration). The biophysical effects of weather may be mediated by the numerous possible adaptive actions $\mathbf{b} = [b_1, ..., b_M]$ of producers, who may have forward-looking beliefs about their local growing season climate and thus may be more or less prepared for the weather crops will experience. Thus, a producer's set of adaptation actions are chosen based on the producer's climate (which they can observe) and also whether

they possess the resources necessary to adapt (e.g. local incomes, which may reflect access to alternative varietals, inputs like fertilizer, or mechanization). Finally, yields may also be affected by a wide range of potentially confounding factors $\mathbf{s} = [s_1, ..., s_L]$ generally unrelated to weather (e.g. soil chemistry). Let $f(\cdot)$ be a function describing the interplay of biophysical processes conditional on weather and producer actions that generates growing season yields:

$$\begin{aligned} y &= f(\mathbf{x}(\mathbf{w}, \mathbf{b}), \mathbf{s}) \\ &= f(x_1(w_1, ..., w_K, b_1, ..., b_M), ..., x_N(w_1, ..., w_K, b_1, ..., b_M), s_1, ..., s_L), \end{aligned} \tag{A.5}$$

where the mth adaptation action b_m is itself a function of expectations over the weather (local climate) and access to resources for adaptation (summarized by local incomes and access to irrigation):

$$b_m = g_m(\text{Climate, Income, Irrigation}), \text{ for } m = 1, ..., M. \tag{A.6}$$

Process-based models (*9*, *10*) explicitly model the components of $\mathbf{x}$, with each $x_n(\cdot)$ as a modeler-specified function of weather parameters, calibrated to specific field locations, and some modeler defined producer adaptive actions. These models can then simulate future yields, given their specifications of biophysical processes and producer actions. However, a key challenge of this approach is that plants and humans are complex, making it difficult to fully specify $f(\cdot)$. It is difficult to model all biological processes $\mathbf{x}$, the interplays between them, and the often suboptimal (from the perspective of yields) actions taken by resource-constrained and profit-maximizing producers found in diverse socioeconomic contexts.

Rather than attempting the difficult task of explicitly modeling $f(\cdot)$, we instead note that we would like to simply differentiate the surface it describes, i.e. differentiate Eq. A.5, with respect to the k^{th} weather element w_k:

$$\left.\frac{\partial y}{\partial w_k}\right|_{\mathbf{b}} = \sum_{j=1}^{N} \frac{\partial y}{\partial x_n} \left.\frac{\partial x_n}{\partial w_k}\right|_{\mathbf{b}} \tag{A.7}$$

where $\partial y/\partial w_k\big|_{\mathbf{b}}$ describes the "reduced form" effect of weather parameter w_k on yields y conditional on adaptive actions $\mathbf{b}$, as mediated through all relevant biophysical processes $(x_1, ..., x_N)$ without having to explicitly model each such process. Prior econometric research (e.g. *11*, *93*) estimated an average value for $\partial y/\partial w_k$ without attempting to condition on $\mathbf{b}$, an approach that integrates over the existing distribution of adaptive behaviors without explicitly modeling them (*6*). Such an approach is useful for understanding average effects of weather today—and is powerful in its simplicity—but it is not able to project future scenarios in which the distribution of adaptive behaviors by producers changes. Prior process-based modeling research that considers adaptations prescribes how some elements of $\mathbf{b}$ enter their models of $x_n(\mathbf{w}, \mathbf{b})$ and evolve in the future (*9*, *10*, *13*), although as discussed above these changes in $\mathbf{b}$ are assumed to maximize yields and do not necessarily reflect realistic producer behavior.

Like Equation A.3, Equation A.7 is not directly empirically tractable because the full vector of adaptations $\mathbf{b}$ are not observable. However, similar to how the effect of climate-driven adaptation could be captured

without explicit observation of adaptation in Equation A.4, the effect of climate-driven changes in $\mathbf{b}$ can be captured without observing them explicitly. We are interested in the effect that climate-driven *changes* in $\mathbf{b}$ have on *changes* to $\frac{\partial y}{\partial w_k}$. Denote the local climate as vector $\mathbf{C} \equiv (\bar{T}, \bar{P}, \bar{T} \times \bar{T})$. As described in the main text, in our implementation, we allow the vector $\mathbf{C}$ to contain the average temperature of a location ($\bar{T}$), the average precipitation ($\bar{P}$) and their product. Then the effect of climate-driven adaptations on $\frac{\partial y}{\partial w_k}$ can be computed using a definite integral:

$$\begin{aligned} \left.\frac{\partial y}{\partial w_k}\right|_{\mathbf{b}(C_2)} - \left.\frac{\partial y}{\partial w_k}\right|_{\mathbf{b}(C_1)} &= \int_{C_1}^{C_2} \sum_{m=1}^{M} \frac{\partial^2 y}{\partial w_k \partial b_m} \frac{\partial b_m}{\partial \mathbf{C}} d\mathbf{C} \\ &= \int_{C_1}^{C_2} \frac{\partial^2 y}{\partial w_k \partial \mathbf{C}} d\mathbf{C} \end{aligned} \tag{A.8}$$

for an arbitrary transition from some initial climate C_1 to a final climate C_2. This expression says that the change in the effect of weather on yields due to adaptations to a change in climate can be computed by integrating the effect that each possible adaptive action has for each incremental change in climate between C_1 and C_2. The benefit of Equation A.8 is that all dimensions of adaptation are made implicit, alleviating the need to track them individually and explicitly, but they are nonetheless accounted for. This is analogous to Equation A.4, which made the effect of adaptation on slope coefficients implicit by noting that it is driven by climate. In our analysis, we aim to empirically estimate $\frac{\partial^2 y}{\partial w_k \partial \mathbf{C}}$ for many dimensions of weather and climate, so that adaptive responses to climate change can be accounted for in our empirical model of the effect of weather on yields.

In addition, as pointed out in Equation A.6, adaptation may also be a function of resources, denoted here by local income I and irrigation access R.[3] We therefore also simultaneously estimate how these factors alter the yield-weather response $\frac{\partial y}{\partial w_k}$

$$\frac{\partial^2 y}{\partial w_k \partial I} = \sum_{n=1}^{N} \frac{\partial y}{\partial x_n} \sum_{m=1}^{M} \frac{\partial^2 x_n}{\partial w_k \partial b_m} \frac{\partial b_m}{\partial I} \tag{A.9}$$

$$\frac{\partial^2 y}{\partial w_k \partial R} = \sum_{n=1}^{N} \frac{\partial y}{\partial x_n} \sum_{m=1}^{M} \frac{\partial^2 x_n}{\partial w_k \partial b_m} \frac{\partial b_m}{\partial R} \tag{A.10}$$

which captures the overall effect of each variable through each possible adaptive action b_m and its influence on each biophysical pathway x_n.

In practice, we estimate $\frac{\partial^2 y}{\partial w_k \partial \mathbf{C}}$, $\frac{\partial^2 y}{\partial w_k \partial I}$ and $\frac{\partial^2 y}{\partial w_k \partial R}$ simultaneously in an empirical model where the baseline effects of weather are also estimated. This is achieved by specifying nonlinear interactions between measures of weather (selected via cross-validation) and up to five key summary statistics informing producer

[3] Theoretically, other types of non-income resources could be accounted for explicitly (e.g. market access), but we restrict our analysis to focus on income because 1) socioeconomic structures correlated with global incomes (e.g. roads, institutions) will be captured by income, and 2) income is the only variable for which standard projections are available, via the Shared Socioeconomic Pathways (*40*). Irrigation is accounted for explicitly because competing forces make the sign of its future adoption uncertain: adaptation and income growth could drive increased access to irrigation, but groundwater and water-cycle constraints could drive reduced access to irrigation. We thus hold future irrigation fixed at location-specific present-day levels, as a conservative approach.

adaptive decisions: local measures of long-run average temperature, long-run average precipitation, their interaction, income, and access to irrigation (details in Appendix D). These local summary statistics capture the range of ways in which producer adaptive actions in response to expectations over climate, socioeconomic conditions, and irrigation affect the responsiveness of crop yields to weather.

Our reduced-form econometric approach thus seeks to measure the effect of weather distributions on yields, net of adaptive adjustments and other actions related to development. Our empirical strategy is designed to achieve this by exploiting exogenous variation in w_k conditional on local climate, income, and irrigation, without explicitly observing or modeling the full set of biophysical processes $(x_1, ..., x_N)$, the full set of adaptive actions $(b_1, ..., b_M)$, nor the full set of non-weather processes $(s_1, ..., s_L)$.

Construction of weather terms (w_k). A large number of candidate weather variables are constructed from raw weather data based on previous literature (*11*, *32*, *34*, *35*, *36*). We assemble variables that prior analyses report were influential for at least one crop, although individual variables might not ultimately be included in the specification for all or any crops. *Degree day* terms were constructed following (*11*), with kink points selected for each crop by a 10-fold cross validation search over potential kinks. *Growing-season-phase precipitation* was summed within month by grid cell, and then transformed (*36*). Construction of *vapor pressure deficit* followed ref. (*35*). The *count of rain days* was calculated by grid cell as days with positive precipitation (*34*). *Extreme rain* was identified by constructing the 1980-2010 rainfall distribution for each grid cell in the GMFD daily precipitation data, and aggregating the amount of rainfall or number of days of rainfall in excess of the 95^{th} percentile of this distribution (*34*). *Count of extreme rain days* was measured following *extreme rain* except grid cell-days were counted instead of summed within grid cell.(*34*) *Drought* was defined using a 10-fold cross validation search over percentile cutoffs in the administrative-unit growing season total precipitation distribution, largely following (*45*). *Minimum temperatures* were calculated as the average of daily grid cell minimum temperatures within each month, following following (*45*). For all weather terms, weighting and aggregation to administrative units were done as described in (*40*) with cropped area weights from ref. (*94*). See Appendix D for full details on the construction of each weather variable.

Cross-validation Step Zero: Residualizing data for causal inference. Cross-validation is typically applied in prediction problems where causal inference is not the primary interest. We adapt the cross-validation procedure in order to apply it to our context, in which causal inference is an objective. To do this, we first select non-parametric controls for unobservable factors (i.e., fixed effects and time trends) so as to isolate plausibly random variation in our set of weather measures (*11*, *22*, *38*). Specifically, we use administrative unit i (typically county) fixed effects $\mu_i^{(\cdot)}$, absorbing time-invariant confounds such as soil quality; country-year fixed effects $\rho_{ct}^{(\cdot)}$, absorbing country-by-year price and trade policy confounds; and state or province quadratic time trends $h_s^{(\cdot)}(t)$, absorbing slow-moving, local confounds such as the diffusion of new technologies or local variation in prices (Eqs. A.11 – A.13). Relying on the Frisch-Waugh-Lovell Theorem for partitioned regression (*95*), we partial-out the variation in outcomes y_{it} on these non-parametric controls:

$$y_{it} = \mu_i^y + h_s^y(t) + \rho_{ct}^y + \tilde{y}_{it} \tag{A.11}$$

We do not select from among these controls in our cross-validation procedure, as we wish to ensure that all of these terms are accounted for in our final model specification, regardless of the outcome of the cross-validation procedure. The objective in this step is to isolate random variation in weather shocks for the purpose of causal inference and not to predict yields via these controls. Next, we partial-out the variation in our vector of regressors $\mathbf{X}_{it}$ that is associated with the same set of nonparametric control variables:

$$\mathbf{X}_{it} = \mu_i^X + h_s^X(t) + \rho_{ct}^X + \tilde{\mathbf{X}}_{it} \tag{A.12}$$

We then use the residual variation $\tilde{y}_{it}$ and $\tilde{\mathbf{X}}_{it}$ in our cross validation procedures, regressing $\tilde{y}_{it}$ on elements of $\tilde{\mathbf{X}}_{it}$. In our specification, y_{it} is log(yields) in administrative unit i and year t, and $\mathbf{X}_{it}$ is the vector of weather measures constructed in the prior step, with potential interactions as described below. Our final specifications differ by crop (Appendix D).

Cross-validation Step One: Selection of Weather Measures. Using the residualized variables $\tilde{y}_{it}$ and $\tilde{\mathbf{X}}_{it}$, we initially implement k-fold cross validation over 10 random folds to systematically evaluate a broad range of weather measures: vapor pressure deficit, degree days, minimum temperature, drought, various non-linearities in growing season precipitation, the count of rainy days, the count of extreme rain days, and the total amount of extreme rain.

When using cross-validation to select weather measures, each model is required to have *at least* one temperature term (i.e., degree days and/or minimum temperature) and one "precipitation" term (i.e., precipitation polynomials, amount of extreme rain, count of extreme rain days, count of rain days, and/or vapor pressure deficit).[4] In this step, weather terms are each interacted with a fixed set of covariates: growing season average daily maximum temperature ("long-run temperature"), growing season average monthly precipitation ("long-run precipitation"), $\log(GDP_{pc})$ ("income"), and the share of cropped area equipped for irrigation ("irrigation"). Holding the set of covariate interactions fixed at this stage ensures that weather variable selection occurs using models that are at least as flexible as those selected after the second cross-validation step, without having to simultaneously explore the full set of potential combinations of weather measures and covariate interactions (which would number 103,904 separate models). In selecting a candidate set of weather terms over which to study adaptation we seek to optimize over parsimony and explanatory power, selecting a high performing model where additional weather terms do not individually contribute substantial fit gains (see Tables S7 and S8).

Not all weather terms can be reliably projected by climate models, and models containing these candidate variables were explored in the cross validation procedure (Figure S4), but ultimately excluded in projections of climate change since they could not be projected with reasonably high confidence.[5]

One exception to this data-driven approach for variable selection occurs in the case of rice. A wide

[4] This model constraint was imposed because temperature and precipitation are known to be correlated, and efforts to account for the causal effects of one without controlling for the other would be vulnerable to systematic bias.(*11*)

[5] As discussed in the main text, we found that growing season drought is the most important factor for predicting cassava yields (24.0% gain in variance predicted, Table S7). Drought is also important for rice yields, as is the count of rain days (6.4% and 8.0% gain in variance predicted, Table S7). The count of rain days is also moderately important for maize yields (6.6% gain in variance predicted, Table S7). Taken together, these results indicate the importance of nuanced projections of future precipitation distributions for a restricted set of global staple crops.

literature on minimum temperature effects on rice yields (*31*, *32*, *45*, *96*) leads us to include t_{min} in our adaptation analysis for rice, even though average out-of-sample R^2 gains from including t_{min} in a degree day model are relatively small (2.9%, Table S8). Spring and winter wheat are estimated with common temperature and precipitation responses for the spring/summer months, and separate fall and winter responses just for winter wheat (spring wheat does not have fall and winter seasons). For complete specifications, see Figure S4 and Section D.

Cross-validation Step Two: Selection of Variables that Mediate Adaptation. In our second cross-validation step we select a set of covariate interactions to model producer adaptation, where covariates reflect the factors that mediate producer adaptation (Eq. A.6). Conditional on the constraints of plant physiology, access to resources, and their understanding of their climate, producers make choices over plant varieties and other adaptive measures. We cannot observe these choices directly, but we infer them through observing changes in the response of crops to weather. For example, if a given location is on average quite hot, producers are likely to chose to plant crop varietals that are more resilient to heat stress, which leads to less observed temperature sensitivity in yields.

In this cross-validation step, we take as given the set of weather parameters selected from the first step. We allow for the previously described interactions between weather variables and income, irrigation, long-run temperature, and long-run precipitation, as well as the product of long-run temperature and long-run precipitation. Further, we allow for the nonlinear precipitation response to vary over phases of the growing season or to be constant over the growing season, with "phases" of the growing season defined by a systematic model search (see Appendix Table S4). Finally, we also allow for interaction terms between degree-day responses and precipitation.

In this step, we again employ k-fold cross validation with 10 folds containing random blocks of data grouped by state/province. Here, the test of model performance is the ability to model yields for a set of states or provinces which are held out of the data. This matches one of the intended uses of our interaction surface, which is to model the heterogeneous response of yields to weather for locations with no yield data available.

In our climate projections, long-run average precipitation ($\bar{P}$) values range over 17 standard deviations outside the mean in our data. To prevent extrapolating adaptation behavior to $\bar{P}$ values far outside of our data, we imposed a single-knot linear spline in $\bar{P}$ for each weather measure ($z_a(\bar{P}_i)$, $z_b(\bar{P}_i)$, and $z_c(\bar{P}_i)$ below). These knots were chosen using a within-R^2 search over knot locations (see Appendix D for details).

Example: Specification for Maize Following our cross validation procedures, the final maize specification is:

$$
\begin{aligned}
y_{it}^{maize} = \\
& DD_{it}^{8-31} \cdot (\beta_1 + \gamma_1 \bar{T}_i + \gamma_2 z_a(\bar{P}_i) + \gamma_3 \bar{T}_i z_a(\bar{P}_i) + \gamma_4 I_i + \gamma_5 R_i) + \\
& DD_{it}^{31+} \cdot (\beta_2 + \gamma_6 \bar{T}_i + \gamma_7 z_b(\bar{P}_i) + \gamma_8 \bar{T}_i z_b(\bar{P}_i) + \gamma_9 I_i + \gamma_{10} R_i) + \\
& prcp_phase1_{it} \cdot (\beta_3 + \gamma_{11} \bar{T}_i + \gamma_{12} z_c(\bar{P}_i) + \gamma_{13} \bar{T}_i z_c(\bar{P}_i) + \gamma_{14} I_i + \gamma_{15} R_i) + \\
& prcp_phase1_{it}^2 \cdot (\beta_4 + \gamma_{16} \bar{T}_i + \gamma_{17} z_c(\bar{P}_i) + \gamma_{18} \bar{T}_i z_c(\bar{P}_i) + \gamma_{19} I_i + \gamma_{20} R_i) + \\
& prcp_phase2_{it} \cdot (\beta_5 + \gamma_{21} \bar{T}_i + \gamma_{22} z_c(\bar{P}_i) + \gamma_{23} \bar{T}_i z_c(\bar{P}_i) + \gamma_{24} I_i + \gamma_{25} R_i) + \\
& prcp_phase2_{it}^2 \cdot (\beta_6 + \gamma_{26} \bar{T}_i + \gamma_{27} z_c(\bar{P}_i) + \gamma_{28} \bar{T}_i z_c(\bar{P}_i) + \gamma_{29} I_i + \gamma_{30} R_i) + \\
& prcp_phase3_{it} \cdot (\beta_7 + \gamma_{31} \bar{T}_i + \gamma_{32} z_c(\bar{P}_i) + \gamma_{33} \bar{T}_i z_c(\bar{P}_i) + \gamma_{34} I_i + \gamma_{35} R_i) + \\
& prcp_phase3_{it}^2 \cdot (\beta_8 + \gamma_{36} \bar{T}_i + \gamma_{37} z_c(\bar{P}_i) + \gamma_{38} \bar{T}_i z_c(\bar{P}_i) + \gamma_{39} I_i + \gamma_{40} R_i) + \\
& \mu_i + h_s(t) + \rho_{ct} + \epsilon_{it} \qquad \text{(A.13)}
\end{aligned}
$$

with

$$
z_a^{maize}(\bar{P}) = \begin{cases} \bar{P} & \text{if } \bar{P} \leq 200\text{mm} \\ 200 & \text{otherwise} \end{cases} \quad z_b^{maize}(\bar{P}) = \begin{cases} \bar{P} & \text{if } \bar{P} \leq 100\text{mm} \\ 100 & \text{otherwise} \end{cases} \quad z_c^{maize}(\bar{P}) = \begin{cases} \bar{P} & \text{if } \bar{P} \leq 250\text{mm} \\ 250 & \text{otherwise} \end{cases}
$$

where y_{it} is log(yields) in administrative unit i in year t, DD_{it}^{8-31} represents degree days from 8C to 31C, which is interacted with each of average growing season daily maximum temperature ($\bar{T}_i$), splines in average growing season total precipitation ($z_{[\cdot]}(\bar{P}_i)$), the interaction between $\bar{T}_i$ and $z_{[\cdot]}(\bar{P}_i)$, average log($GDPpc$) (I_i), and area equipped for irrigation (R_i). The remaining weather terms have similar interactions. $prcp_phase[P]_{it}$ represents monthly precipitation summed within growing-season-phase P, for $P \in 1, 2, 3$. μ_i, $h_s(t)$, and ρ_{ct} are administrative unit i (typically county) fixed effects, absorbing time-invariant confounds such as soil quality; country-year fixed effects, absorbing country-by-year price and trade policy confounds; and state or province quadratic time trends, absorbing slow-moving, local confounds such as the diffusion of new technologies or local variation in prices.

Note that the terms in A.13 reflect rows (weather variables) and columns (mediating variables) illustrated in Figure S2B. See Appendix D for full details of the final model specification for each crop.

The overall fit of our empirical model to the historical data is high, with an R^2 of 0.8453 for maize. For reference, (*11*) report a model R^2 of 0.7654 for maize when focusing on just the Eastern United States, where data quality is high relative to much of the globe.

Projections and the Partial SCC We integrate our econometric results with the Data-driven Spatial Climate Impact Model (DSCIM) (*40*, *41*) to develop projections and partial SCC estimates (Appendix J.5). Calculations were conducted as described in refs. (*40*, *41*), over 24,378 geographically granular regions, 33

climate models, and 1,920 Monte Carlo draws of statistical uncertainty per crop. Following (*40*) we project the impacts of climate change net of adaptation and its costs, relative to a counterfactual in which incomes grow but the climate is held fixed (See Appendix F). Because the context in which we infer adaptation costs differs from ref. (*40*), the theory we employ in our projections is briefly outlined in the Appendix G, where we describe how we derive adaptation costs measured in terms of yields. Figures in the main text show crop-specific projections and aggregate caloric projections in percentage terms. Projections represent weighted averages of log yield estimates, converted to percentage terms. Crop impacts are aggregated over space using area weights (Appendix B), over climate models using SMME weights (Table S9), and over crops using calorie weights (*97*). See Appendix F for full details of the projection methodology.

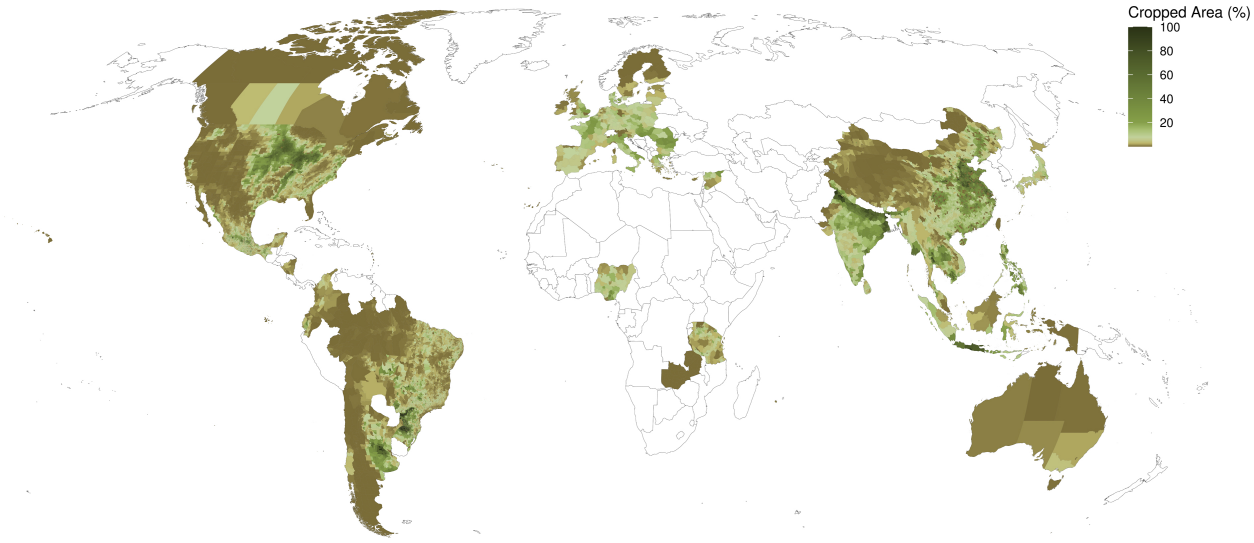
In order to calculate a partial SCC we must value climate-induced changes in yields for both producers and consumers. Our approach to this valuation follows ref. (*61*) and models consumers and producers of calories with constant elasticity of demand and supply, drawing demand and supply elasticities from the literature (*61*, *98*, *99*). We allow for frictionless crop trade within continent but zero trade between continents, and we test sensitivity to this assumption by also exploring frictionless global trade and autarky (i.e., zero trade between countries). We also consider the potential impacts of crop switching, shifting of cropped areas, and international trade by drawing on previous model-based literature that estimates the extent to which these additional margins of adjustment mitigate welfare losses (see Appendix J). In calculating the SCC, we follow (*41*) to calculate results for constant discount rates (2%, 2.5%, 3%, 5%) and (*41*, *76*) for Ramsey discounting ($\rho = 0, \eta = 2$). See Appendix J for full details of the valuation methodology.

One challenge to this analysis is that our measures of climate are cross-sectional in nature, thus correlations between climate and omitted variables that determine the shape of the yield-weather response could potentially bias our estimates of adaptation. If such correlations exist, they might be regional in nature or otherwise only impact limited subsamples of our data. As a partial test of this possibility, we examine non-parametric estimates of the association between climate and temperature sensitivity and find that the associations we rely on are systematic and pervasive throughout the data (Figure S5). This suggests that any unknown omitted variable would have to be consistently correlated with climate throughout all of our sample, from all regions the world, in order to impact our analysis.

In addition, we note that our valuation of agricultural damages from climate change and the partial SCC only accounts for the crops in our sample, which account for a large share of global calories but a smaller share of total agricultural revenues. The present analysis does not include effects of climate change on other sources of agricultural revenue such as livestock, citruses, and other specialty crops. We look to future work to incorporate these output categories.

B Agricultural Data

This section details the agricultural outcome data assembled for this study. Subnational yield data are described in Table S1 and Figure S1 below. Administrative units with low levels of production (less than 100 tons per year on average) were dropped, representing 4.8% of all observations. Weather data range from 1948 – 2010 (Appendix A.1), so yields from those years are used in our analysis. Details of other datasets are given in Appendix A.1 and briefly summarized here. Area equipped for irrigation is from FAO Aquastat, which is cross sectional and fixed in projections (*91*); cropped areas and growing seasons are from SAGE[6] (*94*). Historical and future weather, income, and long-run climate data follow (*40*), with the following exceptions: weather and climate data are cropped area weighted on aggregation (using SAGE "anycrop" area-weights); long-run temperature is calculated as average daily maximum temperature over the growing season; long-run precipitation (not used in (*40*)) is calculated as average total growing season precipitation; average income is calculated for 2$^{\text{nd}}$-administrative division level (ADM2)[7] units whenever yields are available at that resolution.



Supplementary Figure S1: Yield data coverage by subnational administrative unit. Most data are reported at the second administrative level (e.g. county level) or equivalent. Color denotes the average fraction of land area that is cropped in sample. See Appendix Table S1 for detailed descriptions of the data collected for each country.

[6] Occasionally, crop growing seasons in ref. (*94*) for specific crops in specific regions have growing seasons are described as being in excess of one year. We truncate these growing seasons to a single 12-month period, which may span two calendar years.

[7] This is equivalent to counties in the United States.

Country	Adm. Unit[a]	Stats Reported[b]	Crops[c]	# Adm. Units	# Years	N	Source
ARG	adm2	ah, ap, p, y	m, r, s, sm, w	425	47	44,224	source
AUS	adm1	ap, p, y	w	8	137	832	source
AUT	adm2	ah, p, y	m, s, w	9	35	691	source
BEL	adm2	ah, p, y	m, w	11	35	654	source
BGR	adm2	ah, p, y	m, r, s, w	6	10	52	source
BOL	adm1	ah, p, y	c, m, r, s, sm, w	9	30	1,011	source
BRA	adm2	ah, ap, p, y	c, m, r, s, sm, w	5,370	42	566,451	source
CAN	adm1	ah, ap, p, y	m, s, w	9	108	1,473	source
CHL	adm1	ap, p, y	m, r, w	8	34	610	source
CHN	adm2	ap, p, y	m, r, w	2,005	24	111,979	source
COL	adm1	ah, p, y	c, m, r, s, sm, w	32	14	1,634	source
CYP	adm2	ah, p, y	w	1	17	17	source
CZE	adm2	ah, p, y	m, s, w	8	12	247	source
DEU	adm2	ah, p, y	m, w	40	30	649	source
DNK	adm2	ah, p, y	w	5	4	20	source
ECU	adm1	ah, ap, p, y	m, r, s, w	24	14	631	source
ESP	adm2	ah, p, y	m, r, s, w	17	32	1,364	source
EST	adm2	ah, p, y	w	1	15	15	source
FIN	adm2	ah, p, y	w	5	18	73	source
FRA	adm2	ah, p, y	m, r, s, w	25	33	1,732	source
GBR	adm1	ah, p, y	w	11	33	284	source
GRC	adm2	ah, p, y	m, r, w	13	26	590	source
HUN	adm2	ah, p, y	m, r, s, w	7	15	327	source
IDN	adm1	ah, p, y	c, m, r, s	26	23	2,343	source
IND	adm2	ap, p, y	m, r, s, w	302	57	35,467	source
IRL	adm2	ah, p, y	w	2	20	40	source
ITA	adm2	ah, p, y	m, r, s, w	21	33	1,594	source
JPN	adm1	ah, ap, p, y	r	47	33	1,551	source
KHM	adm1	ah, ap, p, y	r	21	21	441	(*82*)
LAO	adm2	ah, ap, p, y	r	143	5	695	(*82*)
LKA	adm1	ah, ap, p, y	r	26	30	1,558	source
LTU	adm2	ah, p, y	m, w	1	19	26	source
LUX	adm2	ah, p, y	m, w	1	32	42	source
LVA	adm2	ah, p, y	w	1	17	19	source
MEX	adm2	ah, ap, p, y	m, w	559	21	45,023	source
MLT	adm2	ah, p, y	w	1	2	2	source
MMR	adm1	ah, ap, p, y	r	14	20	280	(*82*)
MYS	adm1	ap, p, y	r	13	18	233	(*82*)
NGA	adm1	ap, p, y	c, m, r	37	12	1,177	source

NIC	adm1	ah, ap, p, y	m	17	11	356	source
NLD	adm2	ah, p, y	m, w	12	35	583	source
PHL	adm1	ah, p, y	c, m, r	73	29	5,991	source
POL	adm2	ah, p, y	m, s, w	16	13	420	source
PRT	adm2	ah, p, y	m, r, w	7	25	267	source
ROU	adm2	ah, p, y	m, r, s, w	8	15	400	source
SVK	adm2	ah, p, y	m, s, w	4	15	160	source
SVN	adm2	ah, p, y	m, s, w	2	3	13	source
SWE	adm2	ah, p, y	w	6	17	90	source
SYR	adm1	ah, p, y	m, s, w	15	29	966	source
THA	adm1	ah, ap, p, y	r	76	19	1,432	(*82*)
TZA	adm2	ap, p, y	m, r, w	124	8	1,860	source
USA	adm2	ap, p, y	m, r, s, sm, w	2,902	59	399,445	source
VNM	adm1	ap, p, y	c, m, r, s	60	20	5,374	source
ZMB	adm2	ap, p, y	c, m, r, s, sm	72	16	1,871	(*83*)

Supplementary Table S1: Agricultural data used in this analysis. Where both area planted and area harvested data were available, area planted was used to calculate yields to account for situations of complete crop failure. [a]adm1: state/province; adm2: county/municipio. [b]ah: area harvested; ap: area planted; p: production; y: yield. [c]m: maize; s: soybean; r: rice; w: wheat; c: cassava; sm: sorghum.

C Two-Stage Cross Validation in a Causal Inference Context

Appendix A.2 describes our two-step approach to model selection. The primary contribution of this paper is not to advance the field of machine learning; however because we do utilize cross-validation in a causal inference context, it is useful to understand some connections between our approach and some other studies that consider related methodological issues. Thus, this section discusses our approach in the context of the broader literature on machine learning methods and causal inference.

Cross validation is widely used for feature selection in machine learning (ML) models whose goal is to predict an observable outcome (*100*). This type of pure prediction problem is distinct from one in which the goal is causal inference. A growing literature has recognized this distinction (*101*, *102*), while also exploring avenues through which ML can be adapted to a causal inference context (e.g., *103*, *104*, *105*, *106*, *107*).

One branch of this literature (*105*, *106*) studies "double ML" techniques to control for confounds to a treatment of interest when the set of potential confounds is high-dimensional. This is distinct from the context in this paper. The treatment in our context is weather, which is exogenous and stochastic. Thus, we do not require double ML techniques to control for a potentially high-dimensional set of nuisance parameters. Rather, we follow (*11*, *22*) in directly isolating plausibly-exogenous weather shocks for causal identification using a rich set of fixed effects and time trends that non-parametrically control for trending and constant confounds.

A second branch of the literature uses ML techniques to identify heterogeneity in average treatment effects (*103*, *107*), which is closer in spirit to the context of this paper. However, (*103*, *107*) leverage ML to search for treatment effect heterogeneity across a high-dimensional space of covariates where potentially important sources of treatment effect heterogeneity are not *a priori* known. In such a context, an important concern is whether sampling variability in the estimated treatment effects associated with some covariates will sometimes lead to the spurious conclusion that there exists a "heterogeneous" treatment effect when none actually are present. While the ideas of prior work on this problem inform our approach, our context differs because the potential sources of heterogeneity that we consider are limited (climate, income, and irrigation), motivated by prior findings in the existing literature, and constrained to the set of variables for which standard projections exist. Thus, we use a structured approach that relies on expert knowledge to select the forms of heterogeneity that we consider, rather than adopting an unstructured "kitchen sink" approach that considers a vast number of covariates. For example, (*103*) raises concerns about the use of random forests to identify patterns of significant heterogeneity, allowing each covariate in a high dimensional set to be arbitrarily partitioned over its support. (*103*) points out that this can lead to under-rejection of patterns of heterogeneity that do not exist. In contrast, we start with a limited set of variables that the existing literature has already suggested to be important, and we enforce greater structure on the patterns of heterogeneity that we consider – dramatically reducing the likelihood that we recover patterns of estimated heterogeneity that are purely spurious.

One concern for our approach, related to the ideas raise by (*103*), is the role of the multi-step procedure we use to select models for each crop. We break up the cross validation search for model parameters into two steps

because simultaneously searching for weather parameters and forms of heterogeneity involves a prohibitive number of potential models. Instead we first determine which dimensions of weather most affect global yields for a given crop. Then, having selected a parsimonious set of weather dimensions, we determine which sources of heterogeneity are most important for the weather treatment effects. In our first cross validation step, we recognize that any weather variable selected may need to perform well in a final model with multiple different covariate interactions, which leads us to include a fixed set of covariate interactions (long-run temperature and precipitation, income, and irrigation) for each weather term.[8] However, a disadvantage of this approach is a weather variable with no true heterogeneity in its weather responses might be less likely to be selected. In practice, we consider this possibility to be unlikely, as it would imply that a given crop's weather response did not vary with the varietal of the crop selected, nor with access to fertilizer and other inputs, nor with the use of irrigation. However, we are able to directly test whether this issue affects our analysis since our final model is known and there are a limited number of covariates. VPD is the variable to which this concern might most apply, since it the sole weather variable that is projected well in climate models and which we do not select for any crop. We explicitly test whether allowing VPD to enter the first cross validation step without any interactions leads to improvements in its out-of-sample predictive performance, and find that it does not.

A second concern with our approach could center on the parsimony we apply to the selection of weather terms in the first cross validation step. The parsimony requirement we apply follows from our overall approach in this paper which draws on disparate findings from the broad existing literature on climate impacts to agriculture and seeks to succinctly highlight those factors which can be projected by climate models are are meaningfully determinative of future yield projections. Nonetheless, it is possible that this approach causes us to drop potentially important weather terms from the model. In Appendix E we explicitly test perturbations of the finals models by re-including key weather variables and find that this is unlikely to be the case across the crops we consider here.

C.1 Results

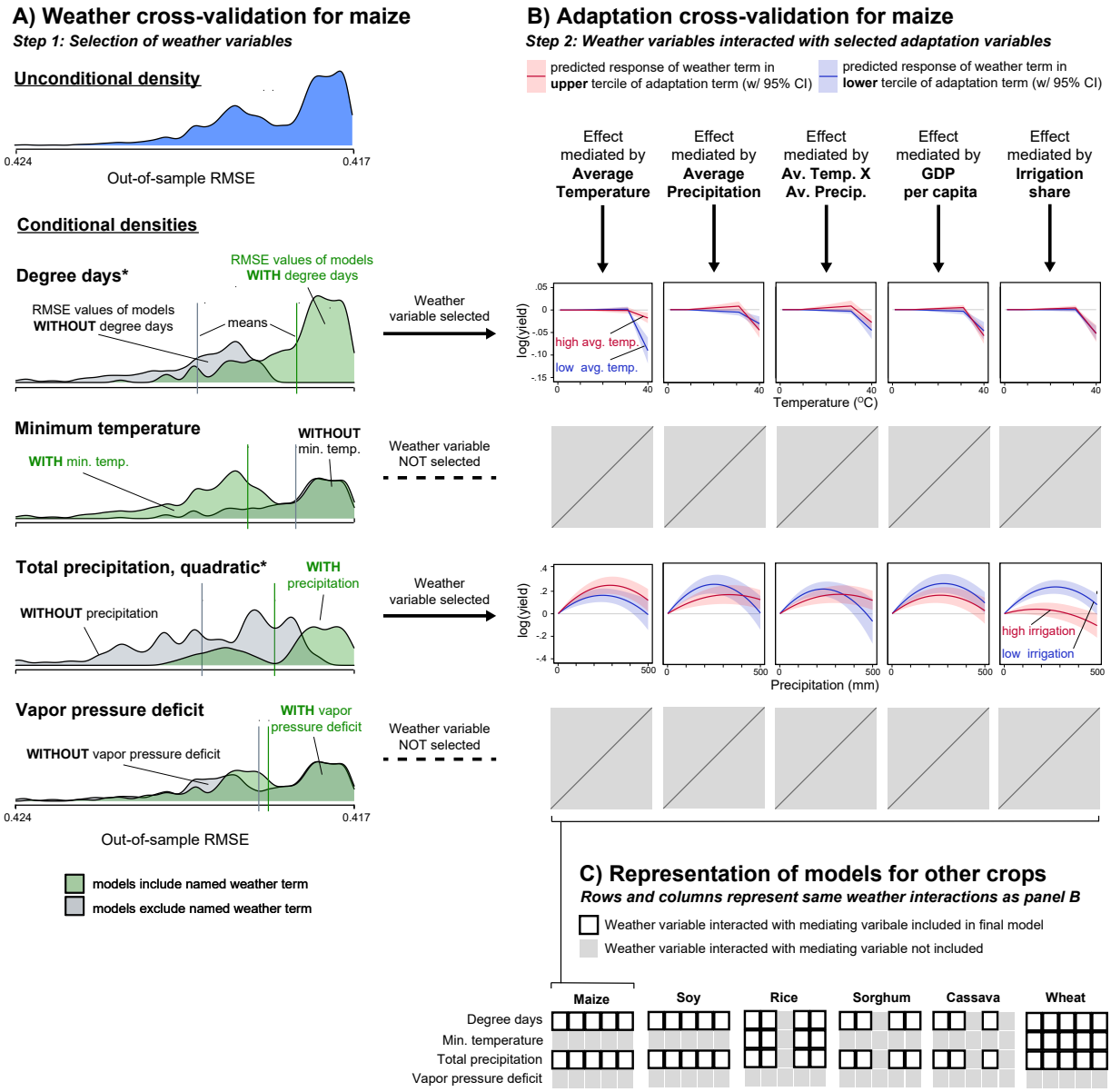
Here we show further results from our cross validation process. Our cross validation process is fully detailed in Appendix A.2 and is summarized in Figure S2 below, which uses maize as an example. Panel A of that figure describes our first cross validation step, the selection of weather variables. Some candidate weather variables are dropped at this step, and some are carried forward to our second cross validation step, the selection of adaptation channels (Panel B). Panel C visually summarizes the final model terms for all crops. Further details are given in the figure caption.

Figure S3 shows detailed results out-of-sample-RMSE results for each candidate model of the weather term selection process, for each crop. Each dot represents a single candidate model (some combination of candidate weather terms). Candidate models are rank-ordered from lowest out-of-sample-RMSE (best performing model) to highest out-of-sample-RMSE. Further details are given in the figure caption.

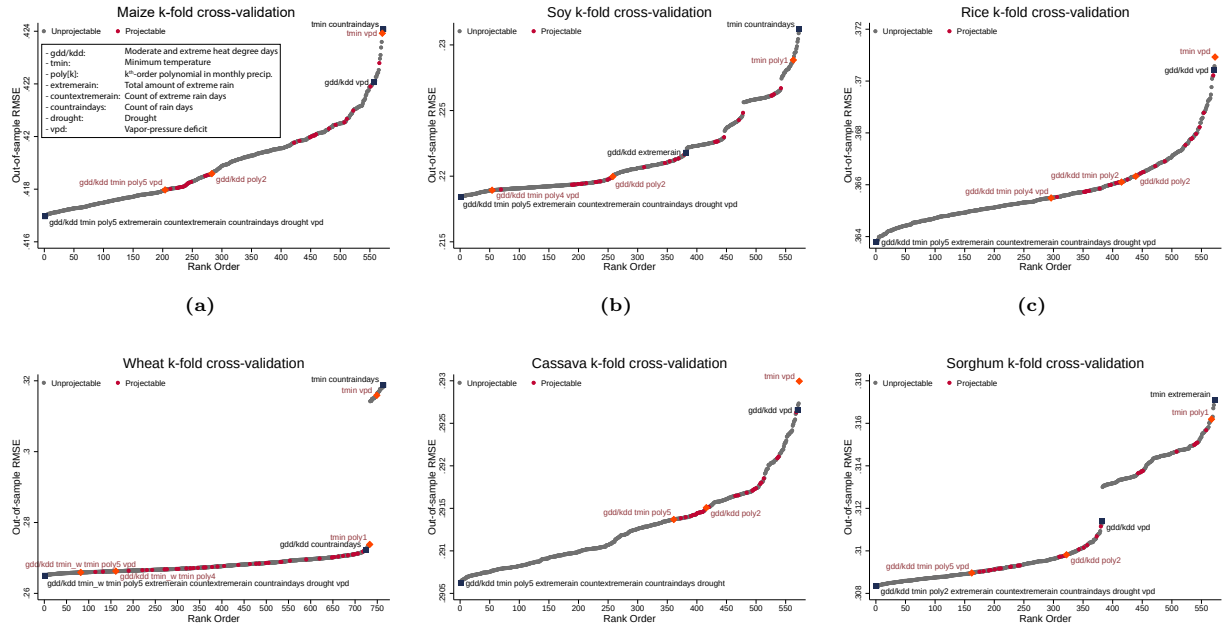
Figure S4 summarizes the out-of-sample-RMSE performance of individual candidate weather terms across

[8] As documented in Appendix A.2.

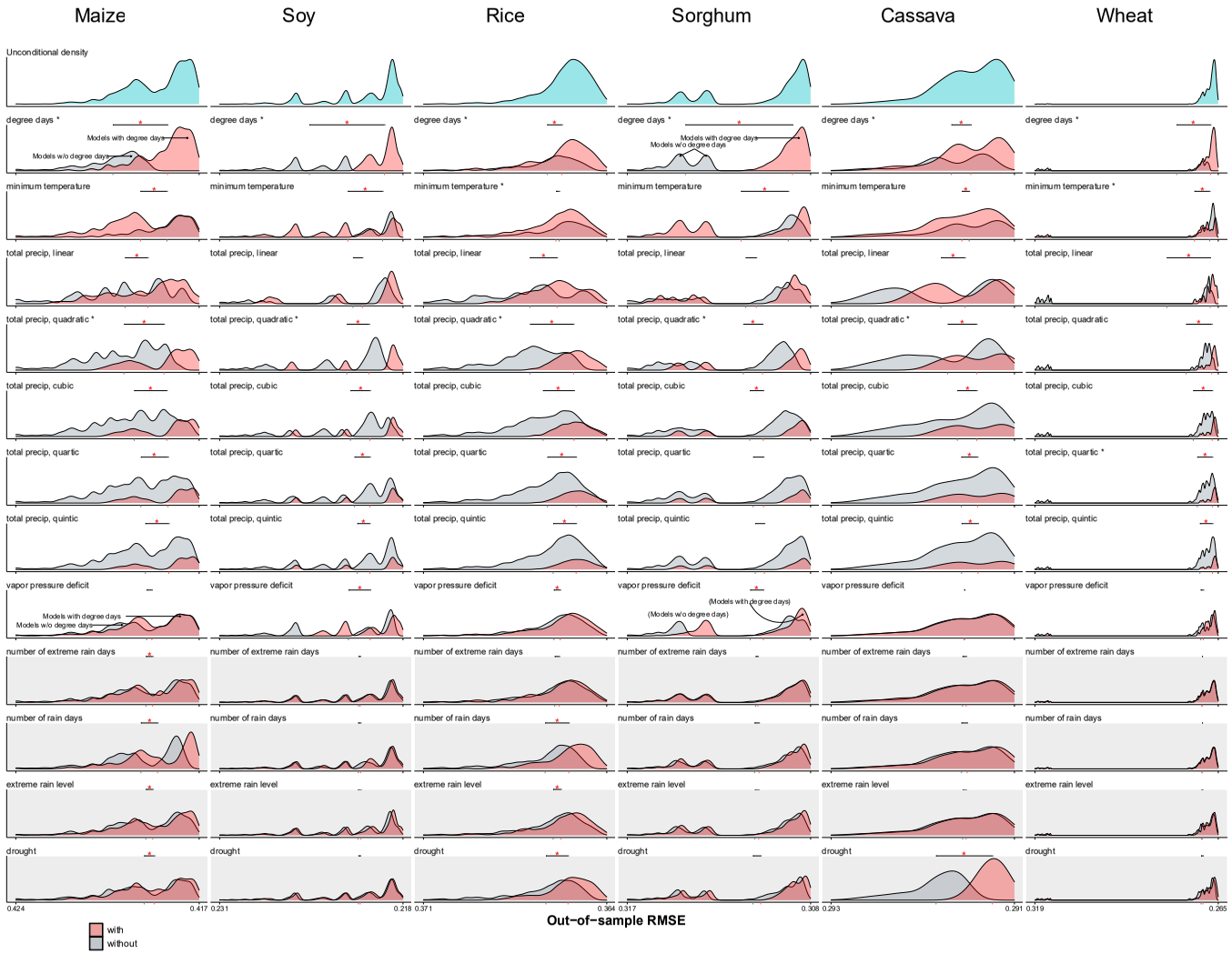
all candidate models, separately by each crop. Columns represent crops, rows represent particular weather terms. Individual plots show the kernel density of out-of-sample-RMSE for candidate models containing a given weather term (pink) or not containing that weather term (grey). The x-axis has been inverted so that lower out-of-sample-RMSE (better model performance) is on the right. Further details are given in the figure caption.



Supplementary Figure S2: Structured crop yield model selection for weather and mediating variables. For each staple crop, cross validation is used to first select key weather variables that influence yields (rows) and then applied to select mediating variables that capture adaptation or resource access (columns). Each selected mediating variable interacts with each selected weather variable. All observations are residualized prior to model selection, in order to remove cross-sectional and time series confounders. All candidates models are tested for each crop, **(A)-(B)** illustrate the process just for maize. **(A)** First step: Cross validation is used to select weather variables that influence maize (see Figures S4 and S6 for all crops). Top panel (blue) displays the unconditional distribution of out-of-sample (OOS) root-mean-squared error (RMSE) for all candidate models. Subsequent rows display pairs of conditional distributions that partition the sample. Green distributions depict model performance for all model permutations that include the indicated weather variable; grey distributions represent all model permutations that exclude the weather variable. Vertical lines indicate average values for each distribution. Strongly non-overlapping distributions indicate that models including the weather variable systematically tend to outperform those that exclude it. Fully overlapping distributions indicate that the indicated weather variable used to stratify models does not improve model fit. Weather terms with black stars were retained in the maize model. **(B)** Second step: using cross-validation to select mediating variables that capture adaptation to climate (e.g. average temperature) or resource access (e.g. GDP per capita). Candidate mediating variables are all interacted with weather variables from **(A)**. Sub-panels depict the mediating influence of the these factors (columns) on the response to weather variables (rows). Grey panels indicate pairs of variables that are not selected for the final model. Colors indicate a weather response that is empirically recovered for a lower (blue) or upper (red) tercile, although actual model specifications are continuous interactions. All coefficients and interactions are estimated simultaneously from a single joint model. Standard errors robust to auto-correlation over time within first level administrative units (e.g. states) and across all units within country-year. **(C)** Similar to **(B)**, but indicating weather-mediating variable pairs selected in the final model (white squares) for each crop.



Supplementary Figure S3: Rank ordering of out-of-sample RMSE performance of different models in the first step cross validation (selection of weather measures): a lower value of out-of-sample RMSE indicates better model performance. Models where all weather measures are projectable by climate models are plotted as red dots, those that contain at least one detailed precipitation measure that is not well-projected by climate models are plotted as grey dots. Generally, the model carried forward for selection of adaptation dimensions is the model labeled "gdd/kdd, poly2," with exception of rice and wheat, where we also carry forward t_{min}. Plots are for: (a) Maize, (b) Soybean, (c) Rice, (d) Wheat, (e) Cassava, (f) Sorghum.



Supplementary Figure S4: Cross validation for selection of weather variables, testing over 8,000 models across all six crops. The top row displays the kernel density of model out-of-sample (OOS) RMSE values for each crop; subsequent rows display conditional densities for each weather term. Pink represents all model permutations including the given weather term; grey represents all model permutations excluding the given term. Black bars indicate the average fit difference from including the term, and red stars indicate significance ($p < 0.05$, t-test). Weather terms with black stars were carried forward to the next cross validation procedure. The bottom four rows represent weather terms that cannot be reliably projected by existing climate models.

D Econometric Estimation: Crop Specifications

Here we present the details of our econometric estimation and results for each crop. For each crop, we performed the following analytical sequence.

1. Calculate weather measures. Degree days (DDs) were calculated following (*11*), who use the method of (*108*) to fit a continuous time sinusoidal interpolation of temperature between daily t_{min} and t_{max} and calculate the area under the curve that falls above the lower threshold and, for GDDs, below the upper threshold.[9] As (*11*) point out, this measure more effectively captures exposure to temperature extremes than does a DD measure based on daily average temperature. Precipitation is a grid-cell by month measure, with precipitation summed within month before polynomial transformations were performed. Minimum temperature t_{min} (including winter t_{min} for winter wheat) and drought were calculated following (*32*). Minimum temperature was aggregated at the daily level, and drought was defined as a binary variable over a percentile cutoff of total growing season precipitation at the administrative unit level. Vapor pressure deficit was calculated following (*35*), using the Tetons (1930) transformation[10] of daily minimum and maximum temperatures which assumes fully saturated vapor pressure at the day's minimum temperature. The count of rain days (*34*) was calculated as a binary value for daily precipitation > 0. The count of extreme rain days and total extreme precipitation (*34*) were calculated as daily binaries and sums (respectively) of rainfall in excess of the 95^{th} percentile of the grid cell 1950-1980 distribution of daily precipitation. All weather measures except drought were calculated at the grid-cell level and then aggregated using SAGE "anycrop" weights. All weather measures employ the median plant and harvest dates from SAGE for the respective crop growing season.

Degree-day cutoffs for each crop Table S2 displays the results of a 10-fold cross-validation search for the optimal thresholds for each crop. These capture the threshold temperature below which cumulative degree days are beneficial to a specific crop ("growing" degree days or GDD) and above which cumulative degree days are harmful to a specific crop ("killing" degree days or KDD). For example, the beneficial degree days for maize occur between 8°Cand 31°C, and the harmful degree days occur above 31°C. Wheat has multiple thresholds in Table S2, reflecting that wheat is grown at different times of year and varieties have different properties. Winter wheat is planted in the fall and overwinters, and therefore degree day cutoffs are defined separately for the fall and winter phases of the crop, also selected using 10-fold cross-validation.

Defining drought for each crop. Table S3 displays the results of a 10-fold cross-validation search for the optimal drought threshold for each crop. These thresholds are expressed in terms of the percentile of location specific seasonal rainfall that leads to a loss in crop yields.

2. Cross validation selection of weather measures. This step is fully described in Methods Appendix

[9] KDDs do not have an upper threshold.

[10] $VPD = 0.6107\left(e^{\frac{17.269T_{max}}{237.3+T_{max}}} - e^{\frac{17.269T_{min}}{237.3+T_{min}}}\right)$

	Growing	"Killing"	Fall		Winter	
Crop	degree days (GDD)	degree days (KDD)	GDD	KDD	GDD	KDD
Corn	8 - 31	≥31	-	-	-	-
Soy	8 - 31	≥31	-	-	-	-
Rice	14 - 30	≥30	-	-	-	-
Sorghum	15 - 31	≥31	-	-	-	-
Cassava	10 - 29	≥29	-	-	-	-
Wheat	1 - 11	≥11	0 - 5	≥5	1 - 17	≥17

Supplementary Table S2: Degree day cutoffs (°C) for each crop. Degree day definitions and the cross-validation procedure for choosing cutoffs are as described in Appendix app:crop-specs. Because winter wheat is planted in the fall and overwinters, degree day cutoffs are defined separately for the fall and winter phases of the crop.

Crop	Drought %ile
Corn	25
Soy	8
Rice	25
Sorghum	25
Cassava	23
Wheat	18

Supplementary Table S3: Precipitation percentiles defining "drought." Result of a cross-validation search over total growing season precipitation to define cutoffs for "drought" for each crop. See Appendix D for details.

A.2. The results for each crop are shown in Figures S4 and S3.

3. Growing Phase Precipitation. After choosing the function form of the precipitation response in the first cross validation step but before selecting dimensions of adaptation in the second cross validation step (see Appendix A.2), potential groupings of months were determined which allow the effect of precipitation to differ by phase of the growing season. This step is not cross validation, but instead is model selection across nested models. The objective is to determine whether the marginal yield response to precipitation is heterogeneous across months or if the precipitation across months should be pooled; and if so, how should pooling be structured. Month groupings were determined by constructing the following sequence of F-tests:

1. Test for a differential precipitation response between the first month and all remaining months of the growing season by testing the marginal effects at 100mm, 300mm, and 500mm of monthly precip.

2. If the result from (1) indicates a significant difference with $p < 0.05$, insert a "phase" break in the growing season and restart this procedure with the remaining months.

3. If the result from (1) does not indicate a significant difference with $p < 0.05$, group this month with any earlier months and restart with the next month in the season.

4. We then repeated steps 1-3 starting from the last month of the growing season (rather than the first month) as a check on the process. If month groupings from this step differed from those of the previous step, we used visual inspection of month-specific precipitation responses to resolve differences.

The final groupings are listed in Table S4 below. Whether or not these month groupings of growing season

phases were used (vs. using total growing season precipitation) was selected during the second cross validation step.

Crop	Phase 1	Phase 2	Phase 3	Phase 4
Maize	1	2-4	5+	-
Soybean	1	2	3-4	5+
Rice	1-2	3-5	6+	-
Spring & Winter wheat*	1	2-3	4+	
Sorghum	1	2-3	4+	-
Cassava	1	2-6	7-9	10-12

Supplementary Table S4: Growing season phases for precipitation effects. Month groupings for estimation of precipitation effects, determined by the sequence of f-tests described above for all crops except wheat. In the second stage cross validation, total growing season precipitation was selected for cassava and for spring and winter wheat (for winter wheat this is the total over the spring/summer months, see * below). For all other crops, precipitation-by-growing-season-phase responses were selected in the second stage cross validation. *For spring and winter wheat, month groupings were examined for the "spring/summer" portion of the growing season only. For spring wheat this was the entire growing season; for winter wheat this was the last five months of the growing season. For winter wheat, phases of the growing season were defined as: "spring/summer" are the last five months of the growing season, "fall" is the first two months of the growing season, and "winter" is the remaining unassigned months between fall and spring/summer. For winter wheat, the fall and winter phases were required to have separate precipitation and temperature responses.

4. Cross validation selection of adaptation dimensions. Definitions of our climate, income, and irrigation covariates used in our estimation are given below. This step is otherwise fully described in Methods Appendix A.2.

- *Long-run average temperature ($\bar{T}$)*: $\bar{T}$ captures correlations with producers' expectations over crop exposure to extreme heat, and is calculated as the average daily maximum temperature for all days within the growing season, over the panel length. The average is taken within panel unit, which is typically at the adm2 level (counties) in our data. For winter wheat, only days in the "spring/summer" phase of the growing season are used.

- *Long-run average precipitation ($\bar{P}$)*: $\bar{P}$ captures correlations with producers' expectations over growing season precipitation, and is calculated as the average monthly precipitation for all months within the growing season, over the panel length. The average is taken within panel unit, which is typically at the adm2 level (counties) in our data. For winter wheat, only months in the "spring/summer" phase of the growing season are used.

- *Long-run average income (I)*: I captures correlations with access to credit, farming technologies, fertilizer and seed varietals, crop insurance, and other socioeconomic influences on farming practices. Following (*40*), it is calculated as the average of panel unit $\log(GDP_{percapita})$, which is measured at the ADM1 unit (state/province) level.

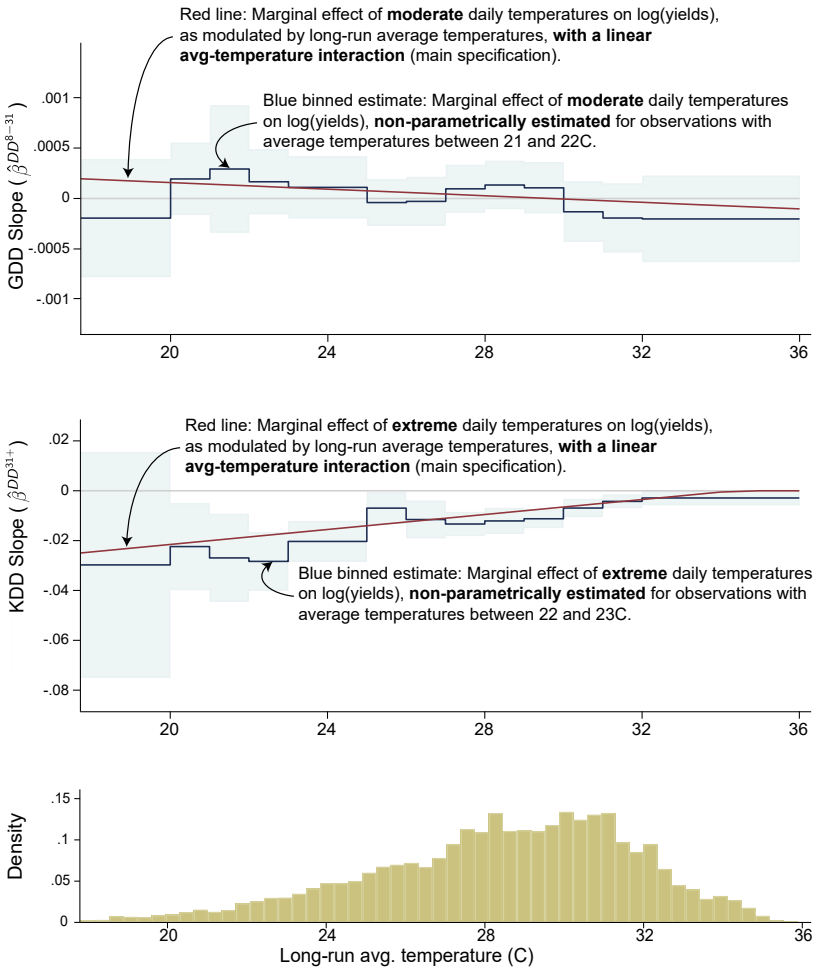
- *Area equipped for irrigation (R)*: R is measured as area equipped for irrigation, which is a cross sectional

measure from around the year 2005 which we aggregate using cropped area weights to the panel unit of our data, so that the measure is interpreted as the fraction of cropped area that is equipped for irrigation within a given panel unit.

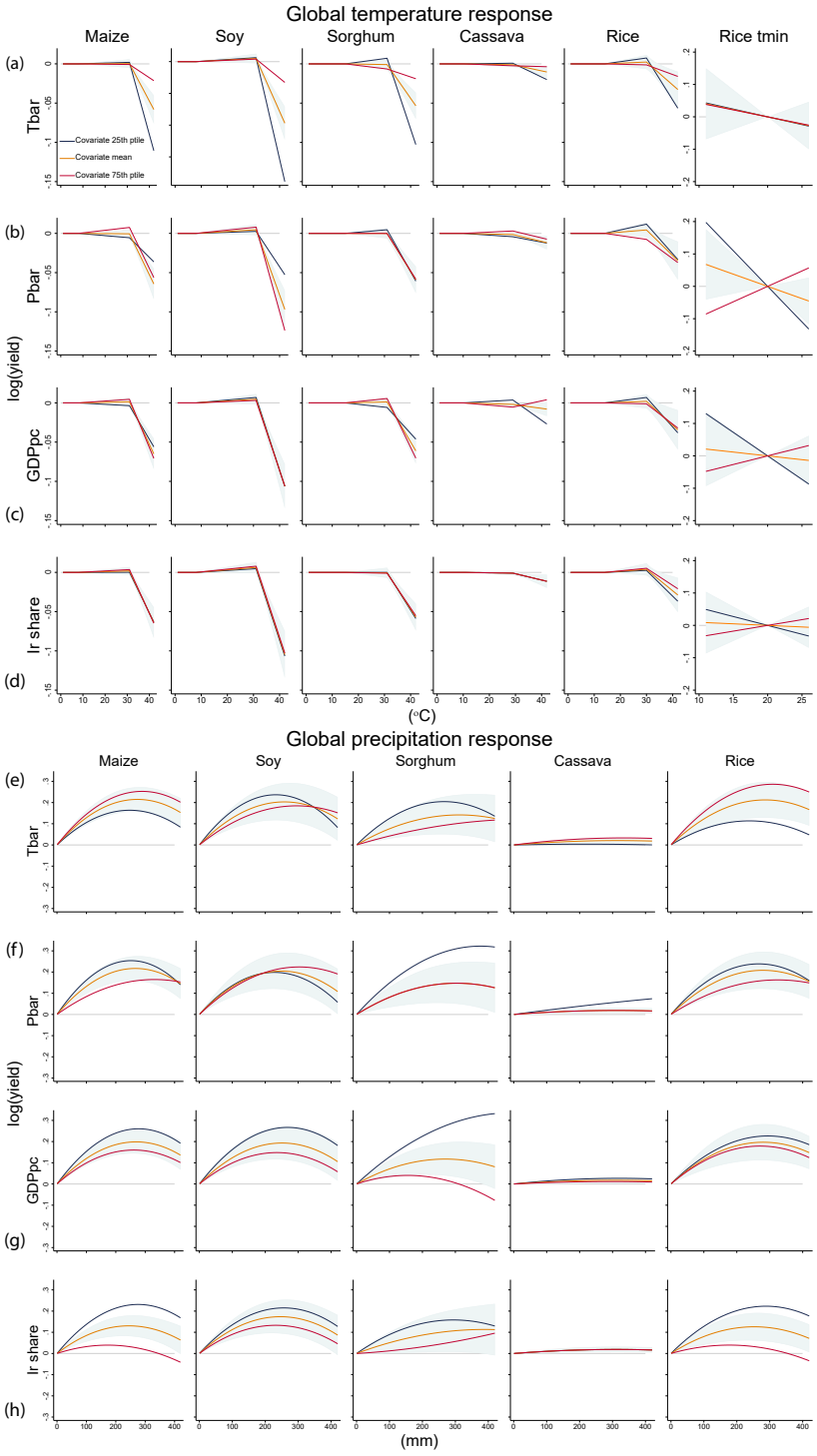
5. Knot choice for spline in long-run average precipitation. In our climate projections, long-run average precipitation ($\bar{P}$) values range up to 17 standard deviations outside the mean in our data. To prevent extrapolating adaptation behavior to $\bar{P}$ values far outside of our data, we imposed a single-knot linear spline in $\bar{P}$ for each weather measure, above which the value of $\bar{P}$ was fixed at the knot value during estimation. These knots were chosen using a within-R^2 search over knot locations, searching from the 5^{th} to 95^{th} percentiles of the crop's $\bar{P}$ support over 25mm increments. Knots for all crop×weather variable combination are shown in Table S5. An example depiction of the fit of the final model to a non-parametric binned-estimator of the degree-day slopes for maize is shown in Figure S5. In this result, the main specification was used with the following exception: moderate and extreme heat degree-day slopes were individually estimated for each 1C bin of long-run temperature, instead of the linear interaction in long-run temperature in the main specification (γ_1 and γ_6 in Eq. A.13, for example). All degree-day slopes for all long-run temperature bins were estimated simultaneously, which represents substantially more parameters than the main model. As can be seen in Figure S5, though the binned degree-day slopes are more noisy, their pattern over long-run temperature is consistent with the linear long-run temperature interaction in the main specification.

Crop	GDD	KDD	Precipitation	Tmin	Tmin_w
Maize	200	100	250	-	-
Soy	275	150	225	-	-
Rice	200	300	250	175	-
Sorghum	100	125	100	-	-
Cassava	250	75	100	-	-
Wheat	100	100	125	125	25

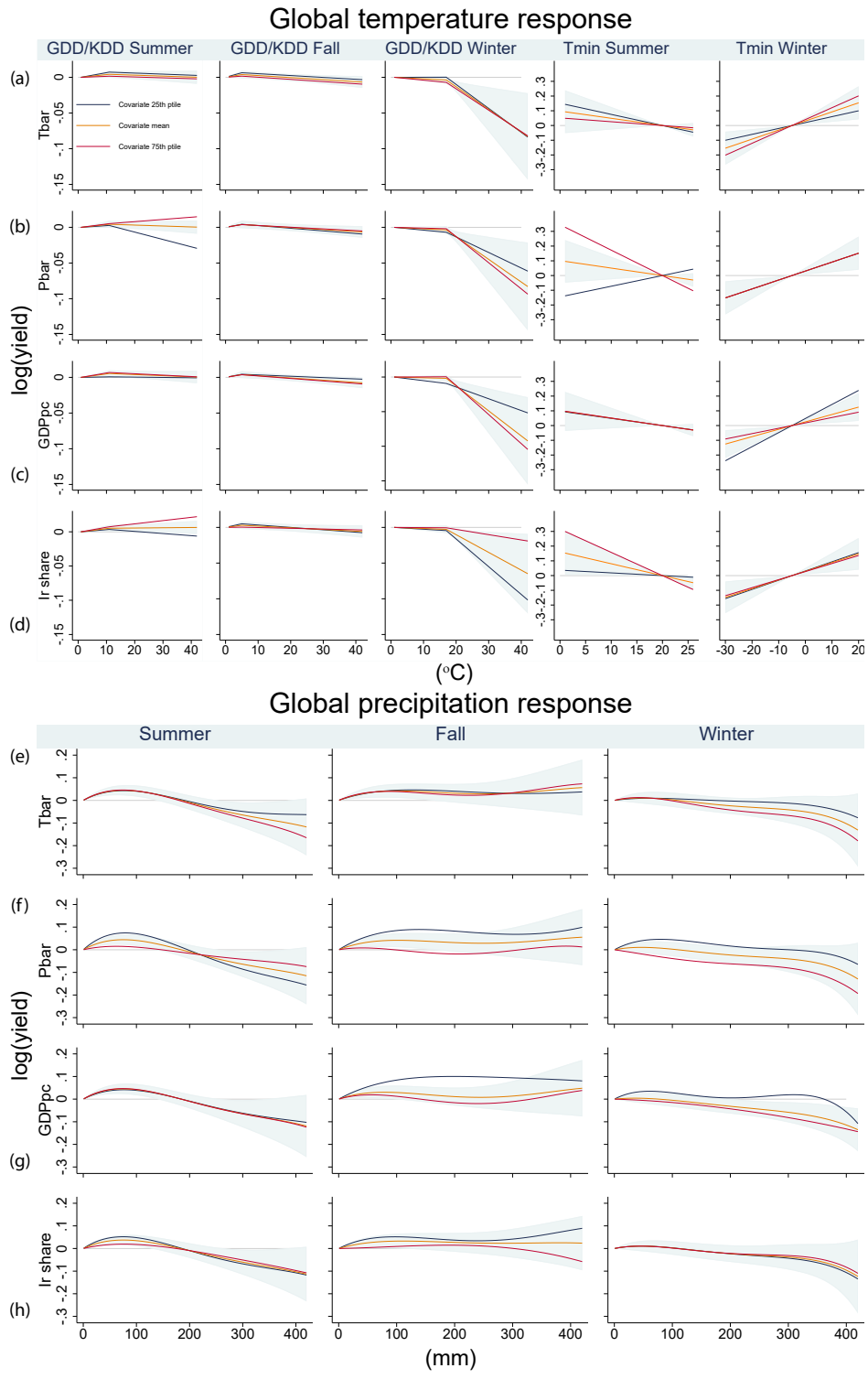
Supplementary Table S5: Spline knots for long-run precipitation $\bar{P}$. Spline knots chosen through a cross validation search as described in Appendix D. The knot for winter daily minimum temperature Tmin_w applies only to winter wheat.



Supplementary Figure S5: Non-parametric estimation of the marginal effects of moderate and extreme heat as a function of long-run average temperature for maize. Red lines correspond to the estimated marginal effects, parameterized by γ_1 and γ_6 in Eq. A.13, used in the main specification (linear interaction with long-run temperature). Blue lines represent highly flexible estimates that are not constrained to take on a linear form. Top panel: the marginal effect of moderate heat (degree-days from 8-31C), estimated separately for each 1C bin of long-run temperature in the data. The red line shows how the marginal effect of moderate heat varies over long-run temperature in our main specification, which corresponds to the effect of γ_1 in Eq. A.13. Middle panel: Same, but for the marginal effect of extreme heat (degree days above 31C). Bottom panel: The distribution of long-run average temperature in the data. Both degree-day slopes in all long-run temperature bins were estimated simultaneously.



Supplementary Figure S6: Interaction terms resulting from the second cross validation step. Empirically estimated temperature and precipitation response surfaces, by crop and by adaptation parameter. Columns are crops, rows are adaptation parameters (covariates). Yellow: all covariates evaluated at the sample mean; blue: covariate of interest evaluated at its lower tercile; red: covariate of interest evaluated at its upper tercile. Note the top panel includes an extra column for rice (t_{min}). Also note: cassava does not include irrigation in the model, thus no irrigation interaction effects are plotted for this crop. Standard errors robust to correlated shocks within state over space and time and within country-year.



Supplementary Figure S7: As Fig. S6, but for wheat: interaction terms resulting from the second cross validation step. Empirically estimated temperature and precipitation response surface for wheat, by adaptation parameter. Columns are seasons, rows are adaptation parameters (covariates). Yellow: all covariates evaluated at the sample mean; blue: covariate of interest evaluated at its lower tercile; red: covariate of interest evaluated at its upper tercile. Standard errors robust to correlated shocks within state over space and time and within country-year.

Final models. The final models that account for the interacting effect of weather and producer decision-making for each crop are displayed in Figure S6 and below in Equations D.1-D.6. In all equations, $y_{it}^{[crop]}$ refers to log(yield) for a given crop in administrative unit i and year t; μ_i denote administrative unit i (typically county) fixed effects; $h_s(t)$ refers to adm1 (state/province) quadratic time trends; ρ_{ct} are country by year fixed effects; and splines in long-run precipitation are denoted $z_{[\cdot]}(\bar{P}_i)$. Note that coefficients and splines are unique for each crop, but crop-specific indices are omitted for notational simplicity (e.g., $z_a(\bar{P}_i)$ for maize does not equal $z_a(\bar{P}_i)$ for soybean). Spline knots for $\bar{P}$ for each crop-weather pair are given in Table S5. All covariates (climate, income I, and irrigation R terms as defined previously) enter linearly. The growing season may be separated into multiple phases for precipitation effects (see Table S4), which may differ for each crop. Winter wheat growing season has three phases with associated weather variables denoted accordingly below: fall (appended $_fall$), winter ($_wint$), and spring/summer ($_sp\&su$).

Maize:

$$
\begin{aligned}
y_{it}^{maize} = \\
& DD_{it}^{8-31} \cdot (\beta_1 + \gamma_1 \bar{T}_i + \gamma_2 z_a(\bar{P}_i) + \gamma_3 \bar{T}_i z_a(\bar{P}_i) + \gamma_4 I_i + \gamma_5 R_i) + \\
& DD_{it}^{31+} \cdot (\beta_2 + \gamma_6 \bar{T}_i + \gamma_7 z_b(\bar{P}_i) + \gamma_8 \bar{T}_i z_b(\bar{P}_i) + \gamma_9 I_i + \gamma_{10} R_i) + \\
& prcp_phase1_{it} \cdot (\beta_3 + \gamma_{11} \bar{T}_i + \gamma_{12} z_c(\bar{P}_i) + \gamma_{13} \bar{T}_i z_c(\bar{P}_i) + \gamma_{14} I_i + \gamma_{15} R_i) + \\
& prcp_phase1_{it}^2 \cdot (\beta_4 + \gamma_{16} \bar{T}_i + \gamma_{17} z_c(\bar{P}_i) + \gamma_{18} \bar{T}_i z_c(\bar{P}_i) + \gamma_{19} I_i + \gamma_{20} R_i) + \\
& prcp_phase2_{it} \cdot (\beta_5 + \gamma_{21} \bar{T}_i + \gamma_{22} z_c(\bar{P}_i) + \gamma_{23} \bar{T}_i z_c(\bar{P}_i) + \gamma_{24} I_i + \gamma_{25} R_i) + \\
& prcp_phase2_{it}^2 \cdot (\beta_6 + \gamma_{26} \bar{T}_i + \gamma_{27} z_c(\bar{P}_i) + \gamma_{28} \bar{T}_i z_c(\bar{P}_i) + \gamma_{29} I_i + \gamma_{30} R_i) + \\
& prcp_phase3_{it} \cdot (\beta_7 + \gamma_{31} \bar{T}_i + \gamma_{32} z_c(\bar{P}_i) + \gamma_{33} \bar{T}_i z_c(\bar{P}_i) + \gamma_{34} I_i + \gamma_{35} R_i) + \\
& prcp_phase3_{it}^2 \cdot (\beta_8 + \gamma_{36} \bar{T}_i + \gamma_{37} z_c(\bar{P}_i) + \gamma_{38} \bar{T}_i z_c(\bar{P}_i) + \gamma_{39} I_i + \gamma_{40} R_i) + \\
& \mu_i + h_s(t) + \rho_{ct} + \epsilon_{it} \quad \text{(D.1)}
\end{aligned}
$$

The grid of included interaction coefficients described by the γ terms in Equation D.1 are depicted visually as the grid in Figure 2. Note that for maize

$$
z_a^{maize}(\bar{P}) = \begin{cases} \bar{P} & \text{if } \bar{P} \leq 200\text{mm} \\ 200 & \text{otherwise} \end{cases} \quad z_b^{maize}(\bar{P}) = \begin{cases} \bar{P} & \text{if } \bar{P} \leq 100\text{mm} \\ 100 & \text{otherwise} \end{cases} \quad z_c^{maize}(\bar{P}) = \begin{cases} \bar{P} & \text{if } \bar{P} \leq 250\text{mm} \\ 250 & \text{otherwise} \end{cases}
$$

as shown in Table S5.

The remaining crop models follow. Crop-specific spline knots for $z_a(\bar{P}), z_b(\bar{P}), z_c(\bar{P})$, and (for rice and wheat) $z_d(\bar{P})$ and $z_e(\bar{P})$ are given in Table S5.

Soybean:

$$
\begin{aligned}
y_{it}^{soybean} = \\
& DD_{it}^{8-31} \cdot (\beta_1 + \gamma_1 \bar{T}_i + \gamma_2 z_a(\bar{P}_i) + \gamma_3 \bar{T}_i z_a(\bar{P}_i) + \gamma_4 I_i + \gamma_5 R_i) + \\
& DD_{it}^{31+} \cdot (\beta_2 + \gamma_6 \bar{T}_i + \gamma_7 z_b(\bar{P}_i) + \gamma_8 \bar{T}_i z_b(\bar{P}_i) + \gamma_9 I_i + \gamma_{10} R_i) + \\
& prcp_phase1_{it} \cdot (\beta_3 + \gamma_{11} \bar{T}_i + \gamma_{12} z_c(\bar{P}_i) + \gamma_{13} \bar{T}_i z_c(\bar{P}_i) + \gamma_{14} I_i + \gamma_{15} R_i) + \\
& prcp_phase1_{it}^2 \cdot (\beta_4 + \gamma_{16} \bar{T}_i + \gamma_{17} z_c(\bar{P}_i) + \gamma_{18} \bar{T}_i z_c(\bar{P}_i) + \gamma_{19} I_i + \gamma_{20} R_i) + \\
& prcp_phase2_{it} \cdot (\beta_5 + \gamma_{21} \bar{T}_i + \gamma_{22} z_c(\bar{P}_i) + \gamma_{23} \bar{T}_i z_c(\bar{P}_i) + \gamma_{24} I_i + \gamma_{25} R_i) + \\
& prcp_phase2_{it}^2 \cdot (\beta_6 + \gamma_{26} \bar{T}_i + \gamma_{27} z_c(\bar{P}_i) + \gamma_{28} \bar{T}_i z_c(\bar{P}_i) + \gamma_{29} I_i + \gamma_{30} R_i) + \\
& prcp_phase3_{it} \cdot (\beta_7 + \gamma_{31} \bar{T}_i + \gamma_{32} z_c(\bar{P}_i) + \gamma_{33} \bar{T}_i z_c(\bar{P}_i) + \gamma_{34} I_i + \gamma_{35} R_i) + \\
& prcp_phase3_{it}^2 \cdot (\beta_8 + \gamma_{36} \bar{T}_i + \gamma_{37} z_c(\bar{P}_i) + \gamma_{38} \bar{T}_i z_c(\bar{P}_i) + \gamma_{39} I_i + \gamma_{40} R_i) + \\
& prcp_phase4_{it} \cdot (\beta_9 + \gamma_{41} \bar{T}_i + \gamma_{42} z_c(\bar{P}_i) + \gamma_{43} \bar{T}_i z_c(\bar{P}_i) + \gamma_{44} I_i + \gamma_{45} R_i) + \\
& prcp_phase4_{it}^2 \cdot (\beta_10 + \gamma_{46} \bar{T}_i + \gamma_{47} z_c(\bar{P}_i) + \gamma_{48} \bar{T}_i z_c(\bar{P}_i) + \gamma_{49} I_i + \gamma_{50} R_i) + \\
& \mu_i + h_s(t) + \rho_{ct} + \epsilon_{it} \quad \text{(D.2)}
\end{aligned}
$$

Rice:

$$
\begin{aligned}
y_{it}^{rice} = \\
& DD_{it}^{14-30} \cdot (\beta_1 + \gamma_1 \bar{T}_i + \gamma_2 z_a(\bar{P}_i) + \gamma_3 I_i + \gamma_4 R_i) + \\
& DD_{it}^{30+} \cdot (\beta_2 + \gamma_5 \bar{T}_i + \gamma_6 z_b(\bar{P}_i) + \gamma_7 I_i + \gamma_8 R_i) + \\
& prcp_phase1_{it} \cdot (\beta_3 + \gamma_9 \bar{T}_i + \gamma_{10} z_c(\bar{P}_i) + \gamma_{11} I_i + \gamma_{12} R_i) + \\
& prcp_phase1_{it}^2 \cdot (\beta_4 + \gamma_{13} \bar{T}_i + \gamma_{14} z_c(\bar{P}_i) + \gamma_{15} I_i + \gamma_{16} R_i) + \\
& prcp_phase2_{it} \cdot (\beta_5 + \gamma_{17} \bar{T}_i + \gamma_{18} z_c(\bar{P}_i) + \gamma_{19} I_i + \gamma_{20} R_i) + \\
& prcp_phase2_{it}^2 \cdot (\beta_6 + \gamma_{21} \bar{T}_i + \gamma_{22} z_c(\bar{P}_i) + \gamma_{23} I_i + \gamma_{24} R_i) + \\
& prcp_phase3_{it} \cdot (\beta_7 + \gamma_{25} \bar{T}_i + \gamma_{26} z_c(\bar{P}_i) + \gamma_{27} I_i + \gamma_{28} R_i) + \\
& prcp_phase3_{it}^2 \cdot (\beta_8 + \gamma_{29} \bar{T}_i + \gamma_{30} z_c(\bar{P}_i) + \gamma_{31} I_i + \gamma_{32} R_i) + \\
& tmin_{it} \cdot (\beta_9 + \gamma_{33} \bar{T}_i + \gamma_{34} z_d(\bar{P}_i) + \gamma_{35} I_i + \gamma_{36} R_i) + \\
& \mu_i + h_s(t) + \rho_{ct} + \epsilon_{it} \quad \text{(D.3)}
\end{aligned}
$$

Wheat:

$$
\begin{aligned}
y_{it}^{wheat} = \\
& DD_sp\&su_{it}^{1-11} \cdot (\beta_1 + \gamma_1 \bar{T}_i + \gamma_2 z_a(\bar{P}_i) + \gamma_3 \bar{T}_i z_a(\bar{P}_i) + \gamma_4 I_i + \gamma_5 R_i) + \\
& DD_sp\&su_{it}^{11+} \cdot (\beta_2 + \gamma_6 \bar{T}_i + \gamma_7 z_b(\bar{P}_i) + \gamma_8 \bar{T}_i z_b(\bar{P}_i) + \gamma_9 I_i + \gamma_{10} R_i) + \\
& prcp_sp\&su_{it} \cdot (\beta_3 + \gamma_{11} \bar{T}_i + \gamma_{12} z_c(\bar{P}_i) + \gamma_{13} \bar{T}_i z_c(\bar{P}_i) + \gamma_{14} I_i + \gamma_{15} R_i) + \\
& prcp_sp\&su_{it}^{2} \cdot (\beta_4 + \gamma_{16} \bar{T}_i + \gamma_{17} z_c(\bar{P}_i) + \gamma_{18} \bar{T}_i z_c(\bar{P}_i) + \gamma_{19} I_i + \gamma_{20} R_i) + \\
& prcp_sp\&su_{it}^{3} \cdot (\beta_5 + \gamma_{21} \bar{T}_i + \gamma_{22} z_c(\bar{P}_i) + \gamma_{23} \bar{T}_i z_c(\bar{P}_i) + \gamma_{24} I_i + \gamma_{25} R_i) + \\
& prcp_sp\&su_{it}^{4} \cdot (\beta_6 + \gamma_{26} \bar{T}_i + \gamma_{27} z_c(\bar{P}_i) + \gamma_{28} \bar{T}_i z_c(\bar{P}_i) + \gamma_{29} I_i + \gamma_{30} R_i) + \\
& tmin_sp\&su_{it} \cdot (\beta_7 + \gamma_{31} \bar{T}_i + \gamma_{32} z_d(\bar{P}_i) + \gamma_{33} \bar{T}_i z_d(\bar{P}_i) + \gamma_{34} I_i + \gamma_{35} R_i) + \\
& \mathbb{1}\{\text{varietal} = \text{winter wheat}\} \times \Big\{ \\
& DD_fall_{it}^{0-5} \cdot (\beta_8 + \gamma_{36} \bar{T}_i + \gamma_{37} z_a(\bar{P}_i) + \gamma_{38} \bar{T}_i z_a(\bar{P}_i) + \gamma_{39} I_i + \gamma_{40} R_i) + \\
& DD_fall_{it}^{5+} \cdot (\beta_9 + \gamma_{41} \bar{T}_i + \gamma_{42} z_b(\bar{P}_i) + \gamma_{43} \bar{T}_i z_b(\bar{P}_i) + \gamma_{44} I_i + \gamma_{45} R_i) + \\
& prcp_fall_{it} \cdot (\beta_{10} + \gamma_{46} \bar{T}_i + \gamma_{47} z_c(\bar{P}_i) + \gamma_{48} \bar{T}_i z_c(\bar{P}_i) + \gamma_{49} I_i + \gamma_{50} R_i) + \\
& prcp_fall_{it}^{2} \cdot (\beta_{11} + \gamma_{51} \bar{T}_i + \gamma_{52} z_c(\bar{P}_i) + \gamma_{53} \bar{T}_i z_c(\bar{P}_i) + \gamma_{54} I_i + \gamma_{55} R_i) + \\
& prcp_fall_{it}^{3} \cdot (\beta_{12} + \gamma_{56} \bar{T}_i + \gamma_{57} z_c(\bar{P}_i) + \gamma_{58} \bar{T}_i z_c(\bar{P}_i) + \gamma_{59} I_i + \gamma_{60} R_i) + \\
& prcp_fall_{it}^{4} \cdot (\beta_{13} + \gamma_{61} \bar{T}_i + \gamma_{62} z_c(\bar{P}_i) + \gamma_{63} \bar{T}_i z_c(\bar{P}_i) + \gamma_{64} I_i + \gamma_{65} R_i) + \\
& DD_wint_{it}^{1-17} \cdot (\beta_{14} + \gamma_{66} \bar{T}_i + \gamma_{67} z_a(\bar{P}_i) + \gamma_{68} \bar{T}_i z_a(\bar{P}_i) + \gamma_{69} I_i + \gamma_{70} R_i) + \\
& DD_wint_{it}^{17+} \cdot (\beta_{15} + \gamma_{71} \bar{T}_i + \gamma_{72} z_b(\bar{P}_i) + \gamma_{73} \bar{T}_i z_b(\bar{P}_i) + \gamma_{74} I_i + \gamma_{75} R_i) + \\
& prcp_wint_{it} \cdot (\beta_{16} + \gamma_{76} \bar{T}_i + \gamma_{77} z_c(\bar{P}_i) + \gamma_{78} \bar{T}_i z_c(\bar{P}_i) + \gamma_{79} I_i + \gamma_{80} R_i) + \\
& prcp_wint_{it}^{2} \cdot (\beta_{17} + \gamma_{81} \bar{T}_i + \gamma_{82} z_c(\bar{P}_i) + \gamma_{83} \bar{T}_i z_c(\bar{P}_i) + \gamma_{84} I_i + \gamma_{85} R_i) + \\
& prcp_wint_{it}^{3} \cdot (\beta_{18} + \gamma_{86} \bar{T}_i + \gamma_{87} z_c(\bar{P}_i) + \gamma_{88} \bar{T}_i z_c(\bar{P}_i) + \gamma_{89} I_i + \gamma_{90} R_i) + \\
& prcp_wint_{it}^{4} \cdot (\beta_{19} + \gamma_{91} \bar{T}_i + \gamma_{92} z_c(\bar{P}_i) + \gamma_{93} \bar{T}_i z_c(\bar{P}_i) + \gamma_{94} I_i + \gamma_{95} R_i) + \\
& tmin_wint_{it} \cdot (\beta_{20} + \gamma_{96} \bar{T}_i + \gamma_{97} z_e(\bar{P}_i) + \gamma_{98} \bar{T}_i z_e(\bar{P}_i) + \gamma_{99} I_i + \gamma_{100} R_i) \\
& \Big\} + \\
& \mu_i + h_s(t) + \rho_{ct} + \epsilon_{it} \qquad \text{(D.4)}
\end{aligned}
$$

Sorghum:

$$
\begin{aligned}
y_{it}^{sorghum} = \\
& DD_{it}^{15-31} \cdot (\beta_1 + \gamma_1 \bar{T}_i + \gamma_2 z_a(\bar{P}_i) + \gamma_3 I_i + \gamma_4 R_i) + \\
& DD_{it}^{31+} \cdot (\beta_2 + \gamma_5 \bar{T}_i + \gamma_6 z_b(\bar{P}_i) + \gamma_7 I_i + \gamma_8 R_i) + \\
& prcp_phase1_{it} \cdot (\beta_3 + \gamma_9 \bar{T}_i + \gamma_{10} z_c(\bar{P}_i) + \gamma_{11} I_i + \gamma_{12} R_i) + \\
& prcp_phase1_{it}^2 \cdot (\beta_4 + \gamma_{13} \bar{T}_i + \gamma_{14} z_c(\bar{P}_i) + \gamma_{15} I_i + \gamma_{16} R_i) + \\
& prcp_phase2_{it} \cdot (\beta_5 + \gamma_{17} \bar{T}_i + \gamma_{18} z_c(\bar{P}_i) + \gamma_{19} I_i + \gamma_{20} R_i) + \\
& prcp_phase2_{it}^2 \cdot (\beta_6 + \gamma_{21} \bar{T}_i + \gamma_{22} z_c(\bar{P}_i) + \gamma_{23} I_i + \gamma_{24} R_i) + \\
& prcp_phase3_{it} \cdot (\beta_7 + \gamma_{25} \bar{T}_i + \gamma_{26} z_c(\bar{P}_i) + \gamma_{27} I_i + \gamma_{28} R_i) + \\
& prcp_phase3_{it}^2 \cdot (\beta_8 + \gamma_{29} \bar{T}_i + \gamma_{30} z_c(\bar{P}_i) + \gamma_{31} I_i + \gamma_{32} R_i) + \\
& \mu_i + h_s(t) + \rho_{ct} + \epsilon_{it} \quad \text{(D.5)}
\end{aligned}
$$

Cassava:

$$
\begin{aligned}
y_{it}^{cassava} = \\
& DD_{it}^{10-29} \cdot (\beta_1 + \gamma_1 \bar{T}_i + \gamma_2 z_a(\bar{P}_i) + \gamma_3 I_i) + \\
& DD_{it}^{29+} \cdot (\beta_2 + \gamma_4 \bar{T}_i + \gamma_5 z_b(\bar{P}_i) + \gamma_6 I_i) + \\
& prcp_{it} \cdot (\beta_3 + \gamma_7 \bar{T}_i + \gamma_8 z_c(\bar{P}_i) + \gamma_9 I_i) + \\
& prcp_{it}^2 \cdot (\beta_4 + \gamma_{10} \bar{T}_i + \gamma_{11} z_c(\bar{P}_i) + \gamma_{12} I_i) + \\
& mu_i + h_s(t) + \rho_{ct} + \epsilon_{it} \quad \text{(D.6)}
\end{aligned}
$$

E Econometric Estimation: Additional Results and Robustness

This section collects additional results and robustness tests related to the econometric and cross-validation portions of our analysis. Table S6 lists the data sources and proportions for winter wheat and spring wheat in our data, as well as those places that do not report a distinction, which is used in our estimation of spring and winter specific response functions. Tables S7 and S8 test the out-of-sample performance of our baseline models if other variables not selected in our cross-validation for variable selection are either included or dropped, respectively.

Wheat varietal by country. As noted in Appendix D, we estimate an empirical model for wheat that differentiates between spring wheat (which is planted in the spring like other annual crops) and winter wheat (which is planted in the fall and overwinters). Most countries do not report which type of wheat is grown in their annual agricultural statistics, as such we assign the wheat varietal for all countries in our data and in projections. Remaining countries not in our data received the global average winter/spring wheat mix and are listed as "All other countries" below.

Supplementary Table S6: Information sources used to assign wheat yields to spring or winter crops.

Country	Spring wheat %	Winter wheat %	Source
Argentina	100	0	https://naldc.nal.usda.gov
Australia	100	0	https://ipad.fas.usda.gov
Austria	0	100	https://ipad.fas.usda.gov
Belgium	0	100	https://ipad.fas.usda.gov
Bolivia	100	0	http://www.fao.org
Brazil	100	0	https://ipad.fas.usda.gov
			Page 78 https://naldc.nal.usda.gov
Bulgaria	0	100	Page 94 https://naldc.nal.usda.gov
Canada	100	0	https://ipad.fas.usda.gov
			https://ipad.fas.usda.gov
Chile	0	100	https://ipad.fas.usda.gov
China	0	100	https://ipad.fas.usda.gov
Colombia	100	0	https://ipad.fas.usda.gov
Cyprus	0	100	https://ipad.fas.usda.gov
Czech Republic	0	100	https://apps.fas.usda.gov
Denmark	0	100	Page 96 https://naldc.nal.usda.gov
Ecuador	100	0	https://ipad.fas.usda.gov
Egypt	0	100	Page 169 https://naldc.nal.usda.gov
Estonia	0	100	Page 269 https://naldc.nal.usda.gov
Finland	0	100	Assumed similar to neighbors
France	0	100	Page 98 https://naldc.nal.usda.gov
Germany	0	100	https://apps.fas.usda.gov

			Page 104 https://naldc.nal.usda.gov
			doi.org/10.1088/1748-9326/aade12
Great Britain	0	100	Page 131 https://naldc.nal.usda.gov
Greece	0	100	https://ipad.fas.usda.gov
Hungary	0	100	https://ipad.fas.usda.gov
			Page 111 https://naldc.nal.usda.gov
India	100	0	Page 177 https://naldc.nal.usda.gov
Iran	0	100	Page 160 https://naldc.nal.usda.gov
			http://www.ine.gob.bo
Ireland	0	100	Page 131 https://naldc.nal.usda.gov
Italy	0	100	Page 112 https://naldc.nal.usda.gov
Kazakhstan	92	8	https://naldc.nal.usda.gov
			https://agris.fao.org/agris-search/
Latvia	0	100	Page 267 https://naldc.nal.usda.gov
Lithuania	0	100	Page 267 https://naldc.nal.usda.gov
Luxembourg	0	100	Assumed similar to neighbors
Mexico	100	0	https://ipad.fas.usda.gov
Morocco	0	100	https://ipad.fas.usda.gov/countrysummary
Netherlands	0	100	Page 131 https://naldc.nal.usda.gov
Pakistan	100	0	https://wheat.pw.usda.gov
Poland	0	100	Page 118 https://naldc.nal.usda.gov
Portugal	0	100	Assumed similar to neighbors
Romania	0	100	Page 124 https://naldc.nal.usda.gov
Russia	41	59	https://www.statista.com/statistics
			https://ipad.fas.usda.gov
Slovakia	0	100	https://ipad.fas.usda.gov
Slovenia	0	100	Page 135 https://naldc.nal.usda.gov
Spain	0	100	Page 125 https://naldc.nal.usda.gov
Sweden	0	100	Page 129 https://naldc.nal.usda.gov
Syria	0	100	https://ipad.fas.usda.gov
Tanzania	100	0	https://ipad.fas.usda.gov
Turkey	0	100	Page 169 https://naldc.nal.usda.gov
Ukraine	0	100	https://ipad.fas.usda.gov
			Page 139 https://naldc.nal.usda.gov
United States	27	73	https://ipad.fas.usda.gov
			Page 24 https://naldc.nal.usda.gov
Uzbekistan	0	100	https://ipad.fas.usda.gov/countrysummary
All other countries	41	59	Average share

Perturbing weather models to examine contributions of individual variables. We examine the contribution of individual weather variables to model performance during "Step 1" of our cross-validation procedure (see Appendix A.2). Note, however, that the apparent contribution of different variables will depend on what other variables are present in the model. Thus, to provide benchmarks, we consider single variable perturbations of the baseline model. To evaluate the effect of excluded weather variables, we introduce each such weather variable as a single variable added to the baseline model to create an "expanded" model and observe how the addition of this variable improves "expanded" model performance over the baseline model. To evaluate the effect of a weather variable already included in the baseline model, we remove individual variables one at a time to create a "restricted" model and observe how inclusion of the removed variable improves baseline model performance over the "restricted" model.

Table S7 shows perturbations of the baseline models in which we add each excluded weather term into the model one at a time, and we show the gain in out-of-sample R^2 (OOS-R^2) in both absolute terms as well as as a percentage of the baseline model OOS-R^2. In the table we see that the largest gain (24%) would come from being able to include drought in the model for cassava; however drought is not a weather term we are able to reliably project into the future. Gains would also come from being able to include drought in the rice model (6.4%) and the count of rainy days – also not reliably projectable – in the rice and maize models (8.0% and 6.8%). None of the "projectable" weather terms improve OOS-R^2 over the baseline by more than 5% except t_{min} for sorghum (5.8%), suggesting that our baseline models effectively balance parsimony against capturing the bulk of weather-induced variation in yields.

Table S8 shows perturbations of the baseline models in which we remove terms from the model one at a time, and show the gain in OOS-R^2 when going from the perturbed model back to the baseline model (for consistency with the approach in Table S7 where the gain is from adding a term), again both in absolute terms and as a percentage of the perturbed model OOS-R^2. We see that every model term adds substantially to the OOS-R^2 of the model, with degree days doubling model OOS-R^2 for sorghum and increasing fits for maize, wheat, and soy by 41%, 54%, and 80%. Inclusion of the "marginal" precipitation term tends to have smaller (though not insubstantial) gains to fit of about 10% - 20%. As noted in the Discussion section of the main text, the t_{min} variable for rice was included because the balance of the literature suggested it is important. However, it is clear in this table that, in our data, t_{min} does not improve model OOS-R^2 to the same extent as the other baseline model terms do across all crops.

Supplementary Table S7: Changes in cross validated out of sample fit due to adding one weather term to the baseline model for each crop. Each line in this table corresponds to a single point in Figure S3.

Crop	Added Measure	Perturbed model % improvement in variance explained
	Reliably projected	
Maize	Baseline (GDD/KDD, pr^2)	N/A
	tmin	0.6%
	pr^3	3.8%
	VPD	0.5%
Soy	Baseline (GDD/KDD, pr^2)	N/A
	tmin	0.8%
	pr^3	2.3%
	VPD	1.5%
Rice	Baseline (GDD/KDD, tmin, pr^2)	N/A
	pr^3	0.6%
	VPD	2.2%
Wheat	Baseline (GDD/KDD, tmin, pr^4)	N/A
	pr^5	1.1%
	VPD	1.8%
Cassava	Baseline (GDD/KDD, pr^2)	N/A
	tmin	2.6%
	pr^3	-0.4%
	VPD	2.2%
Sorghum	Baseline (GDD/KDD, pr^2)	N/A
	tmin	5.8%
	pr^3	0.6%
	VPD	4.6%
	Not reliably projected	
Maize	Count extreme rain days	2.1%
	Count rain days	6.6%
	Amount of extreme rain	3.0%
	Drought	1.9%
Soy	Count extreme rain days	0.5%
	Count rain days	0.9%
	Amount of extreme rain	1.6%
	Drought	0.4%
Rice	Count extreme rain days	0.4%
	Count rain days	8.0%
	Amount of extreme rain	3.7%
	Drought	6.4%

Wheat	Count extreme rain days	0.7%
	Count rain days	0.7%
	Amount of extreme rain	1.5%
	Drought	3.8%
Cassava	Count extreme rain days	2.2%
	Count rain days	2.0%
	Amount of extreme rain	1.3%
	Drought	24.0%
Sorghum	Count extreme rain days	1.2%
	Count rain days	3.2%
	Amount of extreme rain	2.5%
	Drought	2.0%

Supplementary Table S8: Changes in cross validated out of sample fit based on removing one weather term from the baseline model for each crop. Each line in this table corresponds to a single point in Figure S3. Because all models were required to have at least one temperature term, baseline models without t_{min} that drop degree days replace them with t_{min}. For wheat, dropping the quartic polynomial in precipitation is replaced with a quadratic model to preserve tail behavior. See main text discussion of t_{min} for rice.

Crop	**Removed Measure**	**Baseline model % improvement in variance explained**
Maize	Baseline (GDD/KDD, pr^2)	N/A
	GDD/KDD	41.2%
	pr^2	22.2%
Soy	Baseline (GDD/KDD, pr^2)	N/A
	GDD/KDD	80.0%
	pr^2	9.2%
Rice	Baseline (GDD/KDD, tmin, pr^2)	N/A
	GDD/KDD	9.1%
	tmin	2.9%
	pr^2	22.8%
Wheat	Baseline (GDD/KDD, tmin, pr^4)	N/A
	GDD/KDD	53.9%
	tmin	9.0%
	pr^4	8.2%
Cassava	Baseline (GDD/KDD, pr^2)	N/A
	GDD/KDD	9.4%
	pr^2	15.8%
Sorghum	Baseline (GDD/KDD, pr^2)	N/A
	GDD/KDD	101.6%
	pr^2	9.4%

F Projections: Approach

In this section, we describe how we use our empirical estimates of weather effects on crop yields — conditional on climate, income, and irrigation (Appendix D) — to project the future impacts of climate change under different scenarios for adaptation and income growth. We conduct projections over an ensemble of climate models for both high and low future emissions scenarios (RCPs 8.5 and 4.5) and two SSP3 future income trajectories (from IIASA and OECD, Appendix A.1), and employ Monte Carlos to sample from the statistical uncertainty of our empirical estimates. The data and approach to projecting these impacts of climate change follow those used in refs. (*40*, *41*), although with some modification necessary for the context of agriculture. We present an overview here and note key differences. Interested readers should refer to refs. (*40*, *41*) for additional details.

F.1 Projection data

Projections are conducted for each of 24,378 "impact regions" (*40*, *41*) (denoted simply "regions" throughout for parsimony) – which are divisions of the globe into geographic units that have approximately comparable populations and internally consistent climatologies. We employ all 33 climate models used in (*40*) and (*41*), although we drop the ACCESS1-0 RCP 8.5 scenario due to unrealistically large amounts of precipitation by end of century. We rely on a multi-model ensemble of climate models and employ model weights to ensure the distribution of climate sensitivities is consistent with the IPCC AR5 (*40*, *41*). Updated model weights dropping the ACCESS1-0 / RCP 8.5 pair are listed in Table S9.

Estimates of region income are constructed by combining country level income (*89*) with remotely sensed nighttime lights (*109*). In regressions, the $\log(GDPpc)$ income covariate is calculated as a 13-year Bartlett kernel moving average and the climate covariates are calculated as a 25-year Bartlett kernel moving average (see (*40*, *41*) for details). Refs. (*40*, *41*) define "climate" as long-run average temperature $\bar{T}$. In this paper, "climate" consists of an additional covariate, long-run average precipitation $\bar{P}_{it}$. Both $\bar{T}_{it}$ and $\bar{P}_{it}$ are calculated over the primary growing season for a given crop from SAGE (*94*) and aggregated spatially using the SAGE "anycrop" weights, following the same construction as that described in Section D. Irrigation is calculated as described in Section D and held fixed at present-day levels into the future. Future work should explore the impact of alternative irrigation scenarios: increases in incomes and extreme heat exposure may drive increases in future irrigation while aquifer and reservoir draw-down may drive decreases in future irrigation.

F.2 Projected impacts

We consider two climate change scenarios for all projections: a "high emissions" scenario (RCP 8.5) and a "moderate emissions scenario" (RCP 4.5) and present results for each.

We seek to project the impacts of climate change on future crop yields relative to what would have occurred had the climate not changed. Because future incomes will likely rise regardless of warming, the

Climate model	RCP 4.5 weights	RCP 8.5 weights
ACCESS1-0	0.03	0
BCC-CSM1-1	0.09	0.0229
BNU-ESM	0.03	0.036
CANESM2	0.03	0.036
CCSM4	0.0267	0.0229
CESM1-BGC	0.09	0.0229
CNRM-CM5	0.03	0.0229
CSIRO-MK3-6-0	0.03	0.036
GFDL-CM3	0.03	0.04
GFDL-ESM2G	0.04	0.04
GFDL-ESM2M	0.06	0.04
INMCM4	0.06	0.04
IPSL-CM5A-LR	0.03	0.036
IPSL-CM5A-MR	0.03	0.036
MIROC-ESM	0.03	0.04
MIROC5	0.0267	0.0229
MIROC-ESM-CHEM	0.03	0.04
MPI-ESM-LR	0.0267	0.0229
MPI-ESM-MR	0.0267	0.0229
MRI-CGCM3	0.0267	0.09
NORESM1-M	0.0267	0.09
Surrogate CANESM2-89	0.01	0.01
Surrogate CANESM2-94	0.04	0.04
Surrogate CANESM2-99	0.01	0.01
Surrogate GFDL-CM3-89	0.01	0.01
Surrogate GFDL-CM3-94	0.04	0.04
Surrogate GFDL-CM3-99	0.01	0.01
Surrogate GFDL-ESM2G-01	0.01	0.01
Surrogate GFDL-ESM2G-06	0	0.04
Surrogate GFDL-ESM2G-11	0.01	0.01
Surrogate MRI-CGCM3-01	0.01	0.01
Surrogate MRI-CGCM3-06	0.04	0.04
Surrogate MRI-CGCM3-11	0.01	0.01

Supplementary Table S9: Climate model weights used to aggregate projection results across models. To provide an ensemble of climate projections with a probability distribution of GMST responses consistent with that estimated by a probabilistic simple climate model, we use the surrogate model mixed ensemble (SMME) method (*57*) to assign probabilistic weights to climate projections produced by GCMs and to improve representation of the tails of the distribution missing from the ensemble of GCMs. These weights adjust those of (*57*) after dropping the ACCESS1-0 / RCP 8.5 pair due to unrealistic end of century precipitation projections.

impact of climate change must be calculated against a counterfactual state of the world in which incomes have risen but warming did not occur.

As such, our primary object of interest is the impact of climate change when fully accounting for adaptation and its costs, relative to a future scenario in which incomes rise but the climate is held fixed. To fix ideas, consider the climate vector $\mathbf{C}$ (with components consisting of long run temperature, precipitation and their interaction, $\mathbf{C} \equiv \{\bar{T}, \bar{P}, \bar{T} \times \bar{P}\}$) with an associated distribution of weather $\mathbf{w}$ which consists of weather measures such as degree-days, precipitation, and daily minimum temperatures. Following the framework in Section A.2 and the implementation detailed in (*40*), the direct impact of climate change and associated adaptation (marginal terms of Eq. G.5) can be integrated. We normalize these values by price so that impacts and costs are both reported in terms of log(yields). This calculation results in a projection for *yields* $= y(\mathbf{w}_t, \mathbf{C}_t, I_t, R_t)$ that accounts for the benefits of adaptation (note that it is a function of climate, income, and irrigation access, in addition to weather) and total adaptation costs $A(\mathbf{C}_t, I_t, R_t)$, measured in units of *yields* (see Appendix G and Eq. G.5). In addition to accounting for climate, income, irrigation access and weather, note that these projections also account semi-parametrically for various trends and unobserved heterogeneity in sub-national conditions (e.g. soil, infrastructure) through the terms μ, h, and ρ (Equations A.13, D.1–D.6), but they are differenced out when impacts below are computed since they are present in both climate change scenarios and counterfactuals.

We report the following results in our projections:

- **Impact of climate change, without income growth or adaptation:** This object measures the impact of climate change relative to 2015 (roughly the present day), were it the case that producers never experienced income growth and never adapted (i.e. they make decisions based on 2015 climate for all future periods).

$$y^{NoAdaptInc} = y(\mathbf{w}_t, \mathbf{C}_{2015}, I_{2015}, R_{2015}) - y(\mathbf{w}_{2015}, \mathbf{C}_{2015}, I_{2015}, R_{2015})$$

- **Impact of climate change, with the effects of income growth:** This object measures the impact of climate change accounting for changes in income, relative to a counterfactual with those same income increases but without climate change (the "no climate change counterfactual," y^{NCC}). It shows how much changes in income drive changes in weather exposure effects under climate change, without yet allowing for adaptation to climate.

$$y^{IncGrowth} = y(\mathbf{w}_t, \mathbf{C}_{2015}, I_t, R_{2015}) - \underbrace{y(\mathbf{w}_{2015}, \mathbf{C}_{2015}, I_t, R_{2015})}_{y^{NCC}\text{, incomes increase but climate \& weather are fixed}}$$

- **Impact of climate change, with the effects of income growth and adaptation to climate:** This object measures the impact of climate change fully accounting for income growth and adaptation to climate (but without adaptation costs), relative to the no climate change counterfactual. When compared to $y^{IncGrowth}$, it shows how much additional adaptation to climate benefits yields even after

accounting for the effects of income growth, without yet incorporating adaptation costs.

$$y^{FullAdapt} = y(\mathbf{w}_t, \mathbf{C}_t, I_t, R_{2015}) - y^{NCC}$$

- **Impact of climate change with income growth, net of adaptation and its costs:** This is the final object of interest. Adding in adaptation costs (see Appendix G and Eq. G.5), it gives the projected effects of climate change on yields accounting for income growth as well as both adaptation and its costs, relative to the no climate change counterfactual.

$$y^{Total} = y^{FullAdapt} + A(\mathbf{C}_t, I_t, R_{2015})$$

y^{Total} is the object of interest displayed and discussed in Figures 2 and 3 and Table 1 in the main text of the paper.

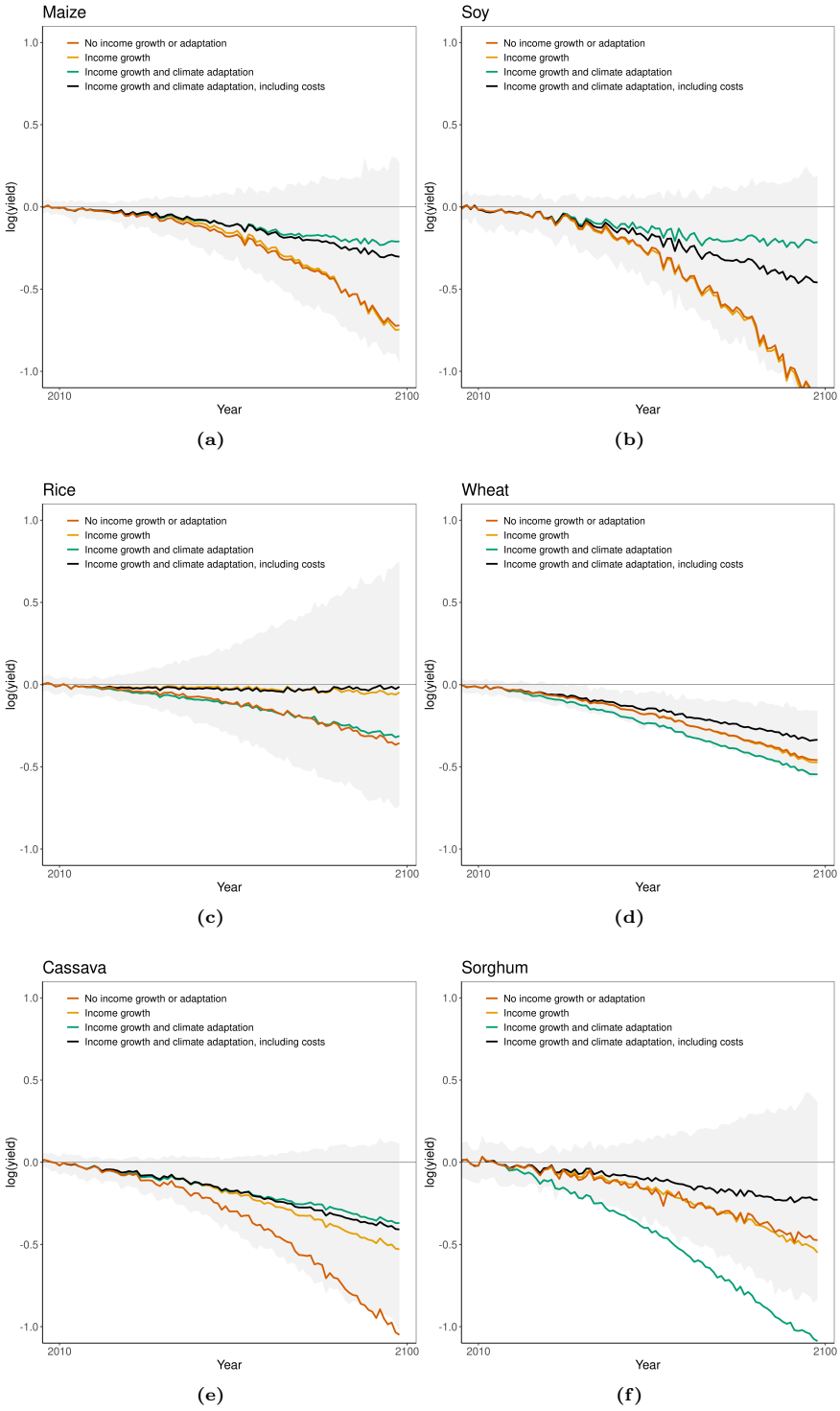
F.3 Extreme heat

In our response surface, we find negative effects of extreme heat on yields for all crops (Figure S6), and multiple studies have a similar finding (*6*). In our many of our projections for specific locations, the effect of extreme heat is gradually mitigated through costly adaptation. We constrain projections such that the marginal effect of extreme heat may become less negative, up to the point where the marginal effect is zero. We do not permit extrapolation of covariates in projections to cause sign-reversals for the effect of extreme heat, as such reversals would simply be an artifact functional form assumptions, have a nonphysical interpretation, and be inconsistent with prior findings in the literature (*6*).[11]

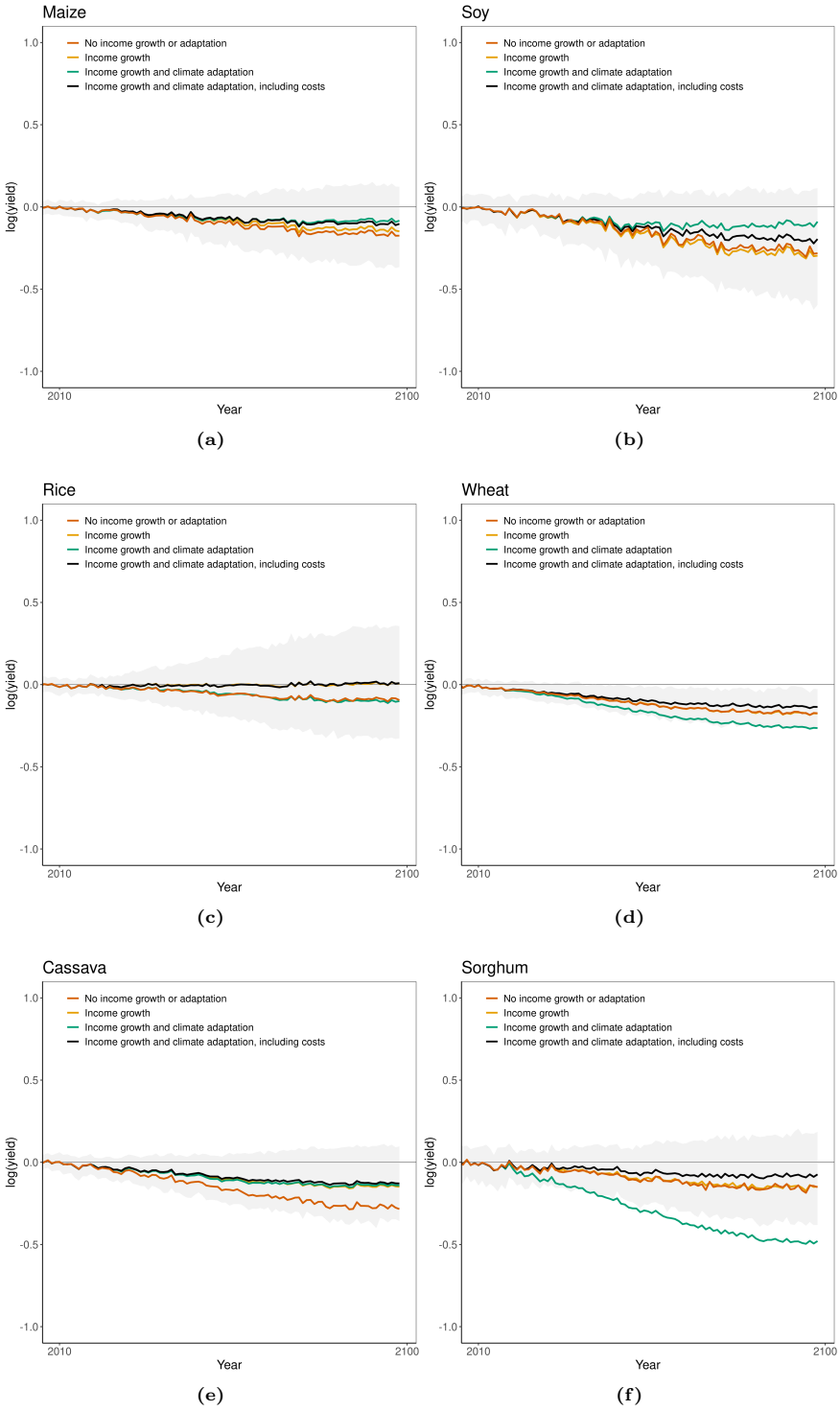
F.4 Projections: No income growth or adaptation, income growth, and income growth and climate adaptation.

All projection results up to this point have shown the "impact of climate change with income growth, net of adaptation and its costs" described in Section F.2. Here we additionally show projections for the other impacts described in Section F.2, none of which include adaptation costs: no income growth or adaptation, income growth, and income growth and climate adaptation. See Section F.2 for further details. We show these projections for RCP 8.5 (Figure S8) and for RCP 4.5 (Figure S9).

[11] If this constraint binds in a given region-year, then any additional adaptation costs associated with extreme heat in that region-year are set to zero.



Supplementary Figure S8: Projected climate impacts under: no income growth or adaptation (orange); income growth (yellow); income growth and climate adaptation (green); and income growth and climate adaptation incorporating adaptation costs (black). Crops are (a) maize, (b) soybean, (c) rice, (d) wheat, (e) cassava, and (f) sorghum. Wheat is a combination of winter wheat and spring wheat projections, weighted by their area share in each region. Incomes taken from Shared Socioeconomic Pathway 3 (SSP3) as modeled by OECD, emissions from the RCP 8.5 warming scenario.



Supplementary Figure S9: Projected climate impacts under: no income growth or adaptation (orange); income growth (yellow); income growth and climate adaptation (green); and income growth and climate adaptation incorporating adaptation costs (black). Crops are (a) maize, (b) soybean, (c) rice, (d) wheat, (e) cassava, and (f) sorghum. Wheat is a combination of winter wheat and spring wheat projections, weighted by their area share in each region. Incomes taken from Shared Socioeconomic Pathway 3 (SSP3) as modeled by OECD, emissions from the RCP 4.5 warming scenario.

G Accounting for the costs of adaptation

We estimate adaptation costs following the approach developed in refs. (*40*) adjusted to the context of producers (farmers) maximizing agricultural profits (rather than individuals maximizing utility over consumption and health, as in (*40*)).[12] Below is a brief derivation of our approach, specific to the agricultural context. Interested readers should see ref. (*40*) for a complete discussion of this approach.

Concept

We estimate the costs of adaptations that are not directly observable to us. The key idea that enables us is the idea that producers will only adapt to the climate when it is in their interest to do so. If we observe adaptation to occur, it is because it is in the interest of the producer; conversely, if adaptation does not occur that indicates that it would not be beneficial on net. Because adaptations we observe appear to make crop yields less vulnerable to extreme weather conditions, it would seem beneficial for all producers to fully adapt and protect their yields from such events. However, we also observe that many farmers do not undertake these adaptations and instead choose to remain vulnerable to weather changes. This suggests that there must exist costs to producers associated with these adaptations, such that the benefits that would accrue through reduced vulnerability do not outweigh these costs. For these producers, choosing to not further adapt to the climate is an optimal strategy. Heuristically, by observing producers that are adapting to the climate and those that are adapting less, we can infer what the unobserved costs of adaptation are. We are able to do this because we can compute what the benefits of adaptation would be for the producer who chooses not to adapt (e.g. simulate their outcomes assuming a different yield response). This bounds the magnitude of costs that the producer must face such that it is optimal for them to not adapt, since the costs must be equal to or greater than these benefits.

Simple Example

A farmer faces uncertainty over the growing season weather and makes planting decisions in order to maximize expected profits given her best guess about the distribution of potential growing season weather. Unanticipated surprises in weather – such as a particularly hot growing season – can cause correspondingly large shocks to crop yields. Based on data, we observe that a simplified version of the farmer's choices are described by Figure S10. Suppose the farmer can choose between a high average yield varietal that is also highly sensitive to extreme heat ("Yield Response$_{\text{warmer climate}}$ + adaptation cost"), and a low average yield varietal that is less sensitive to extreme heat ("Yield Response$_{\text{cooler climate}}$"). If the farmer is in a moderate climate location, where extreme heat is rare, she might choose the high average yield varietal and expect to obtain yield y_1. However, if an unexpectedly hot growing season arrives, that farmer might experience

[12] This approach builds on previous work by (*16*) and is closely related to approach developed in ref. (*92*) to account for adaptation costs implicit in GDP arising from factor reallocations. However, in that case marginal costs and benefits equalize because the outcome (total revenue in equilibrium) is maximized — therefore marginal adaptation costs do not need to be explicitly computed as they are in this agricultural context (where only yields are observed) or in the case of human health (*40*) (where benefits are accrue outside of the market).

extreme yield losses due to the varietal's high sensitivity to extreme heat (point y_3).[13]

If an incremental amount of climate change has occurred (ΔC), this same farmer now *expects* there to be more extreme heat days during the growing season. In that case, the farmer would understand that yields under the *high average* yield varietal would be *lower* on a hot day (y_3) due to the heat sensitivity of the crop varietal chosen. In response, the farmer might adapt and switch to the varietal that is more resistant to extreme heat days. If adaptation had no cost, then the farmer would obtain yield y_4. However the varietal with reduced heat sensitivity also comes with a cost, the lower average yield in this example.[14] In this case, the farmer obtains yield y_5 instead, which is still greater than y_3.

In practice, adaptation costs are not observable by the researcher, so we cannot observe the solid red line ("Yield Response$_{\text{warmer climate}}$ + adaptation cost.") We can, however, estimate the benefits of adaptation (without accounting explicitly for costs) as the dashed red line "Yield Response$_{\text{warmer climate}}$." Under the assumption of a profit-maximizing farmer, the marginal cost for the marginal increment of adaptation equals its marginal benefit. Thus, by estimating the benefits of adaptation, we also can infer by revealed preference the implied marginal costs.

For example, in Figure S10, suppose that a farmer is indifferent on the margin from adopting the practices that produce the yield responses suited for warm and cool (marginally different) climates, and has the outcome denoted at y_1. Because the costs and benefits of the marginal increment of adaptation must be equal, we infer that the underlying adaptations that alter the yield response curve (moving the outcome from y_1 to y_2) – the marginal benefit of adaptation – must be offset by a marginal cost of adaptation that is equal in magnitude: the vertical offset between the dashed red line and the solid red line. These adaptation costs could be average yield effects, or could be associated with monetary expenditures valued in terms of crop yields. To our knowledge, this point was first described by in (*16*). In what follows, we build on this intuition and generalize it so that it may be applied to more complex yield functions where continuous producer adaptations are responding to multiple dimensions of the climate. The remainder of this appendix formally derives the complete approach that we implement empirically.

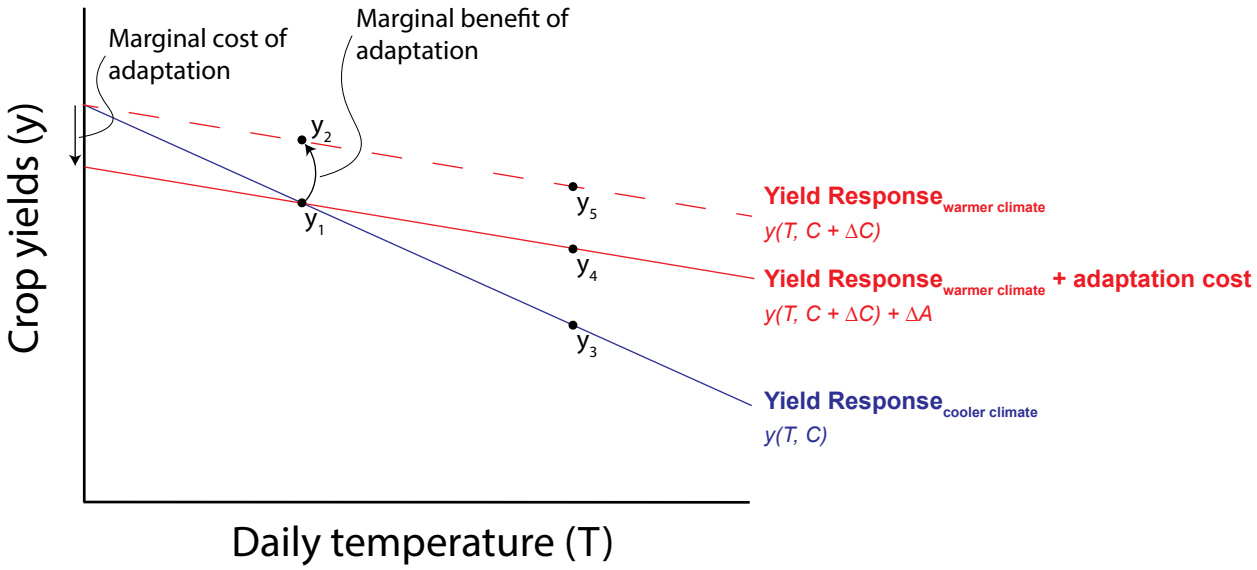
Formalization: Profit maximization

Assume the complete range of all producer-level adaptation actions are captured by the elements of vector **b**, they are continuous, they do not have fixed costs, and they are not durable (do not persist over time) (*38*). Area planted and prices are held fixed relative to a marginal climatic shock, and producers are each individually assumed to be price-takers, they are risk neutral and they have unconstrained access to credit. Note that we account for aggregate (non-marginal) cropped area and price effects in our valuation approach (Section J).

Let profits π be determined by area planted L, yield per acre y, prices p, and costs per acre A. Following ref. (*38*), we use the vector **b** to denote the arbitrarily large set of unobserved adaptive actions producers may take in the course of cultivating staple crops. Denote weather **w** as the vector

[13] Likewise, unexpected yield gains could occur if the temperature is cooler than expected.

[14] Whether or not yields are on average lower, other costs can be converted to units of yield for this purpose.



Supplementary Figure S10: Adaptation costs and benefits in equilibrium Cartoon illustrating the our approach to estimating marginal adaptation costs (Eq. G.4). Crop yields are a function of daily temperature, simplified as a downward sloping line (the actual functions estimated are more complex). The solid blue line is the response of yields in a cooler climate. The dashed red line is the response of yields in a hotter climate, after populations adapt to the warmer climate. The solid red line is yields in the hotter climate, net of the costs of adaptation (expressed in units of crop yield). Adaptation costs are the vertical offset between solid red and dashed red lines. Adaptation costs cannot be observed directly, but they must be present in order for both modes of production in both climates to exist simultaneously in equilibrium, as we observe in data. To see this, note that a profit-maximizing farmer will adapt until the marginal costs and benefits of the next adaptive action just offset. Thus, y_1 is the net productivity (net of adaptation costs) on cooler days under farmer choices in a cooler climate as well as farmer choices in a marginally warmer climate. But without costs to adaptation, the farmer could use the adapted technology to achieve $y_2 > y_1$, yet the farmer is observed to chose y_1. This implies that there is an unobserved cost (vertical displacement from red dashed line to solid red line) that is sufficiently large that it equalizes the net output of the two technologies (adapted and unadapted). At a higher temperature, the outcome y_3 resulting from unadapted technology can be be improved by using the adapted technology (output at y_5) but requires an adaptation cost is incurred, producing the net output at y_4. Calculations in our actual implementation follow the same intuition, but address nonlinear functions and multiple dimensions of adaptation affecting multiple weather variables. Figure adapted from Schlenker, Roberts, and Lobell (2013).

$(GDD, KDD, prcp, prcp^2, tmin, VPD)$[15] and climate $\mathbf{C}$ as the vector $(\bar{T}, \bar{P}, \bar{T} \times \bar{P})$. Then in each period, profit is given by

$$\pi = Ly(\mathbf{w}, \mathbf{b}, \boldsymbol{s})p - LA(\mathbf{b}, \boldsymbol{s})$$

where $\boldsymbol{s}$ represents a vector of weather-invariant and additively seperable cost and/or yield shifters (e.g. soil quality). Profit maximizing producers choose a set of optimal adaptations $\mathbf{b}^*$ at the start of the growing season, which must satisfy the following first-order conditions[16] that equalizes the expected marginal benefits and marginal costs of each form of adaptation:

$$\frac{\partial E[\pi]}{\partial \mathbf{b}} = L\left[\frac{\partial E[y]}{\partial \mathbf{b}}p - \frac{\partial A}{\partial \mathbf{b}}\right] = 0$$

$$\frac{\partial E[y]}{\partial \mathbf{b}}p = \frac{\partial A}{\partial \mathbf{b}} \tag{G.1}$$

which each producer solves (perhaps through trial-and-error, in practice) based on their local climate and resources (income I and irrigation R):

$$\implies \mathbf{b}^* = \mathbf{b}^*(\mathbf{C}, I, R)$$

Thus, the vector of adaptive actions adopted by each producer is a function of local climate conditions.

Estimating the cost of adapting to climate change

Marginal damages from climate change can be quantified as the total derivative of realized producer profits π with respect to a change in the long-run climate.[17] Assuming optimal adaptation, differentiating realized profits with respect to climate we obtain

$$\frac{d\pi}{d\mathbf{C}} = L\left[p\frac{dy}{d\mathbf{C}} - \frac{\partial A}{\partial \mathbf{b}}\frac{\partial \mathbf{b}^*}{\partial \mathbf{C}}\right]. \tag{G.2}$$

where $\dfrac{\partial \mathbf{b}^*}{\partial \mathbf{C}}$ is the Jacobian describing the change in each dimension of optimal adaptation associated with an incremental change in each dimension of climate. We wish to substitute out the derivative of costs A because it is unobserved. Substituting for $\dfrac{\partial A}{\partial \mathbf{b}}$ from Equation G.1 yields

$$\frac{d\pi}{d\mathbf{C}} = L\left[p\frac{dy}{d\mathbf{C}} - p\frac{\partial E[y]}{\partial \mathbf{b}}\frac{\partial \mathbf{b}^*}{\partial \mathbf{C}}\right]. \tag{G.3}$$

[15] This is the full set of potential terms in $\mathbf{w}$ that can be reliably projected by climate models; for any given crop $\mathbf{w}$ is restricted by our cross validation process (see Appendix A.2).

[16] Note that a derivative with respect to the vector $\mathbf{b}$ is a vector of derivatives with respect to each element of $\mathbf{b}$.

[17] Note that producers make adaptation decisions (Eq. G.1) based on their expectation of yields at the start of the growing season, but climate damages are the effect of climate change on realized profits.

To obtain an expression for $\frac{\partial E[y]}{\partial \mathbf{b}}\frac{\partial \mathbf{b}^*}{\partial \mathbf{C}}$ that is measurable with data, we take the total derivative of expected yields with respect to climate

$$\frac{dE[y]}{d\mathbf{C}} = \underbrace{\frac{\partial E[y]}{\partial \mathbf{b}}\frac{\partial \mathbf{b}^*}{\partial \mathbf{C}}}_{\text{Expected effect of adaptations}} + \underbrace{\frac{\partial E[y]}{\partial \mathbf{w}}\frac{\partial \mathbf{w}}{\partial \mathbf{C}}}_{\text{Expected effect of } \Delta\text{weather}}$$

which can be rearranged as

$$\frac{\partial E[y]}{\partial \mathbf{b}}\frac{\partial \mathbf{b}^*}{\partial \mathbf{C}} = \frac{dE[y]}{d\mathbf{C}} - \frac{\partial E[y]}{\partial \mathbf{w}}\frac{\partial \mathbf{w}}{\partial \mathbf{C}} \tag{G.4}$$

expressing $\frac{\partial E[y]}{\partial \mathbf{b}}\frac{\partial \mathbf{b}^*}{\partial \mathbf{C}}$ in terms of observable quantities. Equation G.4 states that the expected marginal gains from adaptation to a change in $\mathbf{C}$ equal the observable effects of climate changes (when populations adapt) minus marginal losses that would occur due to unexpected weather changes that do not allow for long run adaptations. Note that by multiplying both sides of Equation G.1 by $\frac{1}{p}\frac{\partial \mathbf{b}^*}{\partial \mathbf{C}}$ and comparing it to G.4, it is clear that Equation G.4 also captures the costs of adaptation that result from marginal climate changes, expressed in units of crop yields that possess equivalent monetary value.[18] This result is illustrated in Figure S10.

Substituting Equation G.4 into Equation G.3 gives

$$\frac{d\pi}{d\mathbf{C}} = pL\Bigg[\underbrace{\frac{dy}{d\mathbf{C}}}_{\substack{\text{Fully adapted effects}\\ \text{of climate change}\\ \text{on crop yields}}} - \underbrace{\left(\frac{dE[y]}{d\mathbf{C}} - \frac{\partial E[y]}{\partial \mathbf{w}}\frac{\partial \mathbf{w}}{\partial \mathbf{C}}\right)}_{\substack{\text{Estimated marginal adaptation costs}\\ \frac{1}{p}\frac{\partial A}{\partial \mathbf{b}}\frac{\partial \mathbf{b}^*}{\partial \mathbf{C}}}}\Bigg]. \tag{G.5}$$

which on the right-hand side are all terms that can be estimated empirically. Thus, estimating the derivative of yields with respect to climate and with respect to weather allows us to compute the elements of Equation G.5 and the terms in Equation G.2 describing both the impact on yields and adaptation costs resulting from marginal changes in climate.

The fully adapted effects of climate change $\frac{dy}{d\mathbf{C}}$ in Equation G.5 are captured by empirically estimating the relationship between yield and weather in our historical data, conditional on the factors (e.g. climate, income, irrigation) that determine this relationship (Equations A.8-A.10). In estimates of future climate impacts, the distribution of weather that is estimated to occur in each climate condition is projected onto these functions. This captures both the direct effect of weather changes and the benefits of adaptation, but not adaptation costs.

To estimate total adaptation costs, we integrate marginal adaptation costs in the second term of Equation G.5 following the numerical implementation developed in ref. (*40*). That is, the total adaptation costs

[18] The total adaptation benefits associated with the climate shifting from $\mathbf{C}_1$ to $\mathbf{C}_2$ are defined as the dollar value of the difference between the effects of climate change with optimal adaptation and without any adaptation. In contrast to total adaptation costs, this expression relies on the relationship between yields and temperature that holds only at the final climate, $\mathbf{C}_2$. Therefore, when the marginal benefits of adaptation are greater at the final climate than at previous climates, the total benefits of adaptation will exceed total adaptation costs, generating an adaptation "surplus." For example, at a climate between $\mathbf{C}_1$ and $\mathbf{C}_2$, the marginal unit of heat-stress resilience in the choice of maize varietal will have benefits that are exactly equal to its costs. However, at the warmer climate $\mathbf{C}_2$, this same unit of heat-stress resilience becomes inframarginal, and may have benefits that exceed its costs. Ref. (*40*) derives a formal expression for this adaptation surplus.

associated with the climate shifting from some initial state $\mathbf{C}_1$ to a later state $\mathbf{C}_2$ are calculated by integrating the estimable terms from Equation G.5 over a series of small changes in climate. These terms continually evolve with the changing climate $\mathbf{C}$ and are specific to each region in each year. Total adaptation costs in a given period, relative to a baseline period, are the sum of all marginal changes that have been integrated over in preceding periods.

Combining the effects of warming on yields, net of adaptation benefits, with adaptation costs allows us to compute changes in total profits. Damages that result from the climate changing gradually evolving from $\mathbf{C}_1$ to $\mathbf{C}_2$ are then:

$$\pi(T(\mathbf{C}_2), \mathbf{b}(\mathbf{C}_2, I_2, R_2)) - \pi(T(\mathbf{C}_1), b(\mathbf{C}_1, I_2, R_2)) = \int_{\mathbf{C}_1}^{\mathbf{C}_2} \frac{d\pi}{d\mathbf{C}} d\mathbf{C}$$

Which is solved by substituting terms from Eq. G.5. In welfare calculations, these damages can be discounted based on the period in which they occur.

H Projections: Additional Results and Robustness

In this section we display extensions of the main text projection results, results for other scenarios of emissions, and additional robustness checks. Section H.1 shows projection results similar to those in the main text, but for all regions under RCP 8.5, rather than just those that grow the crop in the present day. Section H.2 shows projection results similar to those in Section H.1, but for the RCP 4.5 scenario instead of the RCP 8.5 scenario. Note that our estimates of the economic value of climate change on agriculture use results from a harmonization of both scenarios via their transformation into a damage function. Section H.3 contains figures analogous to Figure 3 in the main text, but using 16 regional aggregates that correspond to the FUND model's regional aggregates (*110*). Section H.4 shows summary results under varying degrees of adaptation along with CO_2 fertilization. Section H.5 contains sensitivity tests for our assumptions regarding the effect of future weather that is outside of the support of the historical data used to estimate our model (Figure S16).

H.1 Projection results for RCP 8.5, all regions

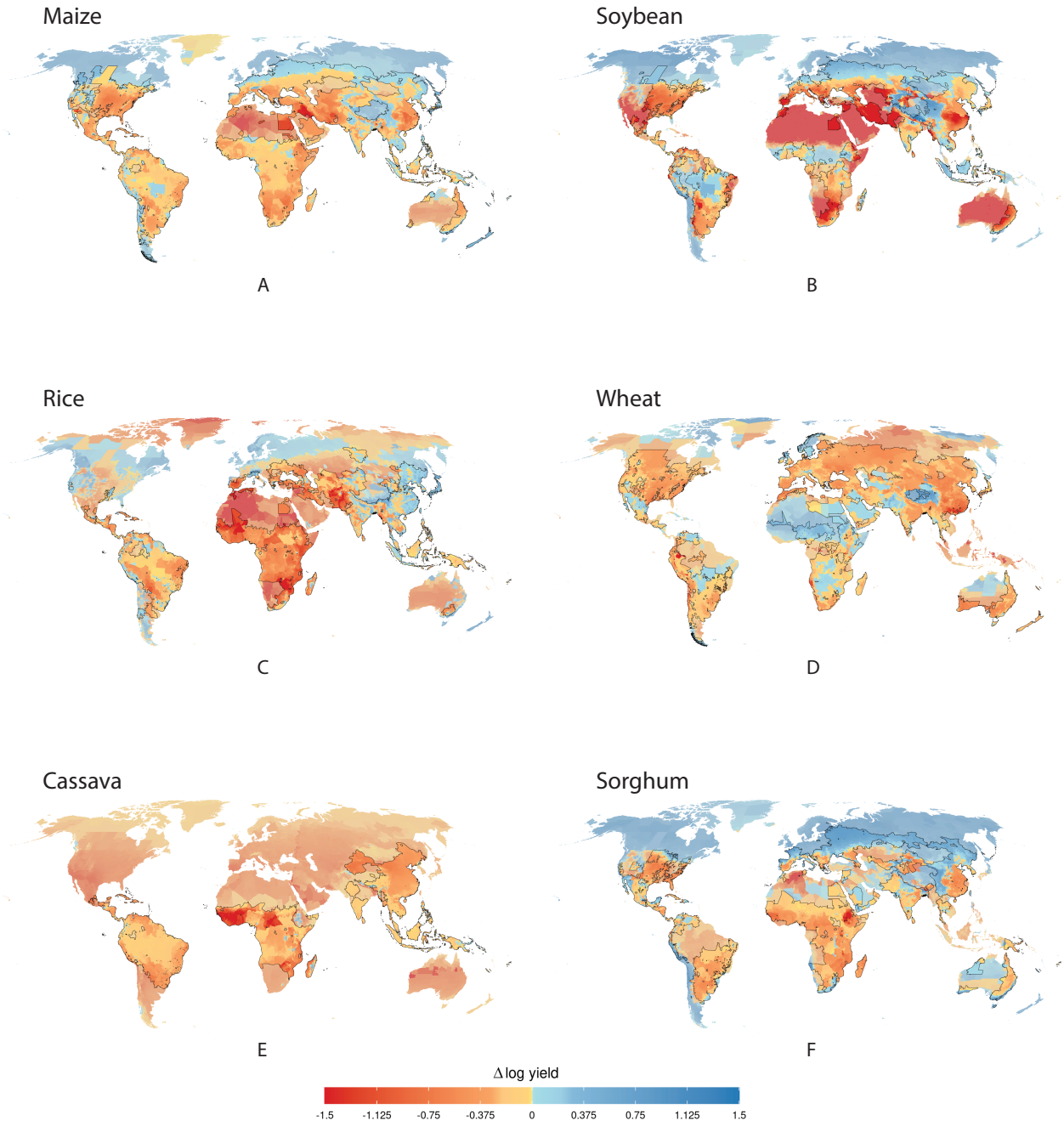
Here we show projection results analogous to Figure 2 in the main text, still for the RCP 8.5 emissions scenario, but here showing all regions in the world, not just those that grow a given crop in the present day (Figure S11). Regions that are currently cropped for each staple are outlined in black. Currently uncropped regions are shaded and colors depict a theoretical change in yield that is not observable. Projected impacts in regions where a crop is not presently grown may represent percentage yield impacts off of a very low baseline yield (e.g. yield gains estimated for Northern Canada and Siberia).

H.2 Projection results for RCP 4.5

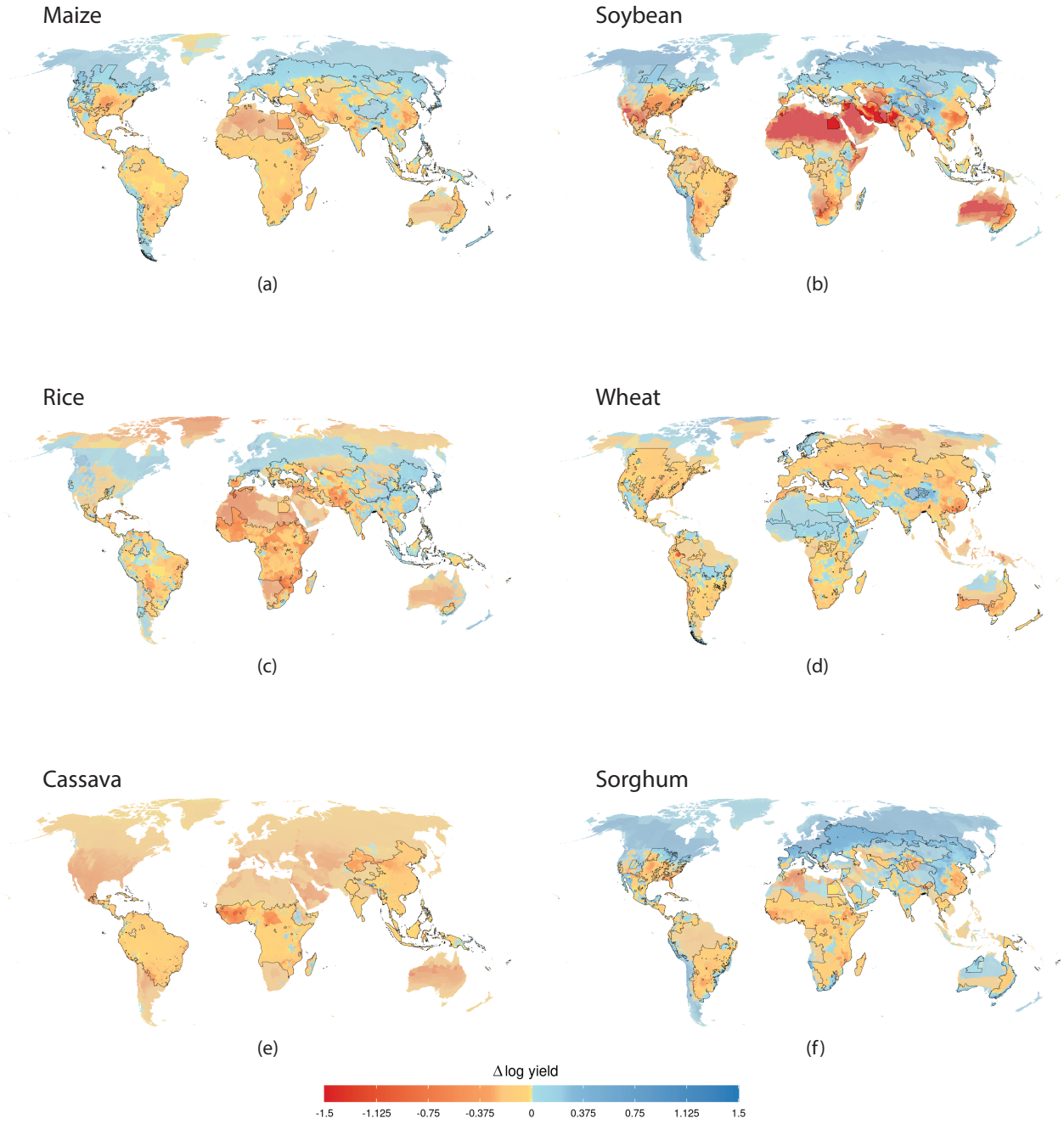
Here we show projection results analogous to Figures 2 and 3 in the main text, but for the RCP 4.5 emissions scenario and all regions in the world (Figures S12 and S13). Lower temperature changes lead to lower overall impacts of warming across all 6 crops, with a number of regions of the world switching from exhibiting negative impacts to exhibiting positive impacts. However, as seen from Figure S13, the central estimate for the aggregated global effect of warming remains negative for all crops (though rice remains close to a zero effect) even in RCP 4.5.

H.3 Regional aggregate results

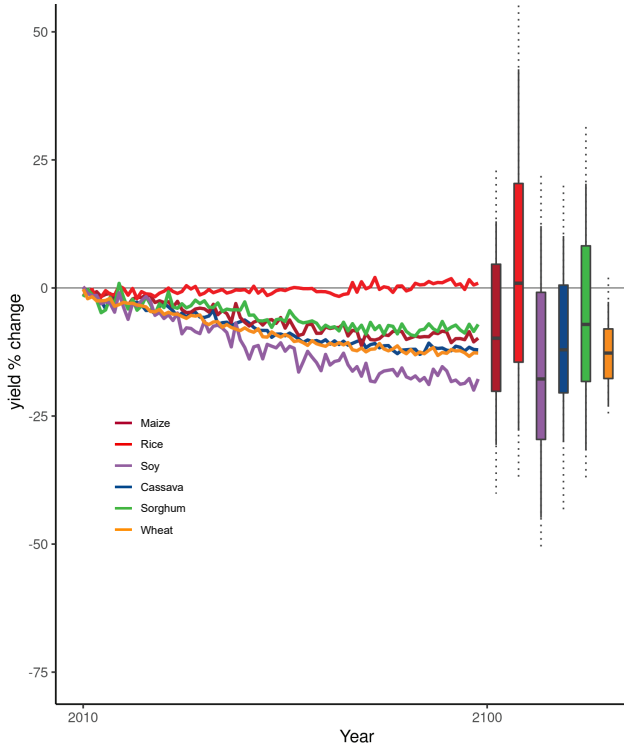
Figures S14 and S15 display aggregated impacts for a set of 16 regions over time. These figures are analogous to Figure 2 in the main text but each panel represents a region of the world as defined in the FUND model (*110*). Each time series is constructed by aggregating impact-region yield projections weighted by their cropped area, showing all crops covering at least 0.2% of harvested area within a given FUND region. Regional results are shown for both RCP 8.5 (Figure S14) and RCP 4.5 (Figure S15). Crops losses are substantial in many of the world's most important growing regions, but there exists substantial regional



Supplementary Figure S11: Projected end-of-century change in log crop yields due to climate change, accounting for adaptation to climate and rising incomes. Colors indicate central estimate in a high emissions (RCP 8.5) scenario, net of estimated adaptation costs, for (a) maize, (b) soybean, (c) rice, (d) wheat, (e) cassava, and (f) sorghum for 2089 - 2098. Regions that are currently cropped for each staple are outlined in black. Currently uncropped regions are shaded and colors depict a theoretical change in yield that is not observable. Wheat is a combination of winter wheat and spring wheat projections, weighted by their area share in each region. Incomes are from Shared Socioeconomic Pathway 3 (SSP3) (*44*). Results for RCP 4.5 are shown in SI Figure S12 and for CO_2 fertilization in Appendix I.

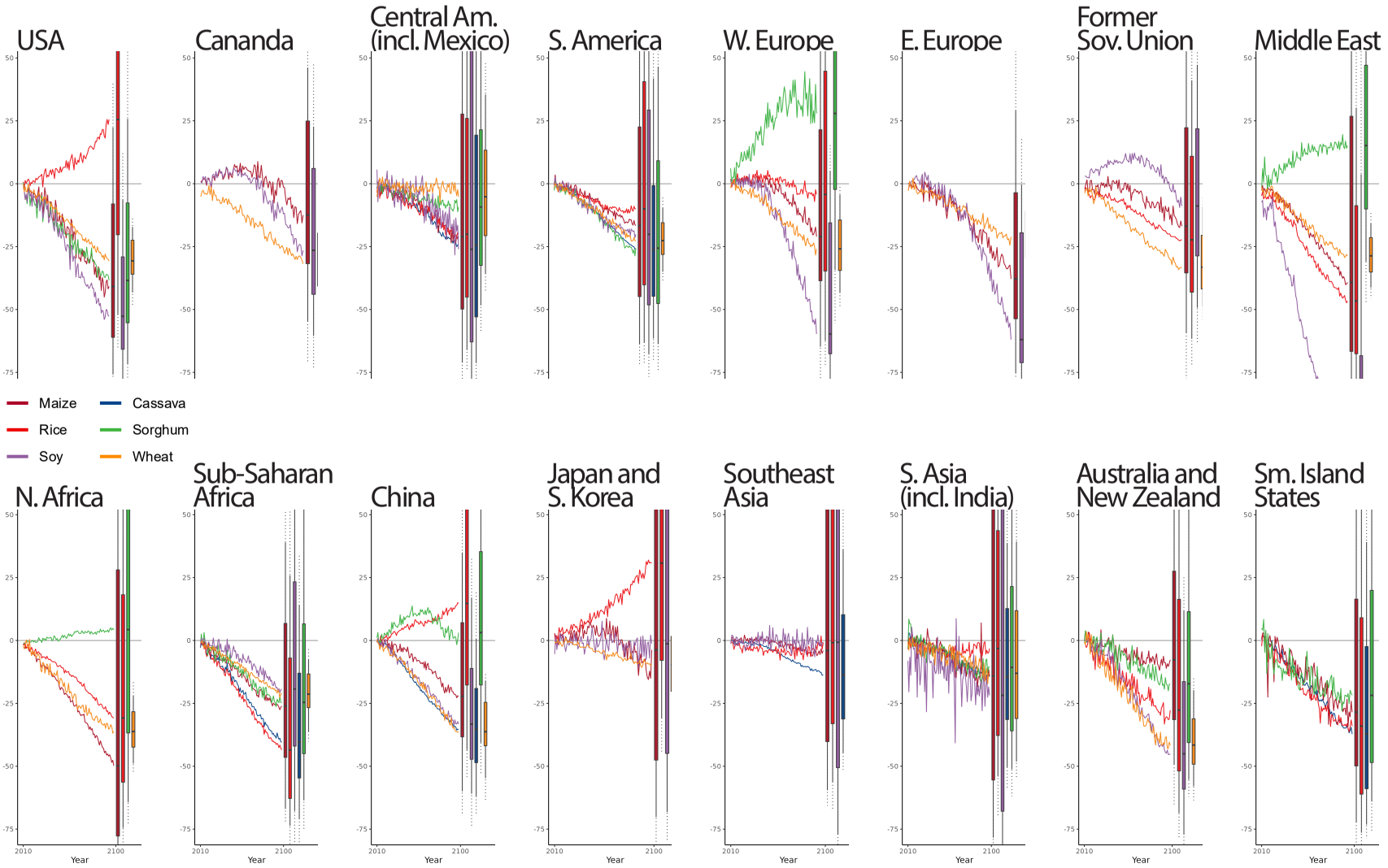


Supplementary Figure S12: Projected climate impacts under income growth and climate adaptation, including adaptation costs, for (a) maize, (b) soybean, (c) rice, (d) wheat, (e) cassava, and (f) sorghum; for the end-of-century decade 2089 - 2098. Wheat is a combination of winter wheat and spring wheat projections, weighted by their area share in each region. Incomes taken from Shared Socioeconomic Pathway 3 (SSP3) as modeled by OECD, emissions from the RCP 4.5 warming scenario. Results for RCP 8.5 are shown in Figure 2.

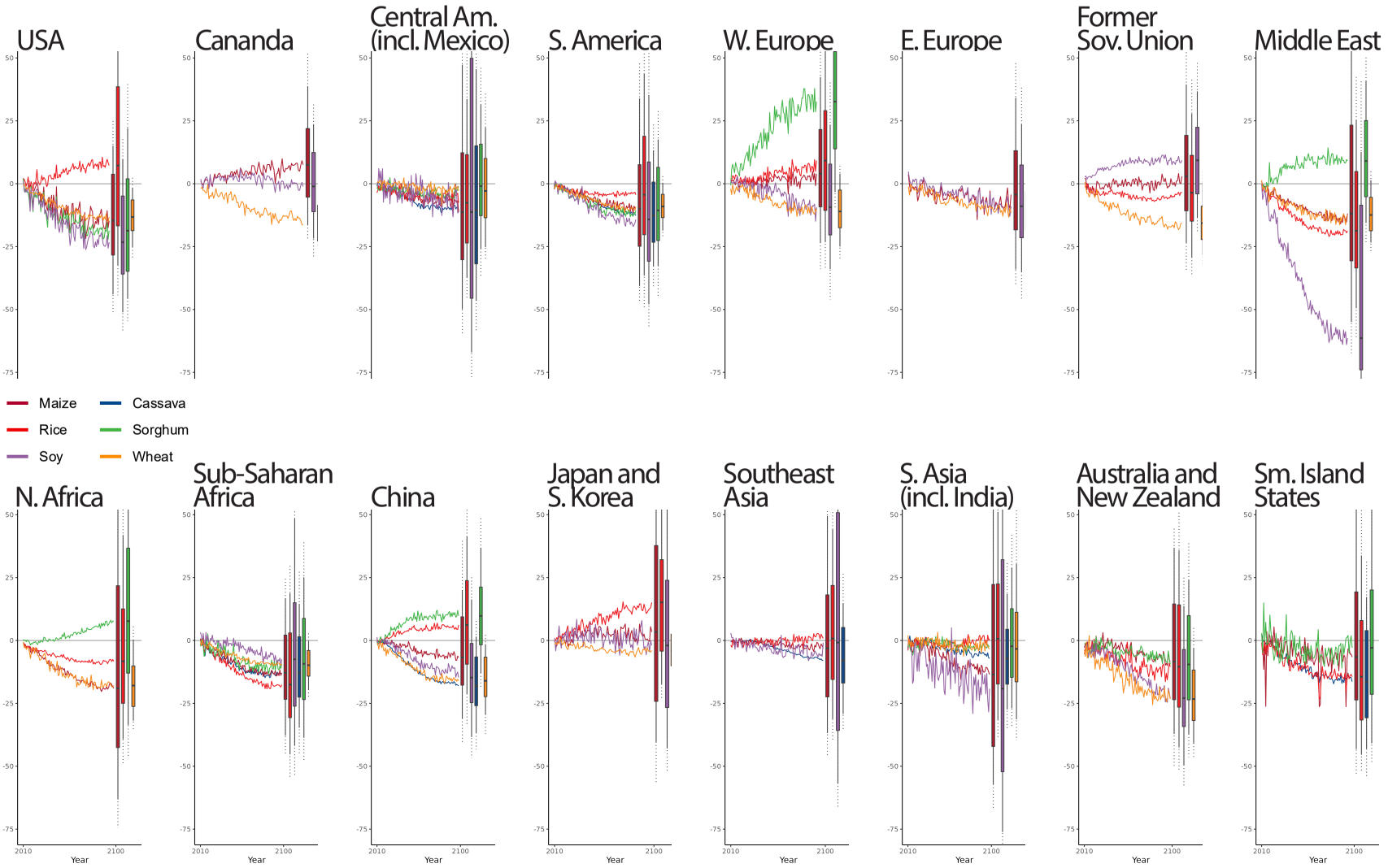


Supplementary Figure S13: Time series of global average climate impacts to grain yields, net of costly producer adaptation and accounting for income growth, for the RCP 4.5 warming scenario. Averages were calculated using crop-specific area weights from SAGE. Box and whisker plots show joint uncertainty in end-of-century impacts over both Monte Carlo statistical uncertainty and 33 climate models. See Figure 3 for the corresponding RCP 8.5 result.

heterogeneity for most crops. Rice often exhibits large benefits of warming due to gains from daily minimum temperatures under adaptation. We also find that Sorghum, a crop that is traditionally grown in drought-prone, warmer, or arid regions, would benefit from warming in areas that currently do not grow much sorghum (e.g. Western Europe). Other crops show varying levels of negative impacts across regions.



Supplementary Figure S14: Time series of global average climate impacts to grain yields, net of costly producer adaptation and accounting for income growth, for the RCP 8.5 warming scenario. Averages calculated using crop-specific area weights from SAGE. The regions shown correspond to region definitions in the FUND model. Box and whisker plots show joint uncertainty in end-of-century impacts over both Monte Carlo statistical uncertainty and 33 climate models. See Figure S15 for the corresponding RCP 4.5 result.



Supplementary Figure S15: Time series of global average climate impacts to grain yields, net of costly producer adaptation and accounting for income growth, for the RCP 4.5 warming scenario. Averages calculated using crop-specific area weights from SAGE. The regions shown correspond to region definitions in the FUND model. Box and whisker plots show joint uncertainty in end-of-century impacts over both Monte Carlo statistical uncertainty and 33 climate models. See Figure S14 for the corresponding RCP 8.5 result.

H.4 Global aggregate results

Table S10 displays crop-specific global projections and aggregate caloric regional projections of yield impacts for mid-century and end-of-century under a high emissions scenario. Impacts are shown for the case of no income benefits nor climate adaptation; income benefits and climate adaptation; and income benefits, climate adaptation, and CO_2 fertilization effects.

	2050			2098		
	(1a) Producer behavior unchanged	(1b) Accounting for adaptation & development	1(c) Adaption, development, & CO_2 fertilization	(2a) Producer behavior unchanged	(2b) Accounting for adaptation & development	2(c) Adaption, development, & CO_2 fertilization
Maize	-12.6	-8	-4.4	-51.4	-26.1	-21.1
	[-23.3,-4]	[-28.7,16.3]	[-25.2,19.9]	[-83,-17.1]	[-68,50.8]	[-63,55.8]
Rice	-8.8	-2.6	3.4	-29.9	-1.3	8.2
	[-16.9,-0.5]	[-28.7,-35.1]	[-22.7,41.1]	[-61,-9.2]	[-66.3,177.7]	[-56.8,187.2]
Soy	-18.1	-12	-6	-68	-36.8	-27.3
	[-35.2,-3.4]	[-37.1,17]	[-31.1,23.1]	[-93.3,-27.5]	[-76,47.1]	[-66.5,56.6]
Wheat	-14.4	-12.3	-6.2	-36.8	-28.5	-19
	[-24,-4.4]	[-23.2,-2.5]	[-17.2,3.5]	[-59.5,-16.9]	[-45.7,-11.6]	[-36.1,-2]
Sorghum	-13.9	-8.3	-4.8	-37.8	-20.4	-15.3
	[-30.7,1.6]	[-33.9,20.9]	[-30.3,24.5]	[-66.3,-9.7]	[-67.4,76.3]	[-62.4,81.4]
Cassava	-21.6	-13.7	-7.7	-65	-33.5	-24
	[-44.3,-4.8]	[-34.7,7.4]	[-28.7,13.4]	[-91.3,-29.9]	[-75.4,31.3]	[-65.9,40.8]
All crops (% calories)	-13.4	-9	-3.7	-45	-23.7	-15.5
	[-24.7,-3]	[-28.5,13.3]	[-23.2,18.6]	[-75,-16.6]	[-62.8,43.8]	[-54.6,51.9]

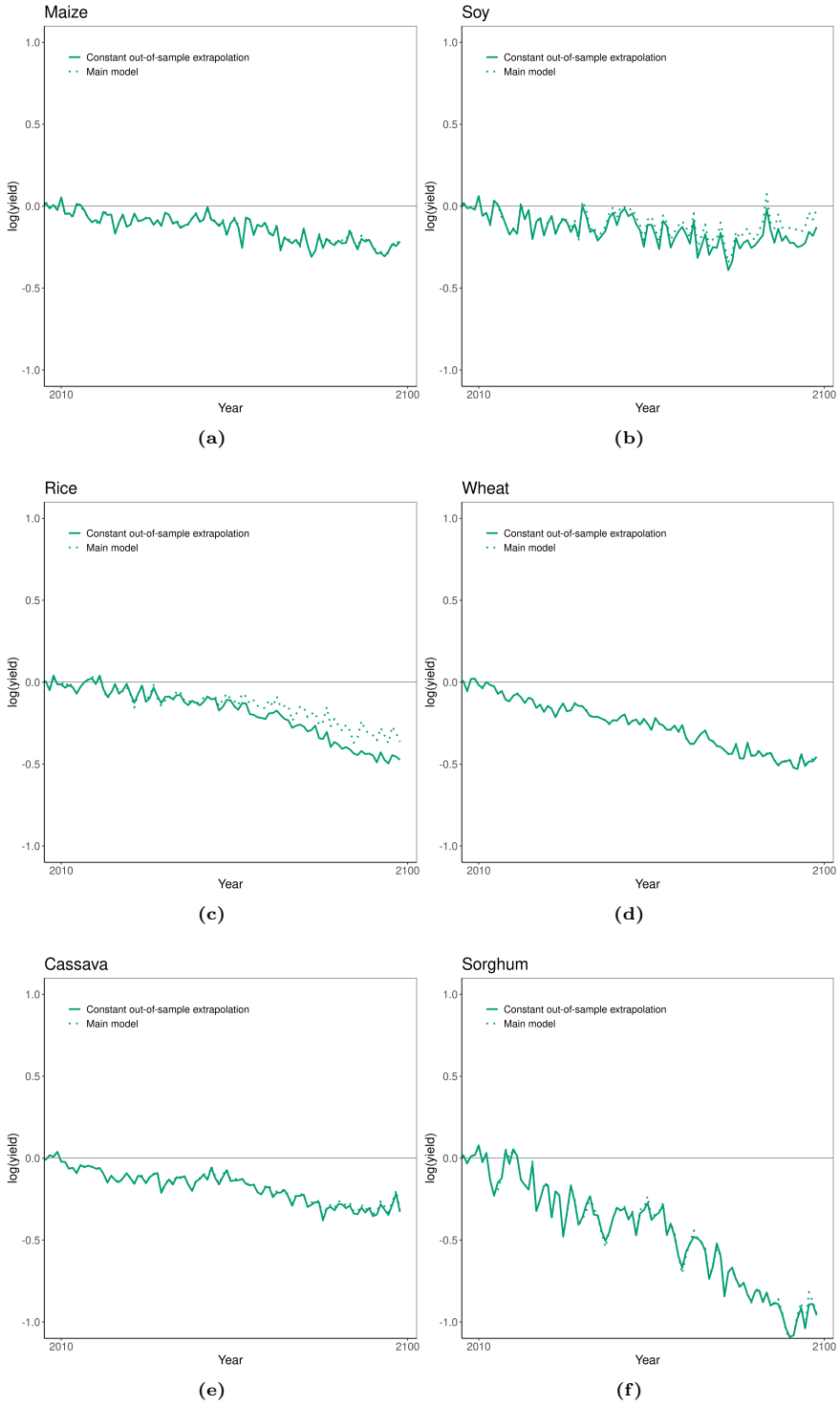
Supplementary Table S10: Projected changes in global average crop yields due to climate change, comparing estimates without adaptation, with adaptation, and with adaptation and CO_2 fertilization. Values indicate estimates in a high emissions (RCP 8.5) scenario, without climate adaptation nor income growth benefits (columns [·]a), with climate adaptation net of estimated adaptation costs and income growth benefits (columns [·]b), and additionally with CO_2 fertilization effects (columns [·]c) for mid-century (columns 1a – 1c) and end-of-century (columns 2a – 2c). Global estimates are of yield % changes by crop, and for total calories across all crops studied. Uncertainty by crop is shown in Figure 3A. Global averages for each crop were calculated using crop-specific area weights from SAGE; total calorie changes were calculated using crop-specific area weights from SAGE and caloric weights from ref. (*97*). Values in brackets represent the 5^{th} and 95^{th} percentiles of the distribution of yield % changes over climate model and statistical uncertainty. Note: averages and distributions shown here are for all high-emissions climate models, regardless of the level of warming, and should not be confused with any particular point on the calorie damage function (Figure 3D).

H.5 Additional projection results and robustness checks

Edge restriction in projections. A concern associated with projecting the impacts of climate change is that future temperature and precipitation exposures may fall outside of the historical support of the data used to estimate our empirical yield responses. Here we test the sensitivity of our projected impacts to an alternative assumption about the shape of the yield response surface outside of the historical support of our data: for all temperature and precipitation values outside of the historical support of our data we set the marginal yield response to zero. This corresponds to a constant out-of-sample extrapolation of our model. We use a single set of cutoffs for all crops: 40C (t_{max}), 400mm (monthly precip.), and 23C ($t_m in$) – the percentiles of each crop's historical distribution reflected by these cutoffs is given in Table S11. As Figure S16 shows, projected incremental impacts from weather exposure outside the historical support of our data only minimally affect our overall results across all crops.

Crop	Tmax	Precipitation	Tmin
Corn	99.5%	98.5%	93.3%
Rice	99.8%	96.5%	88.8%
Soy	99.6%	99.4%	98.5%
Sorghum	99.5%	99.6%	97.1%
Cassava	99.9%	97.6%	92.3%
Spring wheat	99.5%	99.6%	99.4%
Winter wheat	99.8%	99.9%	99.7%

Supplementary Table S11: Percentiles of the temperature and precipitation historical data at which the cutoff values given in the text fall, by crop, used in the constant out-of-sample extrapolation results of Figure S16.



Supplementary Figure S16: Projected climate impacts for: income growth and climate adaptation under our main model (solid green line), and income growth and climate adaptation with constant out-of-sample extrapolation of our model (dashed green line). Crops are (a) maize, (b) soybean, (c) rice, (d) wheat, (e) cassava, and (f) sorghum. Wheat is a combination of winter wheat and spring wheat projections, weighted by their area share in each region. Incomes taken from Shared Socioeconomic Pathway 3 (SSP3) as modeled by OECD, emissions from the RCP 8.5 warming scenario. This set of projections was run with only the CCSM4 climate model.

I Projections: Accounting for CO_2 Fertilization

As part of their growth process, plants consume CO_2 and convert it to biologically useful sugars. CO_2 fertilization is the process by which many types of plants are able to increase their consumption of CO_2 – and hence increase their growth and yields – as atmospheric CO_2 concentrations rise. For these types of plants, the biological process by which CO_2 is transformed into sugars is limited by the available amount of CO_2 in the atmosphere (*63*); these plants are termed "C3" plants and include the crops soybeans, rice, wheat, and cassava. Conversely, "C4" plants have evolved to increase their internal concentrations of CO_2 to three or more times atmospheric concentrations and as such their biological conversion of CO_2 to sugars is not as constrained by atmospheric CO_2 levels. These C4 crops, which include maize and sorghum, do not benefit as much from the CO_2 fertilization effect (*62*, *63*, *64*).

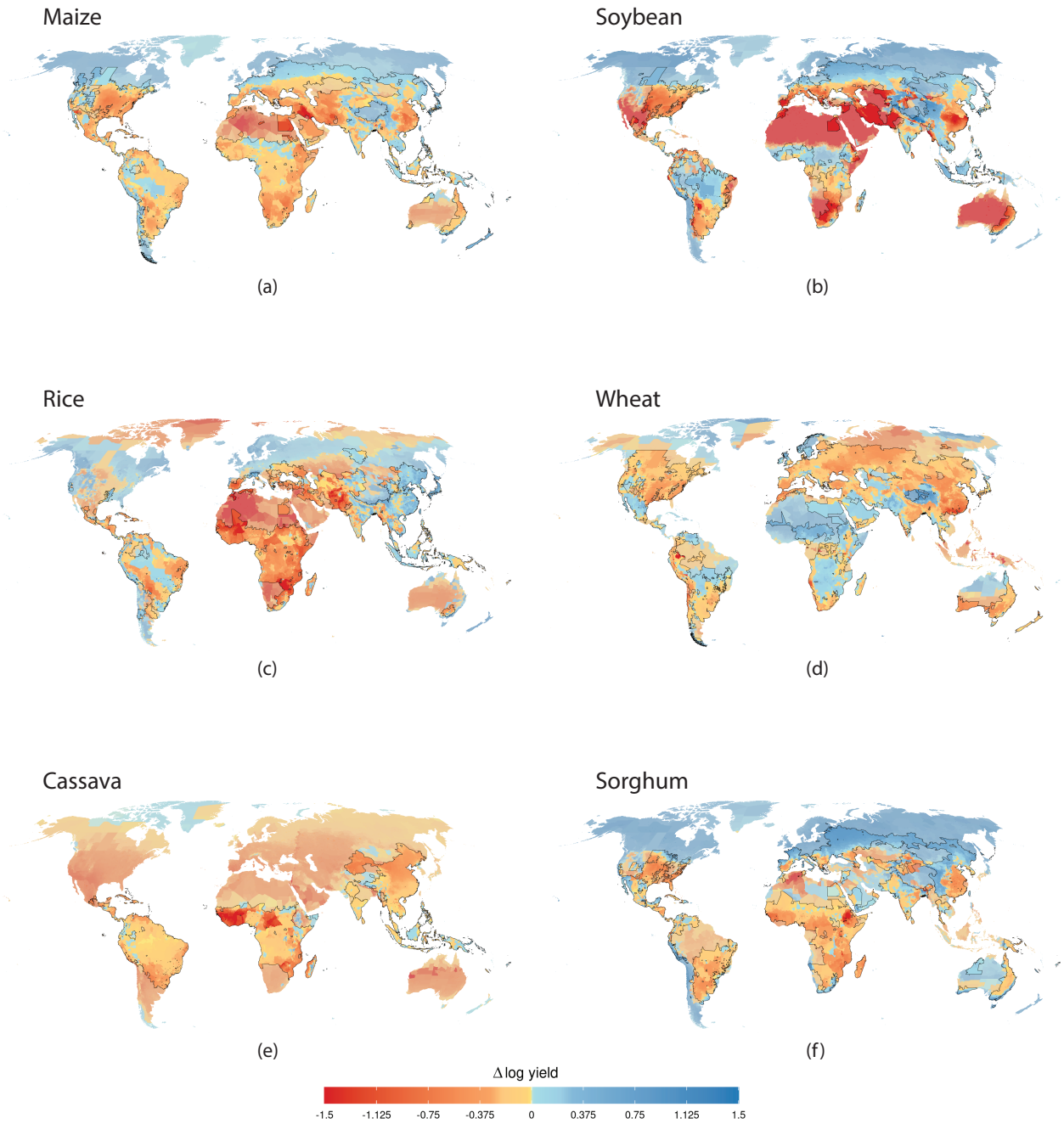
Here, we draw on estimates of the CO_2 fertilization effect for C3 and C4 crops from a recent meta-analysis of the literature (*13*). This analysis estimates the CO_2 fertilization effect (in percentage points) on yields as

$$CO_2_fertilization_{ij} = \beta_i \frac{\Delta CO_{2_{ij}}}{\Delta CO_{2_{ij}} + A_i}$$

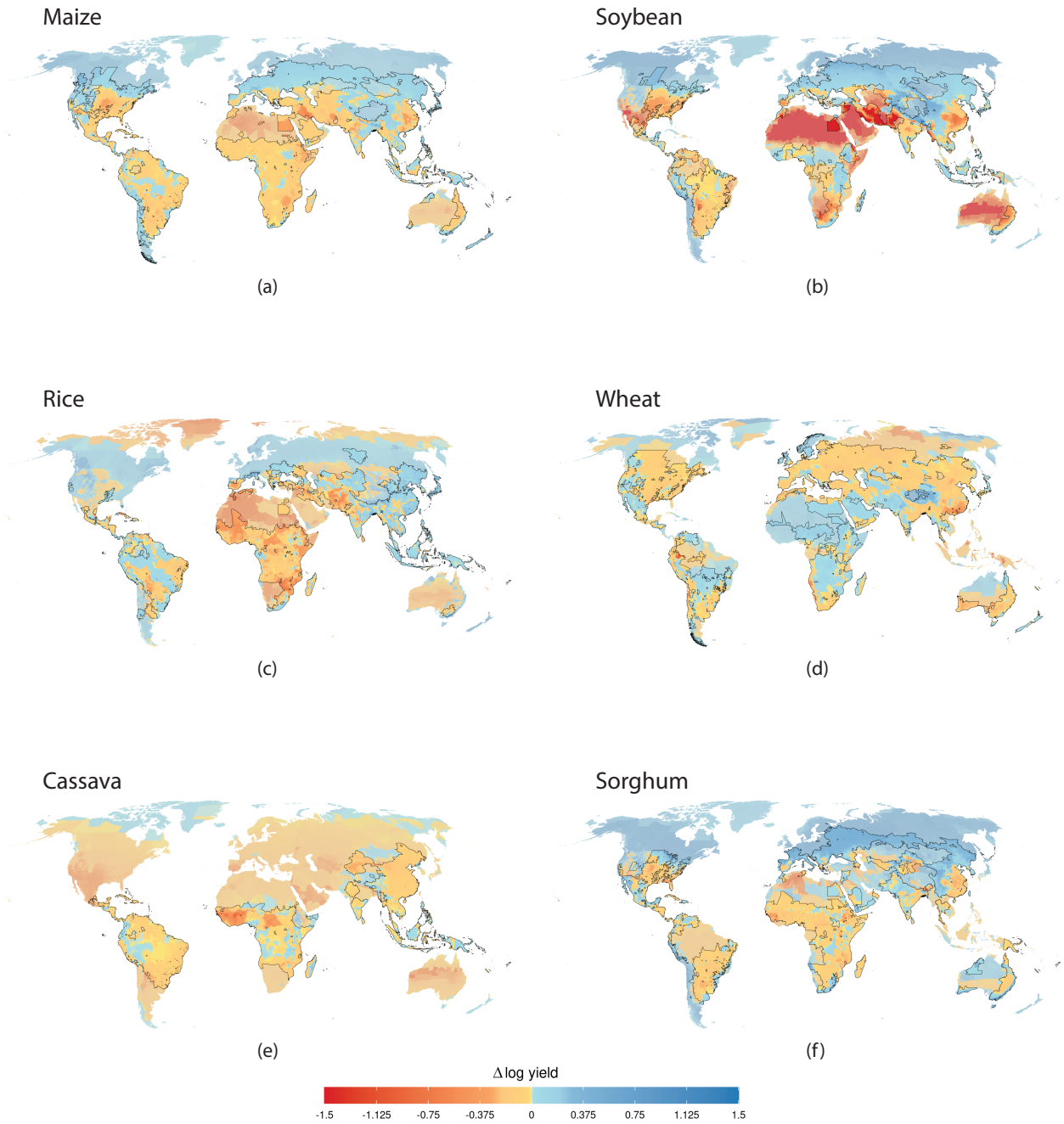
where i indexes C3 or C4, j indexes studies in the meta-analysis, A_i takes a value of 100ppm for C3 crops and 50ppm for C4 crops, and β_i is estimated as 17.20 for C3 crops and 10.82 for C4 crops.

To apply these estimates of CO_2 fertilization to our projections, we estimate this CO_2 fertilization effect for each future year using RCP-specific CO_2 concentrations from [(*111*)], and we subtract off the CO_2 fertilization effect for the year 2015 (the end of our baseline period). We then add this net effect – as log points – to our yield projections for each year. At end-of-century, the CO_2 fertilization effect under RCP 8.5 increases yields by 9.8% and 5.2% for C3 and C4 crops. Under RCP 4.5 end-of-century yields increase by 5.8% and 3.5% for C3 and C4 crops. Global aggregate yield impacts after this adjustment are shown in Figure 3A of the main text.

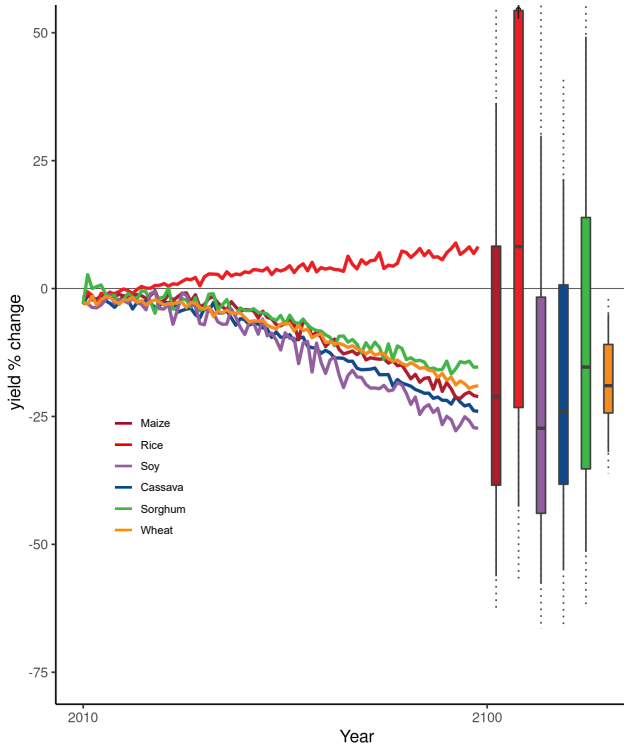
In Figures S17 – S22 displays projection results accounting for the CO_2 fertilization effect. We also test the sensitivity of our partial-SCC estimate to CO_2 fertilization and find it has a moderate effect on the overall estimates (see Tables S12 & S13).



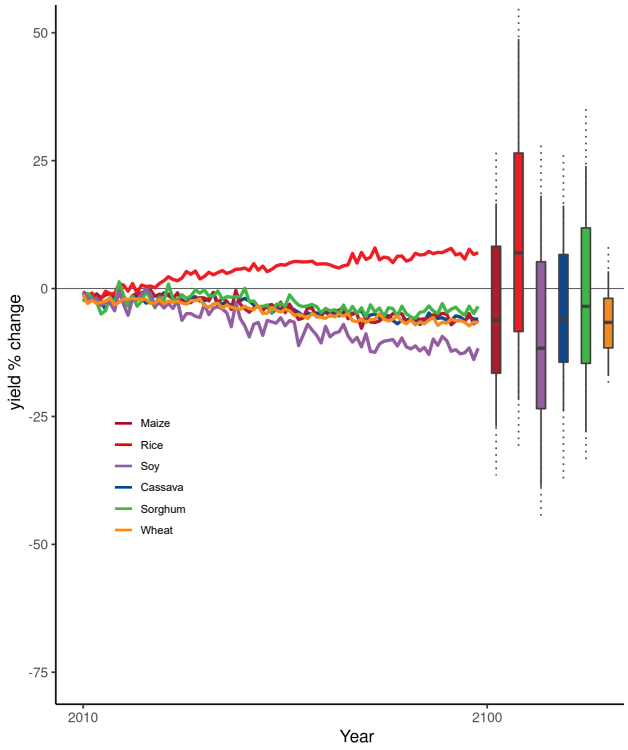
Supplementary Figure S17: Projected climate impacts including CO_2 fertilization under income growth and climate adaptation, including adaptation costs, for (a) maize, (b) soybean, (c) rice, (d) wheat, (e) cassava, and (f) sorghum; for the end-of-century decade 2089 - 2098. Wheat is a combination of winter wheat and spring wheat projections, weighted by their area share in each region. Incomes taken from Shared Socioeconomic Pathway 3 (SSP3) as modeled by OECD, emissions from the RCP 8.5 warming scenario. Results without CO_2 fertilization are shown in Figure 2.



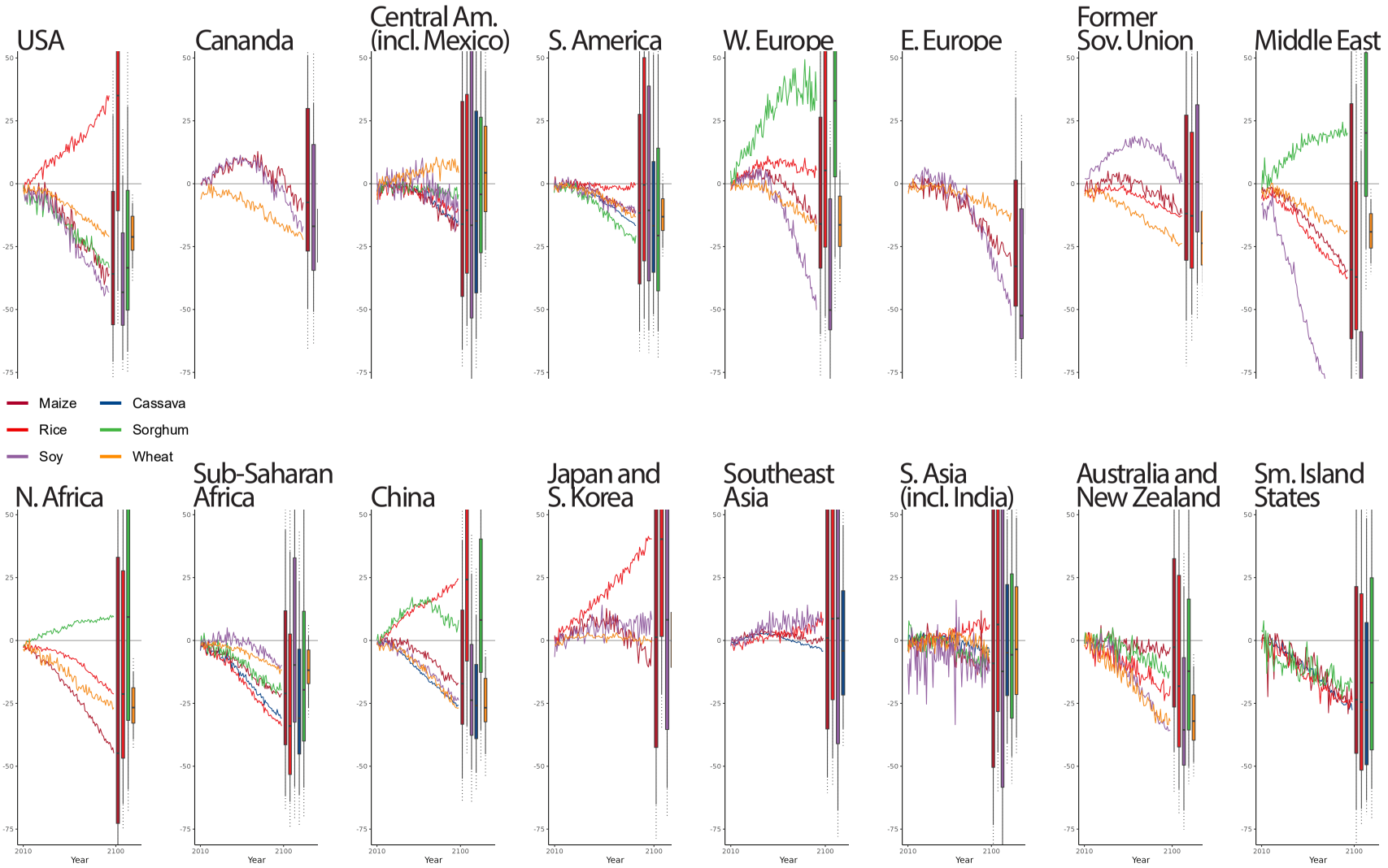
Supplementary Figure S18: Projected climate impacts including CO_2 fertilization under income growth and climate adaptation, including adaptation costs, for (a) maize, (b) soybean, (c) rice, (d) wheat, (e) cassava, and (f) sorghum; for the end-of-century decade 2089 - 2098. Wheat is a combination of winter wheat and spring wheat projections, weighted by their area share in each region. Incomes taken from Shared Socioeconomic Pathway 3 (SSP3) as modeled by OECD, emissions from the RCP 4.5 warming scenario. Results without CO_2 fertilization are shown in Figure S12.



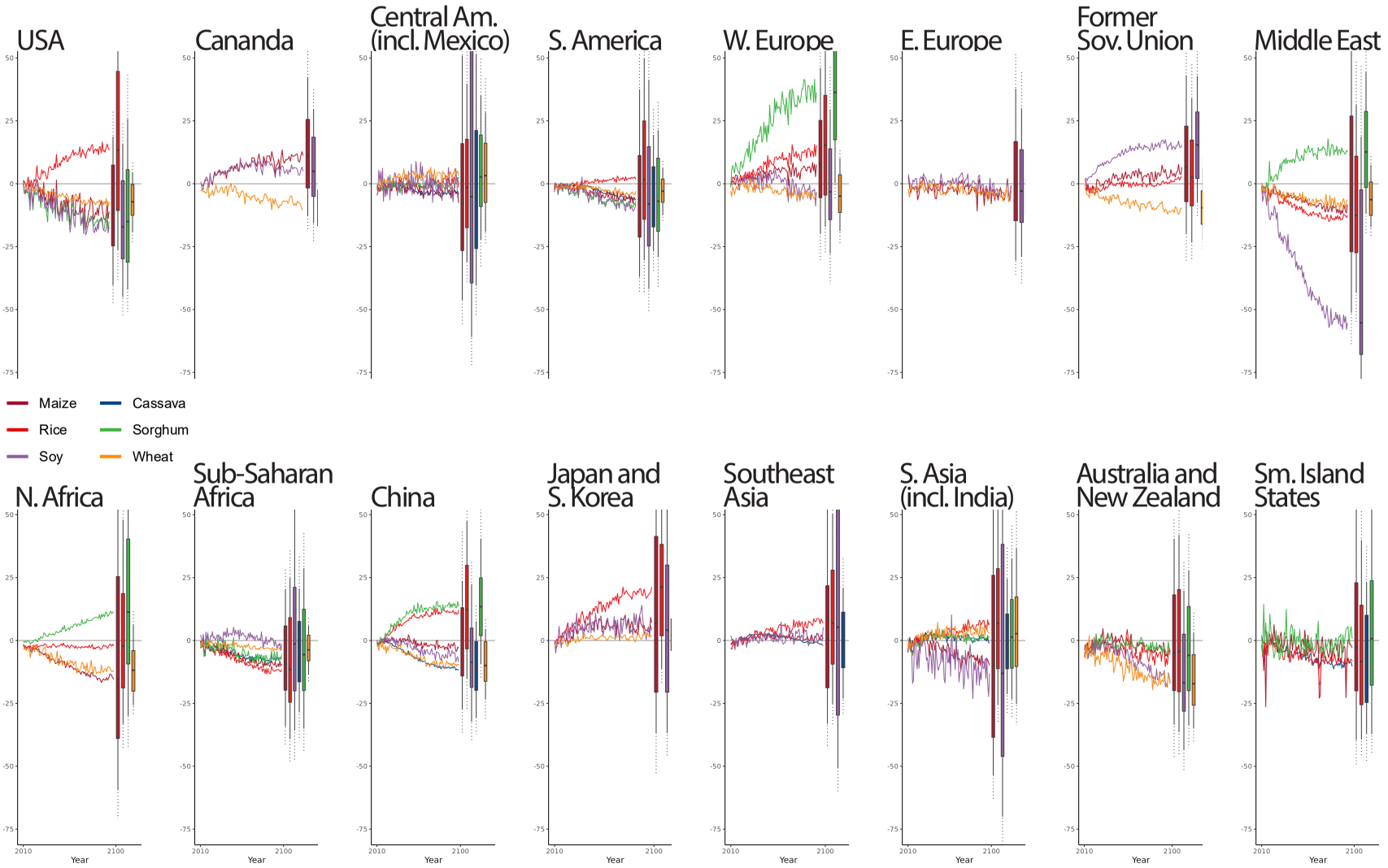
Supplementary Figure S19: Time series of global average climate impacts to grain yields including CO_2 fertilization, net of costly producer adaptation and accounting for income growth, for the RCP 8.5 warming scenario. Averages were calculated using crop-specific area weights from SAGE. Box and whisker plots show joint uncertainty in end-of-century impacts over both Monte Carlo statistical uncertainty and 33 climate models. See Figure 3 for the corresponding result without CO_2 fertilization.



Supplementary Figure S20: Time series of global average climate impacts to grain yields including CO_2 fertilization, net of costly producer adaptation and accounting for income growth, for the RCP 4.5 warming scenario. Averages were calculated using crop-specific area weights from SAGE. Box and whisker plots show joint uncertainty in end-of-century impacts over both Monte Carlo statistical uncertainty and 33 climate models. See Figure S13 for the corresponding result without CO_2 fertilization.



Supplementary Figure S21: Time series of global average climate impacts to grain yields including CO_2 fertilization, net of costly producer adaptation and accounting for income growth, for the RCP 8.5 warming scenario. Averages calculated using crop-specific area weights from SAGE. The regions shown correspond to region definitions in the FUND model. Box and whisker plots show joint uncertainty in end-of-century impacts over both Monte Carlo statistical uncertainty and 33 climate models. See Figure S14 for the corresponding result without CO_2 fertilization.



Supplementary Figure S22: Time series of global average climate impacts to grain yields including CO_2 fertilization, net of costly producer adaptation and accounting for income growth, for the RCP 4.5 warming scenario. Averages calculated using crop-specific area weights from SAGE. The regions shown correspond to region definitions in the FUND model. Box and whisker plots show joint uncertainty in end-of-century impacts over both Monte Carlo statistical uncertainty and 33 climate models. See Figure S14 for the corresponding result without CO_2 fertilization.

J Valuation and the Partial Social Cost of Carbon

In this section we describe our approach to assigning a monetary value to our projected yield impacts of climate change, which enables us to compute a partial social cost of carbon for these agricultural impacts. All estimates of yield impacts in the main text account for within-crop varietal switching (e.g. varieties of maize). Here we additionally account for costly changes in the total amount of agricultural land (along a long-run supply curve) in response to price signals caused by net changes to the overall supply of staple crops under climate change. This movement along the long-run supply curve is in response to the price signal from slow moving (and therefore expected) changes in supply in-line with climate change; annual weather deviations from the long-run trend are unexpected and occur after planting decisions have been made, so producers cannot respond to this component of the price signal. We apply a simple shrinkage estimator (*112*) to the variance in prices to account for the price and quantity effects of storage, though we cannot model "stock-out" conditions should storage approach zero. Consumers demand calories with perfect substitution between crops (e.g. (*61*)), with the distribution of cropped locations and crop types held fixed. Trade is assumed to be frictionless within set markets, and zero between markets; the geographic definitions of markets are varied to show sensitivity to this assumption. Additional sensitivity checks are also introduced.

We further allow for the potential impact for crop switching (e.g. switching from maize to sorghum) and the movement of cropped areas (land conversion). Prior studies have sought to estimate the welfare gains associated with trade, crop switching, and the shifting of cropped locations. We draw on these studies, as detailed below.

J.1 Computing a welfare value for changes in yields

In order to compute a the social welfare value caused by the yield impacts of climate change for any year, we follow (*16*) and model market supply and demand as a constant elasticity system. Here, P and Q refer to the price and quantity of a crop, respectively. Our market model is then:

$$\log(P^S) = \log(k^S) + \epsilon^S \log(Q^S)$$
$$\log(P^D) = \log(k^D) + \epsilon^D \log(Q^D)$$

where the supply and demand elasticities ϵ^S and ϵ^D determine the price-responsiveness of producers and consumers. Movements in this market are illustrated graphically in Figure S23. A reduction in yields, for example, will induce an inward shift in the supply curve from the unperturbed initial equilibrium (Q_0, P_0) to an intermediate point (Q_1, P_0), where $(Q_1 - Q_0)/Q_0$ equals the fractional yield loss associated with the climate impact. In Figure S23a, this is represented as movement from point A to point B.

If producers anticipate that the supply curve has shifted inward relative to a world without climate change, then they expect prices will be higher under climate change. This induces an increase in area planted, resulting in movement along the new supply curve from the intermediate point (Q_1, P_0) to an

equilibrium where the new climate-change supply curve intersects the demand curve (Figure S23a, point C).

We address two additional aspects of agricultural markets: 1) in any given year a component of the weather (climate) is predictable, but a component of the weather is also stochastic; 2) grains are storable goods. The first aspect implies that producers will adjust their area planted based on their expectations of yields at the start of the growing season ($E[S']$ in Figures S23a and b), so that if they expect yields to have been reduced under climate change then they will increase planted area accordingly, up to the point where the expected supply curve meets the demand curve (Q_2^E, P_2^E) (point C in Figures S23a and b). However the stochastic component of weather will induce yield deviations away from expectations, from Q_2^E to Q_2', where $(Q_2' - Q_2^E)/Q_2^E$ is equal to the unanticipated component of the total fractional yield impact (Figure S23b, point D). The second aspect – that grains are storable – implies that storage will smooth the variation in prices and quantities associated with these stochastic weather shocks, injecting grains into the market in unexpectedly bad years and absorbing excess production in unexpectedly good years, resulting in a price shrinkage back toward the expected supply curve from the extreme value $P^D(Q_2')$ to a more moderated value P_2 which lies closer to P_2^E (see Appendix J.4). The final quantity in the market is the quantity Q_2 which is defined by the price P_2 on the demand curve (Figure S23b, point E).

The overall change in social welfare is then simply the change in consumer and producer surplus from (Q_0, P_0) to (Q_2, P_2):

$$\Delta Welfare = \Delta Consumer\ Surplus + \Delta Producer\ Surplus$$

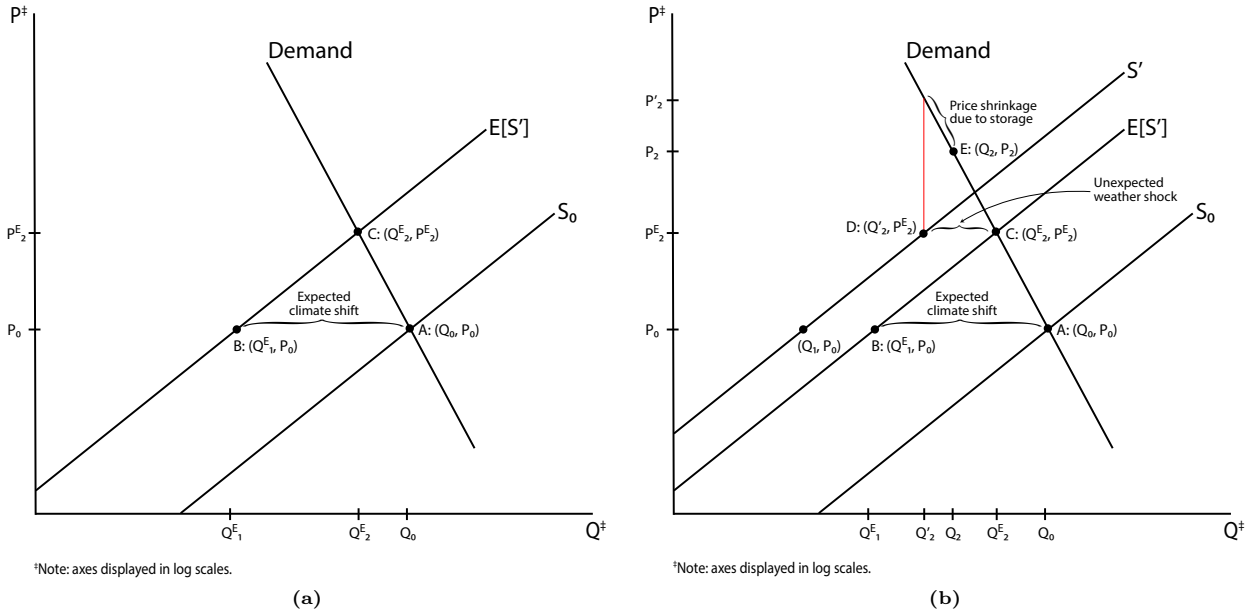
$$\Delta Consumer\ Surplus = \left[\int_0^{Q_2} D(Q)dQ - P_2Q_2\right] - \left[\int_0^{Q_0} D(Q)dQ - P_0Q_0\right]$$

$$\Delta Producer\ Surplus = \left[P_2Q_2 - \int_0^{Q_2} S(Q)dQ\right] - \left[P_0Q_0 - \int_0^{Q_0} S(Q)dQ\right]$$

J.2 Data sources used in valuation

The following data are used as inputs into our valuation calculations.

- Total revenues by country for our 6 crops. We project this into the future using the SSP growth forecasts and the existing empirical relationship in the world between agriculture's share of GDP and GDP per capita (Figure S24). We assume that these 6 crops comprise the same share of agricultural GDP in the future as they do today.
- Demand and Supply elasticities for calories (*16*, *98*, *99*).
- Global Agro-Ecological Zones (GAEZ) "high input" models of levels of crop yields (*113*), which we use to estimate how the ratio between observed yields and the technological frontier (sometimes referred



Supplementary Figure S23: A graphical overview of our approach to the monetization of climate impacts on agricultural yields. We employ a constant elasticity system, which is linear in logs (axes displayed on a log scale). (a) A simplified model, where climate effects on yields are fully anticipated by producers (end-of-season production is known with certainty). The no-climate-change equilibrium is at point A (Q_0, P_0). Climate change causes productivity to contract by a known amount to point B (Q_0, P_1^E) on the new supply curve $E[S']$. Producers know this contraction in supply will result in higher prices, so they plant additional land until the new equilibrium is reached at point C (Q_2^E, P_2^E). (b) The full model, with a shift in yields due to slow-moving climate change which producers expect, a stochastic weather shock which producers do not expect, and storage. As in panel (a), the initial equilibrium is at point A, the no-climate-change equilibrium. Producers expect a productivity shift to supply curve $E[S']$ due to slow-moving climate change and expand area planted until the expected equilibrium point C is reached. Over the course of the growing season stochastic weather is realized, and supply shifts to the supply curve S' and point D. No additional producer response can be made at this point and without storage the price jumps along the red line up to the demand curve. Storage smooths the price spike by adding quantity into the market until the final equilibrium point E (Q_2, P_2). Note that a loss of yields from both anticipated climate change (S_0 to $E[S']$) and stochastic weather ($E[S']$ to S') is shown here, but either term may be positive or negative. See text for further details.

to as the "yield gap") closes with GDP per capita. Note that our climate impacts projections are in terms of log yields, which are interpreted as deviations from a baseline level. We use GAEZ (with an income adjustment) to define the baseline level for all points around the globe.

- Our climate change impacts projections, used to estimate shifts in the supply curve under climate change.[19]

J.3 Conversion of yield impacts into quantity impacts

We calculate Q_0 (caloric production in the no climate-change equilibrium) using GAEZ "high input" yields adjusted for the yield gap associated with a given region's GDPpc (Eq. J.2). This gives a GAEZ income-adjusted yield with irrigation, and another without irrigation (rainfed). We take the weighted average of the two, with weights taken from a given region's area equipped for irrigation (see Appendix A.1). Additionally we use SAGE rasters of planted acreage by crop across the world, and crop-specific calorie per ton conversion factors (see Appendix A.1). Summing across region i and crop j gives:

$$Q_0 = \sum_{i \in I, j \in J} PredictedYield_{ij}^{NoCC} \times \frac{Calories_j}{Ton_j} \times Acres_{ij} \tag{J.1}$$

Our main estimates assume markets clear within continents (so I is a given continent), with frictionless trade within continent and zero trade between continents. We test robustness to this by instead defining markets as either individual countries under autarky (zero trade between countries), or as a single global market with frictionless trade everywhere. Future work should explore the potential impact of bilateral trade costs (*68*, *114*).

Income-Adjusted GAEZ

GAEZ provides information on predicted yield for each crop for every acre in the world. A weakness of GAEZ, however, is that it does not account for technology, which can differ quite substantially across countries and is correlated with GDPpc. We adjust GAEZ high-input potential yields for the yield gap we observe in our data, allowing us to predict how the level of baseline yields evolves as future incomes change.

To apply an income-adjustment to GAEZ, we run the following regression using FAO data on actual country-level yields relative to GAEZ potential yields:

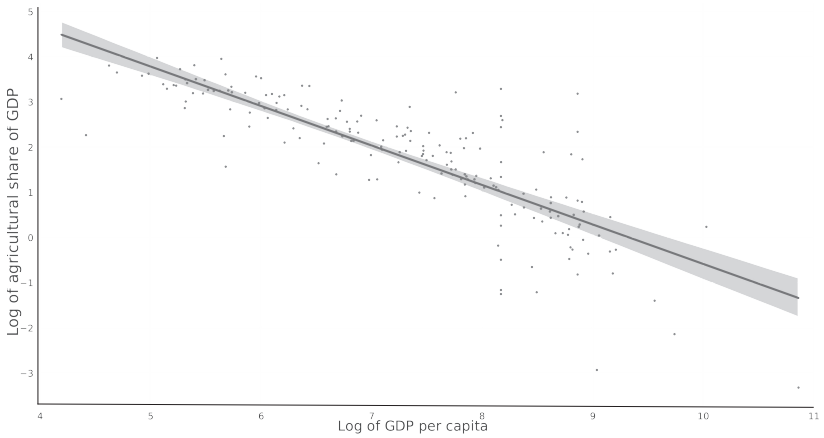
$$\log\left(\frac{ActualYield_k}{GAEZYield_k}\right) = \alpha + \beta_1 \overline{\log(GDPpercapita)}_k + \beta_2 \overline{\log(GDPpercapita)}_k^2 + \epsilon_k \tag{J.2}$$

Here, $\log(\bar{GDPpercapita})_k$ is the 10-year average of $\log(GDPpercapita)$ in country k over the last 10 years of each country's available FAO data. We use logs on both sides of the regression because of the high degree of dispersion in both global yield gaps and GDPpc: the data contain yield gap values in excess of 10

[19] Note: our Monte Carlo results sometimes produce extreme values of predicted yields. For valuation purposes only, we topcode our yields for each crop-year to the maximum value we project from our income-adjusted GAEZ yields for that crop-year (see Eq. J.2).

(which may be explained by mismeasurement at low levels of yields), and GDPpc spans multiple orders of magnitude.

Finally, we calculate the no-climate change equilibrium price per calorie, P_0, as the revenues to our six crops divided by Q_0, where total crop revenues are calculated as $\sum_{i \in I, j \in J} crop_share_agGDP_{ij} \times ag_share_GDP_J \times GDP_J$. Crop shares of agricultural GDP are taken from historical FAO data for each country and held fixed, and agricultural share of GDP comes from a linear regression of 2010 $\log(Ag_share_of_GDP_c)$ on 2010 $\log(GDPpc_c)$ and an intercept (c indexes countries, see Figure S24).



Supplementary Figure S24: Regression model used to predict how the agricultural share of country GDP evolves with income (per capita GDP). This is a cross sectional regression $\log(2010_Ag_share_of_GDP_c) = \alpha + \beta \log(2010_GDPpc_c) + \epsilon_c$.

J.4 Market adjustment and clearing

Fixing (Q_0, P_0) and the supply and demand elasticities (Section J.6) allows us to fully trace out the supply and demand curves for a given market J in a given year. With this information in hand, we follow the methodology laid out in Section J.1 with the following additional details to complete the calculations.

We compute the expected portion of production under climate change (which defines Q_1^E and the expected supply curve $E[S']$ in Figures S23a and b) as no-climate-change production Q_0 minus the moving average of the previous 15 years' climate impact. That is

$$Q_1^E = Q_0 - E[Q_0 - Q_1]$$

with $E[Q_0 - Q_1]$ calculated as a moving average with a Bartlett kernel of 13 years (the same as the averaging period for our income covariate).[20] Recall, this assumes no price adjustment. However, knowledge of Q_1^E and the supply elasticity defines the expected supply curve $E[S']$, which allows us to solve for (Q_2^E, P_2^E) as the intersection of the expected supply curve and the demand curve. This is the expected equilibrium after accounting for the price adjustment leading to increased supply.

[20] We do not take a moving average of previous years' Q_1 values directly because income growth in the current year causes this measure to be systematically biased.

Of course, there will be year-to-year variation in the future. The unexpected portion of a given year's supply shock then simply shifts the expected supply Q_2^E based on the remaining portion of the climate change yield impact:

$$Q_2' = Q_2^E \times \underbrace{\left(1 - \frac{Q_1^E - Q_1}{Q_1^E}\right)}_{\substack{\text{Fraction of expected yields remaining} \\ \text{after accounting for the unexpected} \\ \text{portion of the shock}}}$$

Absent storage, Q_2' would be the final quantity supplied and $P_2' = P^D(Q_2')$ would be the price. Storage reduces the variance in prices by allowing inter-annual arbitrage. Prior work has estimated this smoothing of grain price volatility due to storage (*58*, *112*). Thus, rather than modeling storage explicitly, we apply the shrinkage estimate by ref. (*112*), reducing the estimated raw (i.e. assuming no storage) standard deviation in prices by by 39%. So, we calculate the final price accounting for storage as

$$P_2 = P_2' - 0.39 * (P_2' - P_2^E)$$

and calculate the final quantity supplied into the market as $Q_2 = P^{D^{-1}}(P_2)$.

J.4.1 Welfare adjustments to account for trade, crop switching and land conversion

In response to a permanent shift in the climate, producers may not only change the area they plant in the places where crops are currently grown (discussed above as a shift from Q_1^E to Q_2^E along the expected supply curve $E[S']$, Figure S23); they may also switch which crops they plant, trade in crops with other nations, and even move production to more climatically favorable locations. Prior studies have sought to estimate the welfare gains associated with trade, crop switching, and the shifting of cropped locations (land conversion). The fractions of damages to agriculture averted through these actions have been estimated at 66% (*68*), 66% (*115*), 47% (*70*), and 50% (*67*) using different strategies and approaches. We use the unweighted average of these values (55%) in an adjustment of our estimates that explores the potential reduction of welfare loss through these channels. Thus, we calculate damages allowing for trade, crop switching, and land conversion as $(1 - 0.55)\times$ the value of damages we initially project.

J.4.2 Bounding food expenditures

In a constant elasticity demand system, prices will rise indefinitely as quantity goes to zero. If we were studying all food sources, this could be reasonable. However, here we are studying crops that compose roughly two-thirds of global crop caloric production; we do not estimate or know the impacts on the rest of agricultural output or other sources of calories. If prices rise sufficiently, eventually consumers may substitute toward other calorie sources, in which case the increase in prices for the calorie sources we study would be more limited. To approximate the influence of this behavior in our valuation approach, we place an upper bound on the fraction of income that populations within a market may spend on the crop staples we analyze in any given year. We approximate this bound as the predicted ag_share_GDP in each market-year (see

Figure S24), plus 10 percentage points to account for the fact that if agricultural productivity declines additional resources in agriculture may be required in order to meet basic caloric needs.(*81*) This value is based on the 99 percentile of estimated outcomes reported in ref. (*81*). In sensitivity checks, we consider alternative upper bounds on staple crop expenditures: 1) we add 5 percentage points to ag_share_GDP instead of 10 percentage points (the 95 percentile of from ref. (*81*)); 2) we match the global variance in crop prices for the years 2000-2020 with historical price variance from the FAO, which gives an upper bound of 6% of GDP; 3) we average three estimates from the trade literature(*68*, *69*, *70*) of maximum country-level agricultural sector welfare losses as a fraction of GDP, with an average value of 11% (excluding Malawai from (*68*), which appears to be an extreme outlier). This last alternative is based on welfare loss values which are not estimates of the agricultural expenditures in these models, but still serve as an instructive alternative benchmark.

J.5 Partial Social Cost of Carbon for Staple Crop Production

We compute a partial social cost of carbon for global production of staple crops following the approach used in refs. (*40*, *41*). The procedure is as follows:

1. We fit a damage function of agricultural damages from our Monte Carlo projections under RCP 4.5 and 8.5, two future SSP3 income trajectories (Appendix A.1), and 33 climate models (valued in 2019 USD as described above). Damages are modeled as a quadratic in global mean surface temperature anomaly (Figure S25) for each future year from 2015 to 2098[21] using a five year moving window of Monte Carlo runs.

2. We extrapolate the damage function after 2098 as a constant share of GDP, with the ratio fixed in 2098.[22]

3. We use the Finite Amplitude Impulse Response simple climate model (FaIR, (*116*)) to project warming with and without a 100 GtC pulse of CO_2 in 2015.

4. We compute the marginal agricultural damages in each year associated with the CO_2 pulse, out to the year 2300.

5. We integrate the discounted present value of this stream of marginal damages, using a variety of parameters and approaches recommended by ref. (*71*). We apply both constant discount rates and "Ramsey" discounting (*117*) that accounts for the declining marginal utility of consumption associated with economic development. For Ramsey discounting (*41*) — where the discount rate is given by $\rho+\eta\times g$ — we employ the following values: pure rate of time preference $\rho = 0$;(*41*) intertemporal elasticity of substitution $\eta = 2$;(*76*) and growth rate g for each of the SSP3 income trajectories IIASA and OECD (Appendix A.1). We show Ramsey partial SCC values for the IIASA income trajectory; corresponding values for the OECD income trajectory are very similar.

[21] Our complete set of down-scaled precipitation data stops in 2098.
[22] This differs from (*40*), who fit a time trend to the end-of-century damage function.

Following (*40*), uncertainty in the SCC — which captures economic uncertainty in our damage function and climatological uncertainty in future warming — is calculated as above, with two exceptions. 1) In each year from 2015 to 2098 the damage function is replaced by 19 quantile regressions representing uncertainty in the magnitude of damages, with quantiles taken from the 5^{th} to 95^{th} percentiles at 5% intervals. 2) Each set of quantile-regression damage functions is then projected through a Monte Carlo of FaIR warming uncertainty, and the interquartile range of the final distribution is reported. Additional details on this procedure are detailed in refs. (*40*, *41*).

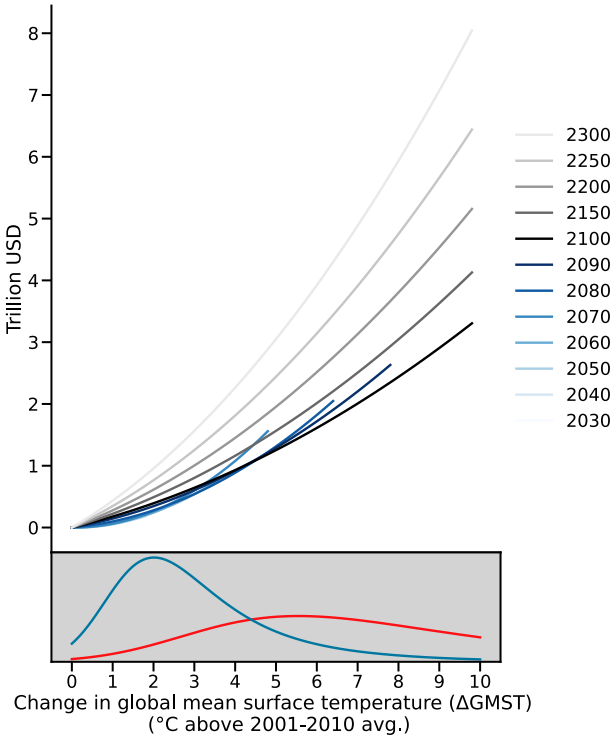
J.6 Scenarios used to compute a partial social cost of carbon

Here we list the parameter values and scenarios we employ in implementing our valuation approach. Due to computational limitations, we do not compute all permutations of possible scenarios. However, we do perturb cases to explore the sensitivity of valuation to each scenario.

- **Market Scale Scenarios:**
  - World - one global market between all producers and consumers clears annually
  - Continent - a market on each continent clears
  - Country - a market within each country clears
- **Supply (*61*, *118*, *119*) and Demand (*61*) Elasticities:**
  - Inelastic scenario - $\epsilon^D : -0.02,\ \epsilon^S : 0.08$
  - Moderately elastic scenario - $\epsilon^D : -0.04,\ \epsilon^S : 0.1$
  - Highly elastic scenario - $\epsilon^D : -0.06,\ \epsilon^S : 0.5$
- **Staple expenditures topcodes:**[23]
  - $ag_share_GDP + 10\%$
  - $ag_share_GDP + 5\%$
  - 6% of GDP - fitted to match historical variance in prices
  - 11% of GDP (*68*, *69*, *70*)
- **Crop switching and land conversion:**
  - Varietal switching - allowing only varietal switching within crops at current locations
  - Flexible production and trade - allowing crop switching, land conversion, and trade between markets. Reduces estimated impacts by 55% (*67*, *68*, *70*, *115*).
- **Discount Rate**

[23] See section J.4.2 for details.

- 2% - Consumption is discounted 2% annually, the long term risk-free rate. Recommended by ref. (*76*)
- 2.5% - Consumption is discounted 2.5% annually. Recommended by ref. (*71*)
- 3% - Consumption is discounted 3% annually. Recommended by ref. (*71*)
- 5% - Consumption is discounted 5% annually. Recommended by ref. (*71*)
- Ramsey - Consumption is discounted based on the pure rate of time preference ($\rho = 0$), an intertemporal elasticity of substitution ($\eta = 2$) and global economic growth (SSP3, IIASA and OECD). Recommended by ref. (*71*)



Supplementary Figure S25: Damage functions fit to our Monte Carlo projections, showing how agricultural damages (valued in $2019) change with increases in global mean surface temperature $\Delta GMST$. Damage functions are shown for every 10 years from 2030 to 2100, and for every 50 years from 2100 to 2300. The distributions at the bottom represent RCP 8.5 warming (red) and RCP 4.5 warming (blue) in 2200. See text, (*41*), and (*40*) for additional details.

Discount rate (%)	Partial SCC: Varietal switching	Partial SCC: + Flexible production and trade
	High emissions scenario: RCP 8.5	
2.0	\$4.65	\$2.09
	[\$2.66, \$10.19]	[\$1.20, \$4.58]
	(\$0.96, \$25.73)	(\$0.43, \$11.58)
2.5	\$3.26	\$1.47
	[\$1.88, \$7.02]	[\$0.85, \$3.16]
	(\$0.68, \$17.78)	(\$0.30, \$8.00)
3.0	\$2.44	\$1.10
	[\$1.41, \$5.10]	[\$0.63, \$2.30]
	(\$0.51, \$13.04)	(\$0.23, \$5.87)
5.0	\$1.10	\$0.50
	[\$0.59, \$2.00]	[\$0.26, \$0.90]
	(\$0.18, \$5.36)	(\$0.08, \$2.41)
Ramsey	\$11.53	\$5.19
	[\$6.44, \$25.08]	[\$2.90, \$11.29]
	(\$2.40, \$63.11)	(\$1.08, \$28.40)
	Low emissions scenario: RCP 4.5	
2.0	\$3.19	\$1.44
	[\$1.91, \$8.01]	[\$0.86, \$3.60]
	(\$0.55, \$21.95)	(\$0.25, \$9.88)
2.5	\$2.31	\$1.04
	[\$1.39, \$5.52]	[\$0.63, \$2.48]
	(\$0.41, \$14.76)	(\$0.18, \$6.64)
3.0	\$1.78	\$0.80
	[\$1.07, \$4.03]	[\$0.48, \$1.82]
	(\$0.32, \$10.68)	(\$0.14, \$4.81)
5.0	\$0.91	\$0.41
	[\$0.49, \$1.67]	[\$0.22, \$0.75]
	(\$0.12, \$4.44)	(\$0.06, \$2.00)
Ramsey	\$8.74	\$3.93
	[\$4.68, \$21.47]	[\$2.11, \$9.66]
	(\$1.53, \$63.35)	(\$0.69, \$28.51)

Supplementary Table S12: The partial social cost of carbon for four different constant discount rates, plus Ramsey discounting, and two emissions trajectories, all for incomes under the Shared Socioeconomic Pathways 3 (SSP3) scenario. IQRs of the partial SCC are calculated over both economic and climate uncertainty and shown in square brackets; 90% confidence intervals over this uncertainty are shown in parentheses. Markets are defined as continents, supply and demand elasticities are 0.1 and −0.04, staple expenditures are topcoded at ag_share_GDP + 10%, CO_2 fertilization is included. "Varietal switching" holds each country's baseline calorie mix between crops as well as where crops are grown fixed into the future, and assumes trade is frictionless within market and zero between markets. "+ Flexible production and trade" includes varietal switching but also allows for international trade, and additionally allows proders to switch crops and change the locations where crops are grown. Ramsey discounting has a pure rate of time preference of 0 and elasticity of intertemporal substitution of 2 (*76*). Ramsey partial SCCs reported are for the IIASA future income trajectory; corresponding values for the OECD trajectory are very similar (Appendix A.1). Variations in key parameters are shown in Table S13. See Appendix J for details.

Elasticities (ϵ^S, ϵ^D)	Market	Max. Expenditure	CO_2 Fertilization	Partial SCC Varietal switching	Partial SCC + Flexible production and trade
		High emissions scenario: RCP 8.5			
0.1, -0.04	Continent	$ag_share_GDP + 10\%$	No	\$5.97	\$2.69
0.1, -0.04	Country	$ag_share_GDP + 10\%$	Yes	\$6.21	\$2.80
0.1, -0.04	Global	$ag_share_GDP + 10\%$	Yes	\$4.14	\$1.86
0.1, -0.04	Continent	$ag_share_GDP + 5\%$	Yes	\$3.71	\$1.67
0.1, -0.04	Continent	11% of GDP	Yes	\$4.37	\$1.97
0.1, -0.04	Continent	6% of GDP	Yes	\$3.30	\$1.48
0.5, -0.06	Continent	$ag_share_GDP + 10\%$	Yes	\$1.37	\$0.62
0.08, -0.02	Continent	$ag_share_GDP + 10\%$	Yes	\$6.42	\$2.89
		Low emissions scenario: RCP 4.5			
0.1, -0.04	Continent	$ag_share_GDP + 10\%$	No	\$5.01	\$2.25
0.1, -0.04	Country	$ag_share_GDP + 10\%$	Yes	\$6.33	\$2.85
0.1, -0.04	Global	$ag_share_GDP + 10\%$	Yes	\$2.40	\$1.08
0.1, -0.04	Continent	$ag_share_GDP + 5\%$	Yes	\$2.82	\$1.27
0.1, -0.04	Continent	11% of GDP	Yes	\$3.03	\$1.36
0.1, -0.04	Continent	6% of GDP	Yes	\$2.54	\$1.14
0.5, -0.06	Continent	$ag_share_GDP + 10\%$	Yes	\$1.11	\$0.50
0.08, -0.02	Continent	$ag_share_GDP + 10\%$	Yes	\$5.12	\$2.31

Supplementary Table S13: Variations in key parameters used to calculate the partial social cost of carbon values in Table S12, for two emissions trajectories using incomes under the Shared Socioeconomic Pathways 3 (SSP3) scenario. Constant 2% discounting used in all cases. See Appendix J for details.